

Washington University in St. Louis

Washington University Open Scholarship

All Theses and Dissertations (ETDs)

1-1-2011

Suprachiasmatic nuclei development: A characterization of transcription factors and the influence of retinal innervation and VIP signaling

Cassandra VanDunk
Washington University in St. Louis

Follow this and additional works at: <https://openscholarship.wustl.edu/etd>

Recommended Citation

VanDunk, Cassandra, "Suprachiasmatic nuclei development: A characterization of transcription factors and the influence of retinal innervation and VIP signaling" (2011). *All Theses and Dissertations (ETDs)*. 656.

<https://openscholarship.wustl.edu/etd/656>

This Dissertation is brought to you for free and open access by Washington University Open Scholarship. It has been accepted for inclusion in All Theses and Dissertations (ETDs) by an authorized administrator of Washington University Open Scholarship. For more information, please contact digital@wumail.wustl.edu.

WASHINGTON UNIVERSITY IN ST. LOUIS

Division of Biology and Biomedical Sciences

Neurosciences

Dissertation Examination Committee:

Paul Gray, Chair

Susan Culican

Erik Herzog

Kristen Kroll

Narendrakumar Ramanan

Paul Taghert

**SUPRACHIASMATIC NUCLEI DEVELOPMENT:
A characterization of transcription factors and the influence of retinal innervation
and VIP signaling**

by

Cassandra Marie VanDunk

A dissertation presented to the
Graduate School of Arts and Sciences
of Washington University in
partial fulfillment of the
requirements for the degree
of Doctor of Philosophy

December 2011

Saint Louis, Missouri

Copyright by
Cassandra Marie VanDunk
2011

ABSTRACT OF THE DISSERTATION

Suprachiasmatic nuclei development:

A characterization of transcription factors and the influence of retinal innervation and
VIP signaling

by

Cassandra Marie VanDunk

Doctor of Philosophy in Biology and Biomedical Sciences (Neuroscience)

Washington University in Saint Louis, 2011

Professor Paul A. Gray, Chairperson

The suprachiasmatic nuclei (SCN) are highly specialized neural structures with an essential behavioral function; creating the rhythm of the mammalian central clock and entraining that internal clock to the external world. The nuclei each consist of approximately 10,000 neurons, each capable of creating near 24 h rhythms, organized into a highly structured network. While the molecular clockwork underlying the rhythm within neurons and network properties have been well studied, how the nuclei are initially specified and how the network develops is poorly understood. Herein, we seek to elucidate the genes and mechanisms involved in the specification and development of SCN neurons, the SCN network, and circadian function.

We first identified genes expressed relatively discretely with the SCN. Using these genes we provided a detailed analysis of transcription factor (TF) and

developmental-gene expression within the SCN from neurogenesis through to adulthood in mice (*Mus musculus*). Through this analysis we identified a genetically distinct neuroepithelium from which SCN neurons are derived and described a gene cascade through which SCN neurons progress as they become postmitotic. In addition, we observed changes in patterns of TF expression through development indicating maturation of nuclei both prenatally and postnatally. We investigated the contribution of critical circadian components in shaping SCN development by monitoring the localization of TF expression in mouse models that lacked either *Atoh7*, necessary for retinal ganglion cell development, or functional VIP peptide or VIP receptor 2 (*VPAC₂*, *Vipr2*). We found that maturation of TF expression patterns within the SCN occurred independent of retinal innervation and VIP signaling, suggesting that localizations may reflect intrinsic differences in subsets of neurons within the nuclei rather than induced changes. Finally, we began to define specific TFs necessary for SCN development using a Cre/loxP system to temporally localize TF deletion. We found that the well-conserved TF, *Six3*, is necessary for the initial formation and specification of SCN neurons, but not involved postmitotically in onset or localization of TF or peptide expression. This work begins to reveal aspects of the development of circadian function, by providing a characterization of SCN anatomical development and the first descriptions of TFs necessary for specification.

ACKNOWLEDGEMENTS

First, and foremost, I would like to thank my advisor, Paul Gray. His encouragement, endless support, and guidance, even when I was reluctant and lacked the confidence, has pushed me to become a better scientist and thinker. I must thank him for not only supporting my scientific pursuits as they pertained to my thesis work, but for also supporting my personal interests and allowing (and HIGHLY recommending) me to pursue other scientific interests through attendance of the Neural Systems and Behavior course at Woods Hole.

I would like to thank the members of the Gray lab past and present Huaiyang Wu, GuangYi Ling, Sri Tupal, and George McMurray for their contributions, assistance, and support. I would especially like to thank George for not only providing technical assistance but also always having a strange story sure to lighten the lab atmosphere.

I would also like to thank my thesis committee members Susan Culican, Erik Herzog, Kristen Kroll, Narendrakumar Ramanan, and Paul Taghert. This committee has provided constructive feedback and critiques, which have shaped my project into what it is today and taught me to really evaluate the types of questions I was asking and the best way to answer them. I would like to especially thank Erik Herzog who not only served as the head of my thesis committee but has provided resources, expertise, guidance, and support throughout my graduate school career.

To my fellow classmates and friends inside and outside of academia, THANK YOU! Graduate school is hard, but you made it a little easier. You have become my family and I can't thank you enough. Special thanks must be given to Matt Thimgan for providing invaluable scientific advice, critiques of my scientific work, and friendship over the years and to Jeffery (Chef Jeff) and Lauren Gerth who have always been my cheering section any time I needed it and for making the North side into an oasis of comfort and support.

It is impossible to thank everyone who has contributed to my growth and successes over the last six years in only one page. So to the Neuroscience program, staff, and community, area businesses that have kept me fed and happy, and all the people that have provided hours of laughter, escape, and support. Thank you.

Finally, to my family. There are not words to describe how thankful I am to you. You have supported me in all my educational decisions (even though it meant being far away) and have always made me feel like I can do this and for that I am eternally grateful. Mom, Dad, Mark, Jamie, and baby Kaya. I love you and thank you.

TABLE OF CONTENTS

ABSTRACT OF THE DISSERTATION.....	ii
ACKNOWLEDGEMENTS.....	iv
TABLE OF CONTENTS.....	v
LIST OF FIGURES AND TABLES.....	viii
CHAPTER 1	
Introduction	1
Suprachiasmatic nuclei as principal circadian rhythm generators.....	2
Molecular clock.....	3
Anatomy and network organization of the SCN.....	5
Origins and development of the SCN.....	7
i. Suprachiasmatic neuroepithelium and premitotic patterning.....	8
ii. Prenatal maturation.....	9
iii. Postnatal maturation.....	10
Influence of the environment on SCN development.....	11
Transcription factors as tools for understanding development.....	13
References.....	15
CHAPTER 2	
Development, Maturation, and Necessity of Transcription Factors in Mouse Suprachiasmatic Nucleus	31
Abstract.....	32
Introduction.....	33
Materials and Methods.....	36
Results.....	41
Identification of SCN candidate transcription factors.....	41
SCN transcription factor expression is diverse and dynamic.....	41
Six3 and Ror α show diurnal variation.....	43
Transcription factors identify the prenatal SCN.....	44
Ror α does not specify postnatal SCN structure.....	47
Identification of the SCN neuroepithelium.....	48
Relationship of early SCN to developmental transcription factors.....	49
Six3 is required for SCN formation.....	52
Discussion.....	54
References.....	60

CHAPTER 3

Role of retinal innervation and vasoactive intestinal polypeptide signaling in mouse suprachiasmatic nuclei development	86
Abstract	87
Introduction	88
Materials and Methods	91
Results	96
Effects of retinal innervation on SCN transcription factor expression	96
Morphological Analysis	96
<i>In situ</i> hybridization Analysis	97
Effects of VIP/VPAC2 signaling on SCN transcription factor expression	99
Morphological Analysis	99
<i>In situ</i> hybridization Analysis: LD	100
<i>In situ</i> hybridization Analysis: DD	101
Discussion	103
References	108

CHAPTER 4

Roles of homeobox protein Six3 in postmitotic GABA-ergic populations of <i>Mus musculus</i>	128
Abstract	129
Introduction	130
Materials and Methods	133
Results	136
Onset of Gad2-cre expression in the SCN	136
Gad2-cre driven conditional knockout of Six3 leads to severe growth deficiencies	136
Role of Six3 in postmitotic specification of SCN neurons	137
Gad2-cre conditional deletion of Six3 may affect extra-SCN structures	138
Discussion	140
References	144

CHAPTER 5

Conclusions and Future Directions	158
Conclusions	159
Development of SCN neuronal subtypes	160
Differential gene expression and the impact of retinal innervation on SCN development	162

Role for Six3 in development.....	164
Future Directions.....	165
SCN formation and specification.....	165
Six3 and the SCN.....	166
References.....	170
CURRICULUM VITAE.....	174

LIST OF FIGURES AND TABLES

CHAPTER 1

Figure 1	Generalized Suprachiasmatic nuclei organization.....	29
Figure 2	Timeline of Suprachiasmatic nuclei development.....	30

CHAPTER 2

Figure 1	Diverse patterns of transcription factor expression in P0 mouse SCN.....	72
Figure 2	The adolescent mouse SCN shows discrete patterns of transcription factor expression.....	73
Figure 3	Six3 and ROR α show diurnal variation in expression.....	74
Figure 4	Dynamic transcription factor expression during SCN prenatal Maturation.....	75
Figure 5	ROR α is not necessary for normal SCN peptide localization.....	76
Figure 6	SCN is derived from a distinct progenitor domain.....	77
Figure 7	Summary of SCN development.....	79
Figure 8	Six3 is necessary for SCN formation.....	81
Supplemental Table 1	Transcription factors with discrete expression within the mouse SCN at P0.....	83
Supplemental Table 2	Transcription factors with discrete mRNA expression within the mouse anterior hypothalamus at E13.5.....	84

CHAPTER 3

Figure 1	SCN presence and location are unaffected by absence of retinal innervation.....	115
----------	---	-----

Table 1	SCN area and length are maintained in the absence of retinal innervation.....	116
Figure 2	Progressive localization of transcription factor expression is maintained in <i>Atoh7</i> knock-outs.....	117
Figure 3	SCN presence and location are unaffected by absence of VIP/VPAC ₂ signaling.....	120
Table 2	SCN location and morphology are maintained in VIP/VPAC ₂ signaling mutants.....	121
Figure 4	Abundance of <i>Rora</i> expression is reduced in VIP and VPAC ₂ mutants kept in constant darkness but not under 12 h light/dark.....	122
Figure 5	Abundance and localization of <i>Rora</i> expression does not correlate with behavioral rhythmicity.....	125
CHAPTER 4		
Figure 1	<i>Gad2-cre</i> induces successful recombination within the SCN.....	149
Figure 2	<i>Six3^{flox/flox}/Gad2-cre(+)</i> mice display severe growth deficiencies visible by P10.....	150
Figure 3	Neonatal localization of SCN transcription factors and peptide expression persist in <i>Six3^{flox/flox}/Gad2-cre(+)</i> mice.....	151
Figure 4	Postmitotic loss of <i>Six3</i> does not affect mature transcription factor expression or peptide localization.....	152
Table 1	SCN size is maintained in animals with postmitotic deletion of <i>Six3</i>	153
Figure 5	Co-expression of <i>Gad1</i> and <i>Six3</i> mRNA is not exclusive to the SCN.....	154
Supplemental Table 1	Regions of overlap of <i>Six3</i> and <i>Gad1</i> mRNA in P2 mouse neural tissue.....	157

-CHAPTER 1-

Introduction

Suprachiasmatic nuclei as principal circadian rhythm generators

The mammalian biological system contains several key generators responsible for creating and maintaining rhythms on different time scales for essential body processes including locomotion, respiration, and circadian function. Key characteristics of rhythm generators are that the rhythms are created endogenously without sensory inputs and can be modulated in order for flexibility in our systems. The localization of these centers within the central nervous system and the development and generation of these rhythms have been fundamental points of interest within the field of neuroscience.

Circadian rhythms are endogenous rhythms that occur on a near 24 h cycle. These rhythms are involved in crucial biological processes such as regulating sleep-wake activity and hormone rhythms (Ibuka et al., 1977; Maywood et al., 2007). The principal circadian rhythm generators are the suprachiasmatic nuclei (SCN), a set of bilateral nuclei that act as central pacemakers; creating, maintaining, and translating signals to the rest of the body in near 24 h rhythms (Welsh et al., 1995; Abrahamson and Moore, 2001; Gachon et al., 2004; Morin and Allen, 2006). The SCN reflect a very unique rhythm generating system, as the rhythm is not created solely from the cellular network; rather, each individual cell possesses the machinery to produce an approximate 24 h rhythm and is considered a potential endogenous oscillator (Welsh et al., 1995). These single cells, organized into a highly structured network, communicate with one another to synthesize a single, robust network output that is then transmitted to downstream targets. A crucial aspect of the circadian system is that SCN activity can be modified or entrained by the

external environment. Timing signals (Zeitgebers), such as light, result in the cells of the SCN modifying or shifting the cycle of the rhythm that they are projecting to the rest of the body. In its simplest form then, the circadian system consists of an input (for entrainment to the external environment), the central pacemaker, and an output (for entraining the rest of the body).

The ability of single cells to create a near 24 h rhythm is not unique to the SCN. Other cell types throughout the body also contain the machinery necessary for this rhythm generation (Panda et al., 2002; Storch et al., 2002; Ueda et al., 2002). Thus, there must be additional mechanisms that allow the SCN to be principal pacemakers for the entire mammalian system. What then makes an SCN neuron an SCN neuron? What makes this cell group develop into a functional circadian rhythm generator? The research presented within this thesis seeks to elucidate the genes and mechanisms necessary for the development of the SCN into principal circadian pacemakers.

Molecular clock

Each cell within the SCN has the same oscillatory potential to create a near 24 h rhythm. This central rhythm is produced by set genes, referred to as “clock genes”, which interact in a series of negative and positive feedback loops (for review (Ko and Takahashi, 2006)). These feedback loops include heterodimers of the proteins CLOCK and BMAL1 that enter the nucleus and bind to specific E-box promoter sequences that enhance the transcription of Period (Per) and Cryptochrome (Cry) genes. PER: CRY

heterodimers then translocate back into the nucleus binding upstream sites on Clock and Bmal genes and ultimately inhibiting their own transcription. Additional posttranslational mechanisms such as phosphorylation by casein kinase 1 (Meng et al., 2008) contribute in making this process occur within a 24 h timescale (Reppert and Weaver, 2002). In addition to this main loop, a second loop is thought to aid in the precision and stabilization of the core rhythm by contributing to the regulation of Bmal1 levels (Emery and Reppert, 2004). CLOCK: BMAL1 induce the transcription of nuclear hormone receptors Rev-erb a,b and ROR a,b, which bind response elements (ROREs) of Bmal1 and regulate its transcription, with Rev-erba acting as a repressor (Preitner et al., 2002) and Rora as a trans-activator (Akashi and Takumi, 2005).

As mentioned, the ability to create a 24 h rhythm with this molecular clockwork is not solely a property of SCN neurons (Panda et al., 2002; Storch et al., 2002; Ueda et al., 2002). Not only can cells of other tissue types create a circadian rhythm, they have been shown to also be cell-autonomous oscillators, able to maintain rhythmicity in the absence of the SCN (Yoo et al., 2004). In addition, Yoo and colleagues (2004) demonstrate that different types of peripheral tissues exhibit slightly different circadian properties. These data suggest that although molecular clockwork is present within multiple tissue types that rhythms within each tissue are specialized. However, what underlies these differences in cellular properties between tissue types is just starting to be understood.

Anatomy and network organization of the SCN

The SCN are bilaterally located within the ventral anterior hypothalamus just dorsal to the optic chiasm and lateral to the third ventricle. Individually, the SCN contain ~10,000 neurons organized into a highly structured network. Each neuron within the SCN is an endogenous oscillator capable of creating near 24 h rhythms (Welsh et al., 1995). These endogenous oscillators have been shown to vary in their afferent input, peptide expression, and response to stimuli (for review (Moore et al., 2002)). The presence of SCN subtypes has prompted attempts at dividing the SCN anatomically and functionally into discrete zones.

Classically, the SCN is subdivided into two complementary regions based on cells expressing the neuropeptides, arginine vasopressin (AVP) and vasoactive intestinal polypeptide (VIP) (Figure 1). These regions, termed loosely dorsomedial or shell and ventrolateral or core (Moore, 1996), respectively, are divisions more a consequence of convenience for means of comparison across species, than steadfast designations. Although the zones are not concrete, they do provide general distinctions from which network function can begin to be understood.

The SCN core contains the highest density of cells and is characterized by neurons expressing VIP, gastrin releasing peptide (GRP), neurotensin (NT), as well as transient calbindin (Silver et al., 1999; Abrahamson and Moore, 2001; Moore et al., 2002; Karatsoreos et al., 2004; Morin et al., 2006; Kriegsfeld et al., 2008). Both GRP and NT have been shown to play a role in communicating phase resetting signals within the SCN

(Gamble et al., 2007), while VIP acts as a key synchronizing agent between individual cellular oscillators and promotes synchrony (Aton et al., 2005). This region has been shown to receive the highest density of direct photic and non-photoc information from the retinohypothalamic tract (RHT) through release of glutamate and PACAP from retinal ganglion cell terminals (Moore and Card, 1985; Cassone et al., 1988; Abrahamson and Moore, 2001). Along with its role in relaying indirect photic signals (Johnson et al., 1989), the inner geniculate leaflet as well as the midbrain raphe nuclei provide non-photoc inputs to the SCN core through the release of neuropeptide-Y and serotonin, respectively (Albers and Ferris, 1984; Biello et al., 1994; Meyer-Bernstein and Morin, 1996; Marchant et al., 1997).

Surrounding the central core is the less cell dense SCN shell, marked by neurons expressing AVP and Met-enkephalin (mENK) (Abrahamson and Moore, 2001). Studies have shown rhythmic release of AVP is a key mechanism utilized by the SCN to entrain peripheral clocks (Castel et al., 1990). The SCN shell receives dense projections from the SCN core and modulatory input, in the form of galanin, from other regions within the anterior hypothalamus and preoptic areas (Levine et al., 1994; Abrahamson and Moore, 2001). In addition to the signaling agents mentioned above, electrical (Yamaguchi et al., 2003) and *gamma*-Aminobutyric acid (GABA) signaling mechanisms (Okamura et al., 1990) have also been implicated in both cell-to-cell and core-to-shell communication (Albus et al., 2005).

Investigation in hamsters, mice, and rats demonstrate that the SCN can be distinguished by functionally distinct regions of differential gene expression (Hastings et al., 1999; Hamada et al., 2001; Jobst and Allen, 2002; LeSauter et al., 2003; Karatsoreos et al., 2004). These studies find rhythms in the expression of *Per1*, *Per2*, and *c-fos* mainly limited to the SCN shell, with highest expression levels occurring during subjective day (Sumova et al., 1998; Guido et al., 1999; Hastings et al., 1999; Yan et al., 1999; Schwartz et al., 2000; Dardente et al., 2002; LeSauter et al., 2003; Karatsoreos et al., 2004). Expression of these genes was absent within the core SCN during both subjective light and dark. However, presenting an animal with a light pulse was able to induce rhythmicity of *Per1*, *Per2*, and *c-fos* within this subdivision, a response gated to pulses given during subjective night (Travnickova et al., 1996; Shigeyoshi et al., 1997). Currently, it is unknown if the anatomical and/or functional subdivisions present within the SCN reflect intrinsic genetic differences between groups of cells or if the regions are induced through development.

Origins and development of the SCN

Research focused on development of circadian rhythmicity has centered primarily on when rhythms emerge. However, given that the clockwork is not unique to cells of the SCN, a better way of understanding the development of circadian function would be to ask what is happening within the nuclei before the clock begins ticking. What genes or signals specify SCN neurons? Where are SCN cells derived from? What is necessary for

the network to mature appropriately? One way to begin to understand this complex process of development is to understand what is already known in order to assess what questions remain. Below I summarize what is known about the SCN during three distinct developmental stages. The first developmental time period examines premitotic patterning, during which specific neuroepithelial zones are established from the surrounding germinal matrix and cells begin to undergo mitosis. The second time period, prenatal maturation, encompasses development between the time when cells are postmitotic and the birth of the animal. The third time period, postnatal maturation, reflects a stage that accounts for changes occurring from birth to development of fully functional nuclei. Previous research has utilized rat models; therefore, all ages described refer to the rat gestational timeline unless otherwise stated. Please refer to Figure 2 for a diagrammatic representation of the developmental timeline.

i. Suprachiasmatic neuroepithelium and premitotic patterning

Tritiated thymidine experiments performed by Altman and Bayer (1978a) proposed that the SCN is derived from a special neuroepithelial zone that forms a shallow ventromedian evagination just caudal to the optic recess during the third wave of hypothalamic development. They further described two separate neuroepithelial zones from which the SCN is derived; a dorsal neuroepithelium that gives rise to neurons of the shell, and a ventral zone where neurons of the core are derived. Neurogenesis was described as occurring approximately five days before birth, with neurons of the core

produced first followed by neurons of the shell (Altman and Bayer, 1978b, a), consistent with the spatiotemporal progression seen in mouse (Shimada and Nakamura, 1973; Okamura et al., 1983; Kabrita and Davis, 2008) and hamster (Davis et al., 1990; Antle et al., 2005).

The zone from which the SCN is derived is situated amidst a large array of early morphogens and signaling gradients along the early ventral floor plate. The genes that may be important for early SCN specification are unknown primarily due to the inability to unequivocally mark the neuroepithelium within the broader context of the developing brain beyond anatomical estimates. Within Chapter 2 we aim to find markers of not only SCN neurons but also the neuroepithelium in order to elucidate early SCN development in the context of the developing telencephalon/diencephalon.

ii. Prenatal maturation

By E17 in rat (E15, in mice, (Kabrita and Davis, 2008)), all the neurons of the SCN are postmitotic (Altman and Bayer, 1978a). It is during this time period between the end of neurogenesis and birth that rhythms begin to emerge and transcription factor, neurotransmitter, and peptide phenotypes are evident. Evaluation of gene expression indicates the presence of *Per1* and *Per2* mRNA as early as E17 (Shimomura et al., 2001) closely followed by the expression of *Clock* and *Bmal1* at E19 (Sladek et al., 2004). The first evidence of single cell rhythmicity is in the diurnal expression of *Per1* mRNA present at E17 (Shimomura et al., 2001). Reppert and Schwartz (1984) demonstrated

rhythms in cellular metabolism by observing diurnal fluctuations in the uptake of 2-deoxyglucose occurring as early as E19. By E22, low amplitude, but significant, circadian rhythms in the firing rates of cells are present in SCN neurons (Shibata and Moore, 1987). It is important to note that at this stage, no clock gene proteins can be visualized, suggesting that the fetal molecular clockwork does not drive the circadian fluctuations present. Although distinctions between SCN neurons and rhythms emerge during this postmitotic stage, it remains unclear whether SCN neuronal subtypes are specified during premitotic or postmitotic stages and what is driving fetal rhythms.

iii. Postnatal maturation

Within the first three days of birth the SCN undergoes many functional changes. Retinal fibers begin to innervate the SCN at birth (P0) providing direct light information able to induce expression of *Per1*, *Per2* (Mateju et al., 2009), and *c-fos* (Weaver and Reppert, 1995; McNeill et al., 2011) by postnatal day three (P3). In addition, although low in amplitude, mRNA rhythms in most clock genes are present (Sumova et al., 2006) and endogenous oscillations of *c-fos* in the SCN shell emerge (Bendova et al., 2004). In mature animals a photic light pulse can induce gene expression within the SCN only during subjective night. Developmentally, the gating of cells responsiveness to light is first seen in clock genes by P5 (Mateju et al., 2009) while the induction of *c-fos* is not gated fully until P10 (Bendova et al., 2004; Mateju et al., 2009). Synaptogenesis within the rat SCN was shown to occur slowly until early postnatal stages during which

synapses are rapidly formed until P10, after which the last 30% of synapse connections are made (Moore and Bernstein, 1989). Interestingly, it is not until synaptogenesis is almost complete that the amplitudes of clock gene fluctuations approach adult levels (Sladek et al., 2004), most likely reflecting cell-to-cell communication increasing network synchrony and strength. Additionally, rhythms in Per, Cry, and Clock proteins are present at similar levels to adult by P10 (Ansari et al., 2009).

Onset of photoperiodic entrainment in clock genes develops gradually. Partial entrainment of Per1 and Per2 to photoperiods is detected at P10, but not until P20 for Cry1 and Bmal1 (Kovacikova et al., 2005). This suggests that although components of the clock are present before birth and rhythms can be detected in early postnatal stages, that maturation of the system in the form of innervation, synaptogenesis, afferent, and efferent connections must occur for the system to be complete and fully functional, ie. entrainable, occurring by P20.

Influence of the environment on SCN development

Although circadian rhythms are driven endogenously, it is not fully understood if SCN network organization or functional development is influenced or dependent on outside environmental factors or extra-SCN input. Possible factors could include maternal rhythms, maternal environment, innervation, spontaneous activity, or sensory input.

Circadian rhythms are seen within the fetal SCN even before functional molecular clockwork, suggesting an alternative clock is driving the fetal SCN. Recent research has suggested that the fetal SCN can be thought of as a peripheral oscillator by the mother (for review (Seron-Ferre et al., [IN PRESS])) and strong evidence has shown that maternal signals such as melatonin (Davis and Gorski, 1988; Viswanathan and Davis, 1997) and dopamine (Weaver et al., 1992; Vitaterna et al., 1994; Weaver and Reppert, 1995; Strother et al., 1998) are fully capable of entraining the fetal and even neonatal mouse SCN. Interestingly, pups born to mothers with non-functional circadian rhythms either through SCN lesion (Reppert and Schwartz, 1986; Davis and Gorski, 1988) or genetic modification (Jud and Albrecht, 2006) develop circadian rhythms normally. These reports demonstrate that the fetal SCN and functional circadian rhythms develop independent of the mothers influence.

Light input can influence circadian behaviors. Recently, it has been shown that rearing animals under various photoperiods has a direct consequence on the free-running behavioral period produced (Ohta et al., 2006; Ciarleglio et al., 2011). Ciarleglio and colleagues (2011) demonstrate that not only were the behavioral locomotor periods affected, but that the changes in period length could also be seen in single cell and tissue level rhythmicity. As would be predicted, the disruption or removal of retinal projections to the SCN results in behaviorally free-running animals. These mice are able to maintain a single, although slightly lengthened, rhythmic period (Laemle and Ottenweller, 1998; Wee et al., 2002). Anatomically, removal of the eye by way of physical removal or

through a naturally occurring mutation resulting in anophthalmia has led to changes in both SCN cell number and location (Silver, 1977; Nagai et al., 1992; Tokunaga et al., 1997). In addition, a number of enucleation studies report changes in the number of cells expressing VIP mRNA and/or protein (reduction, (Laemle and Rusa, 1992); increase, (Holtzman et al., 1989; Okamoto et al., 1990; Denis et al., 1993)). The mechanism of how light influences the determination of circadian period and possibly SCN anatomical development is currently unknown. In Chapter 3 we take a closer look at the impact retinal innervation may have on shaping development of the SCN.

Transcription factors as tools for understanding development

Recently, several groups have performed large-scale transcription factor (TF) screens in order to identify genes expressed in relatively discrete populations of cells (Gong et al., 2003; Gray et al., 2004; Lein et al., 2007; Shimogori et al., 2010). The distinct combinations of TFs expressed, at least in part, pattern the differentiation and specification of distinct cell types. Thus, screens of this nature can serve several purposes. First is the identification of cell and nuclei specific genetic markers. Establishing marker genes for populations not only allows for the tracking of specific cells throughout development, but is also essential for the creation of tools for manipulation of the cell type or population of interest. Secondly, identification of genes present at distinct stages can provide useful lineage and developmental information. TF analysis in this manner has propelled the understanding of specification of heterogeneous

cell groups within both the retina (for review (Peters and Cepko, 2002)) and spinal cord (Matisse and Joyner, 1997). As of yet, no direct investigation into TFs present within the SCN or the relationship between TFs and the formation of the SCN and/or circadian rhythmicity has been undertaken.

Overall, the research contained within this thesis aims to identify genes expressed within the SCN during various stages in development in order to create tools for furthering the understanding of the development of SCN subdivisions, the SCN network, and circadian function. In Chapter 2 we seek to find TFs that can relatively discretely identify the SCN from surrounding nuclei during both prenatal and postnatal stages. We then use a subset of the found TFs to characterize the normal development of the SCN from a period before neurogenesis to weaning, when the SCN is mature. In Chapter 3 we utilize the characterized expression patterns to investigate the influence of several crucial aspects of circadian function, namely retinal innervation and VIP/VPAC₂ signaling, on the development of the SCN and formation of mature TF expression patterns. In addition, we begin to elucidate the roles distinct TFs may play in the formation, specification, and development of the SCN (Chapters 2 and 4) by evaluating proper development in mice with either naturally occurring genetic mutations or temporally controlled gene deletions.

References

- Abrahamson EE, Moore RY (2001) Suprachiasmatic nucleus in the mouse: retinal innervation, intrinsic organization and efferent projections. *Brain Res* 916:172-191.
- Akashi M, Takumi T (2005) The orphan nuclear receptor ROR α regulates circadian transcription of the mammalian core-clock *Bmal1*. *Nat Struct Mol Biol* 12:441-448.
- Albers HE, Ferris CF (1984) Neuropeptide Y: role in light-dark cycle entrainment of hamster circadian rhythms. *Neurosci Lett* 50:163-168.
- Albus H, Vansteensel MJ, Michel S, Block GD, Meijer JH (2005) A GABAergic mechanism is necessary for coupling dissociable ventral and dorsal regional oscillators within the circadian clock. *Curr Biol* 15:886-893.
- Altman J, Bayer SA (1978a) Development of the diencephalon in the rat. I. Autoradiographic study of the time of origin and settling patterns of neurons of the hypothalamus. *J Comp Neurol* 182:945-971.
- Altman J, Bayer SA (1978b) Development of the diencephalon in the rat. III. Ontogeny of the specialized ventricular linings of the hypothalamic third ventricle. *J Comp Neurol* 182:995-1015.
- Ansari N, Agathagelidis M, Lee C, Korf HW, von Gall C (2009) Differential maturation of circadian rhythms in clock gene proteins in the suprachiasmatic nucleus and the pars tuberalis during mouse ontogeny. *Eur J Neurosci* 29:477-489.

- Antle MC, LeSauter J, Silver R (2005) Neurogenesis and ontogeny of specific cell phenotypes within the hamster suprachiasmatic nucleus. *Brain Res Dev Brain Res* 157:8-18.
- Aton SJ, Colwell CS, Harmar AJ, Waschek J, Herzog ED (2005) Vasoactive intestinal polypeptide mediates circadian rhythmicity and synchrony in mammalian clock neurons. *Nat Neurosci* 8:476-483.
- Bendova Z, Sumova A, Illnerova H (2004) Development of circadian rhythmicity and photoperiodic response in subdivisions of the rat suprachiasmatic nucleus. *Brain Res Dev Brain Res* 148:105-112.
- Biello SM, Janik D, Mrosovsky N (1994) Neuropeptide Y and behaviorally induced phase shifts. *Neuroscience* 62:273-279.
- Cassone VM, Speh JC, Card JP, Moore RY (1988) Comparative anatomy of the mammalian hypothalamic suprachiasmatic nucleus. *J Biol Rhythms* 3:71-91.
- Castel M, Feinstein N, Cohen S, Harari N (1990) Vasopressinergic innervation of the mouse suprachiasmatic nucleus: an immuno-electron microscopic analysis. *J Comp Neurol* 298:172-187.
- Ciarleglio CM, Axley JC, Strauss BR, Gamble KL, McMahon DG (2011) Perinatal photoperiod imprints the circadian clock. *Nat Neurosci* 14:25-27.
- Dardente H, Poirel VJ, Klosien P, Pevet P, Masson-Pevet M (2002) Per and neuropeptide expression in the rat suprachiasmatic nuclei: compartmentalization and differential cellular induction by light. *Brain Res* 958:261-271.

- Davis FC, Gorski RA (1988) Development of hamster circadian rhythms: role of the maternal suprachiasmatic nucleus. *J Comp Physiol A* 162:601-610.
- Davis FC, Boada R, LeDeaux J (1990) Neurogenesis of the hamster suprachiasmatic nucleus. *Brain Res* 519:192-199.
- Denis P, Dussailant M, Nordmann JP, Berod A, Saraux H, Rostene W (1993) Vasoactive intestinal peptide/peptide histidine isoleucine mRNA in the eye and suprachiasmatic nucleus of normal and monocularly enucleated rats. *Graefes Arch Clin Exp Ophthalmol* 231:541-545.
- Emery P, Reppert SM (2004) A rhythmic Ror. *Neuron* 43:443-446.
- Gachon F, Nagoshi E, Brown SA, Ripperger J, Schibler U (2004) The mammalian circadian timing system: from gene expression to physiology. *Chromosoma* 113:103-112.
- Gamble KL, Allen GC, Zhou T, McMahon DG (2007) Gastrin-releasing peptide mediates light-like resetting of the suprachiasmatic nucleus circadian pacemaker through cAMP response element-binding protein and Per1 activation. *J Neurosci* 27:12078-12087.
- Gong S, Zheng C, Doughty ML, Losos K, Didkovsky N, Schambra UB, Nowak NJ, Joyner A, Leblanc G, Hatten ME, Heintz N (2003) A gene expression atlas of the central nervous system based on bacterial artificial chromosomes. *Nature* 425:917-925.

- Gray PA, Fu H, Luo P, Zhao Q, Yu J, Ferrari A, Tenzen T, Yuk DI, Tsung EF, Cai Z, Alberta JA, Cheng LP, Liu Y, Stenman JM, Valerius MT, Billings N, Kim HA, Greenberg ME, McMahon AP, Rowitch DH, Stiles CD, Ma Q (2004) Mouse brain organization revealed through direct genome-scale TF expression analysis. *Science* 306:2255-2257.
- Guido ME, de Guido LB, Goguen D, Robertson HA, Rusak B (1999) Daily rhythm of spontaneous immediate-early gene expression in the rat suprachiasmatic nucleus. *J Biol Rhythms* 14:275-280.
- Hamada T, LeSauter J, Venuti JM, Silver R (2001) Expression of Period genes: rhythmic and nonrhythmic compartments of the suprachiasmatic nucleus pacemaker. *J Neurosci* 21:7742-7750.
- Hastings MH, Field MD, Maywood ES, Weaver DR, Reppert SM (1999) Differential regulation of mPER1 and mTIM proteins in the mouse suprachiasmatic nuclei: new insights into a core clock mechanism. *J Neurosci* 19:RC11.
- Holtzman RL, Malach R, Gozes I (1989) Disruption of the optic pathway during development affects vasoactive intestinal peptide mRNA expression. *New Biol* 1:215-221.
- Ibuka N, Inouye SI, Kawamura H (1977) Analysis of sleep-wakefulness rhythms in male rats after suprachiasmatic nucleus lesions and ocular enucleation. *Brain Res* 122:33-47.

- Jobst EE, Allen CN (2002) Calbindin neurons in the hamster suprachiasmatic nucleus do not exhibit a circadian variation in spontaneous firing rate. *Eur J Neurosci* 16:2469-2474.
- Johnson RF, Moore RY, Morin LP (1989) Lateral geniculate lesions alter circadian activity rhythms in the hamster. *Brain Res Bull* 22:411-422.
- Jud C, Albrecht U (2006) Circadian rhythms in murine pups develop in absence of a functional maternal circadian clock. *J Biol Rhythms* 21:149-154.
- Kabrita CS, Davis FC (2008) Development of the mouse suprachiasmatic nucleus: Determination of time of cell origin and spatial arrangements within the nucleus. *Brain Res* 1195:20-27.
- Karatsoreos IN, Yan L, LeSauter J, Silver R (2004) Phenotype matters: identification of light-responsive cells in the mouse suprachiasmatic nucleus. *J Neurosci* 24:68-75.
- Ko CH, Takahashi JS (2006) Molecular components of the mammalian circadian clock. *Hum Mol Genet* 15 Spec No 2:R271-277.
- Kovacikova Z, Sladek M, Laurinova K, Bendova Z, Illnerova H, Sumova A (2005) Ontogenesis of photoperiodic entrainment of the molecular core clockwork in the rat suprachiasmatic nucleus. *Brain Res* 1064:83-89.
- Kriegsfeld LJ, Mei DF, Yan L, Witkovsky P, Lesauter J, Hamada T, Silver R (2008) Targeted mutation of the calbindin D28K gene disrupts circadian rhythmicity and entrainment. *Eur J Neurosci* 27:2907-2921.

Laemle LK, Rusa R (1992) VIP-like immunoreactivity in the suprachiasmatic nuclei of a mutant anophthalmic mouse. *Brain Res* 589:124-128.

Laemle LK, Ottenweller JE (1998) Daily patterns of running wheel activity in male anophthalmic mice. *Physiol Behav* 64:165-171.

Lein ES, Hawrylycz MJ, Ao N, Ayres M, Bensinger A, Bernard A, Boe AF, Boguski MS, Brockway KS, Byrnes EJ, Chen L, Chen L, Chen TM, Chin MC, Chong J, Crook BE, Czaplinska A, Dang CN, Datta S, Dee NR, Desaki AL, Desta T, Diep E, Dolbeare TA, Donelan MJ, Dong HW, Dougherty JG, Duncan BJ, Ebbert AJ, Eichele G, Estin LK, Faber C, Facer BA, Fields R, Fischer SR, Fliss TP, Frensley C, Gates SN, Glattfelder KJ, Halverson KR, Hart MR, Hohmann JG, Howell MP, Jeung DP, Johnson RA, Karr PT, Kawal R, Kidney JM, Knapik RH, Kuan CL, Lake JH, Laramie AR, Larsen KD, Lau C, Lemon TA, Liang AJ, Liu Y, Luong LT, Michaels J, Morgan JJ, Morgan RJ, Mortrud MT, Mosqueda NF, Ng LL, Ng R, Orta GJ, Overly CC, Pak TH, Parry SE, Pathak SD, Pearson OC, Puchalski RB, Riley ZL, Rockett HR, Rowland SA, Royall JJ, Ruiz MJ, Sarno NR, Schaffnit K, Shapovalova NV, Sivisay T, Slaughterbeck CR, Smith SC, Smith KA, Smith BI, Sodt AJ, Stewart NN, Stumpf KR, Sunkin SM, Sutram M, Tam A, Teemer CD, Thaller C, Thompson CL, Varnam LR, Visel A, Whitlock RM, Wohnoutka PE, Wolkey CK, Wong VY, et al. (2007) Genome-wide atlas of gene expression in the adult mouse brain. *Nature* 445:168-176.

- LeSauter J, Yan L, Vishnubhotla B, Quintero JE, Kuhlman SJ, McMahon DG, Silver R (2003) A short half-life GFP mouse model for analysis of suprachiasmatic nucleus organization. *Brain Res* 964:279-287.
- Levine JD, Zhao XS, Miselis RR (1994) Direct and indirect retinohypothalamic projections to the supraoptic nucleus in the female albino rat. *J Comp Neurol* 341:214-224.
- Marchant EG, Watson NV, Mistlberger RE (1997) Both neuropeptide Y and serotonin are necessary for entrainment of circadian rhythms in mice by daily treadmill running schedules. *J Neurosci* 17:7974-7987.
- Mateju K, Bendova Z, El-Hennamy R, Sladek M, Sosniyenko S, Sumova A (2009) Development of the light sensitivity of the clock genes *Period1* and *Period2*, and immediate-early gene *c-fos* within the rat suprachiasmatic nucleus. *Eur J Neurosci* 29:490-501.
- Matise MP, Joyner AL (1997) Expression patterns of developmental control genes in normal and *Engrailed-1* mutant mouse spinal cord reveal early diversity in developing interneurons. *J Neurosci* 17:7805-7816.
- Maywood ES, O'Neill JS, Chesham JE, Hastings MH (2007) Minireview: The circadian clockwork of the suprachiasmatic nuclei--analysis of a cellular oscillator that drives endocrine rhythms. *Endocrinology* 148:5624-5634.
- McNeill DS, Sheely CJ, Ecker JL, Badea TC, Morhardt D, Guido W, Hattar S (2011) Development of melanopsin-based irradiance detecting circuitry. *Neural Dev* 6:8.

- Meng QJ, Logunova L, Maywood ES, Gallego M, Lebiecki J, Brown TM, Sladek M, Semikhodskii AS, Glossop NR, Piggins HD, Chesham JE, Bechtold DA, Yoo SH, Takahashi JS, Virshup DM, Boot-Handford RP, Hastings MH, Loudon AS (2008) Setting clock speed in mammals: the CK1 epsilon tau mutation in mice accelerates circadian pacemakers by selectively destabilizing PERIOD proteins. *Neuron* 58:78-88.
- Meyer-Bernstein EL, Morin LP (1996) Differential serotonergic innervation of the suprachiasmatic nucleus and the intergeniculate leaflet and its role in circadian rhythm modulation. *J Neurosci* 16:2097-2111.
- Moore RY (1996) Entrainment pathways and functional organization of the circadian system. In: *Hypothalamic Integration of Circadian Rhythms. Progress in Brain Research* (R.M. Buijs AK, H.J. Romijn, C.M.A. Pennartz, M. Mirmiran, ed), pp 103-119. Amsterdam: Elsevier.
- Moore RY, Card JP (1985) Visual pathways and the entrainment of circadian rhythms. *Ann N Y Acad Sci* 453:123-133.
- Moore RY, Bernstein ME (1989) Synaptogenesis in the rat suprachiasmatic nucleus demonstrated by electron microscopy and synapsin I immunoreactivity. *J Neurosci* 9:2151-2162.
- Moore RY, Speh JC, Leak RK (2002) Suprachiasmatic nucleus organization. *Cell Tissue Res* 309:89-98.
- Morin LP, Allen CN (2006) The circadian visual system, 2005. *Brain Res Rev* 51:1-60.

- Morin LP, Shivers KY, Blanchard JH, Muscat L (2006) Complex organization of mouse and rat suprachiasmatic nucleus. *Neuroscience* 137:1285-1297.
- Nagai N, Nagai K, Nakagawa H (1992) Effect of orbital enucleation on glucose homeostasis and morphology of the suprachiasmatic nucleus. *Brain Res* 589:243-252.
- Ohta H, Mitchell AC, McMahon DG (2006) Constant light disrupts the developing mouse biological clock. *Pediatr Res* 60:304-308.
- Okamoto S, Okamura H, Takahashi Y, Akagi Y, Yanaihara N, Ibata Y (1990) Contrary effect of eye enucleation on VIP-immunoreactive neurons in the suprachiasmatic nucleus and the superior colliculus of the rat. *Neurosci Lett* 112:137-142.
- Okamura H, Fukui K, Koyama E, Tsutou HL, Tsutou T, Terubayashi H, Fujisawa H, Ibata Y (1983) Time of vasopressin neuron origin in the mouse hypothalamus: examination by combined technique of immunocytochemistry and [3H]thymidine autoradiography. *Brain Res* 285:223-226.
- Okamura H, Abitbol M, Julien JF, Dumas S, Berod A, Geffard M, Kitahama K, Bobillier P, Mallet J, Wiklund L (1990) Neurons containing messenger RNA encoding glutamate decarboxylase in rat hypothalamus demonstrated by in situ hybridization, with special emphasis on cell groups in medial preoptic area, anterior hypothalamic area and dorsomedial hypothalamic nucleus. *Neuroscience* 39:675-699.

- Panda S, Antoch MP, Miller BH, Su AI, Schook AB, Straume M, Schultz PG, Kay SA, Takahashi JS, Hogenesch JB (2002) Coordinated transcription of key pathways in the mouse by the circadian clock. *Cell* 109:307-320.
- Peters MA, Cepko CL (2002) The dorsal-ventral axis of the neural retina is divided into multiple domains of restricted gene expression which exhibit features of lineage compartments. *Dev Biol* 251:59-73.
- Preitner N, Damiola F, Lopez-Molina L, Zakany J, Duboule D, Albrecht U, Schibler U (2002) The orphan nuclear receptor REV-ERB α controls circadian transcription within the positive limb of the mammalian circadian oscillator. *Cell* 110:251-260.
- Reppert SM, Schwartz WJ (1986) Maternal suprachiasmatic nuclei are necessary for maternal coordination of the developing circadian system. *J Neurosci* 6:2724-2729.
- Reppert SM, Weaver DR (2002) Coordination of circadian timing in mammals. *Nature* 418:935-941.
- Schwartz WJ, Carpino A, Jr., de la Iglesia HO, Baler R, Klein DC, Nakabeppu Y, Aronin N (2000) Differential regulation of fos family genes in the ventrolateral and dorsomedial subdivisions of the rat suprachiasmatic nucleus. *Neuroscience* 98:535-547.

- Seron-Ferre M, Mendez N, Abarzua-Catalan L, Vilches N, Valenzuela FJ, Reynolds HE, Llanos AJ, Rojas A, Valenzuela GJ, Torres-Farfan C ([IN PRESS]) Circadian rhythms in the fetus. *Mol Cell Endocrinol*.
- Shibata S, Moore RY (1987) Development of neuronal activity in the rat suprachiasmatic nucleus. *Brain Res* 431:311-315.
- Shigeyoshi Y, Taguchi K, Yamamoto S, Takekida S, Yan L, Tei H, Moriya T, Shibata S, Loros JJ, Dunlap JC, Okamura H (1997) Light-induced resetting of a mammalian circadian clock is associated with rapid induction of the mPer1 transcript. *Cell* 91:1043-1053.
- Shimada M, Nakamura T (1973) Time of neuron origin in mouse hypothalamic nuclei. *Exp Neurol* 41:163-173.
- Shimogori T, Lee DA, Miranda-Angulo A, Yang Y, Wang H, Jiang L, Yoshida AC, Kataoka A, Mashiko H, Avetisyan M, Qi L, Qian J, Blackshaw S (2010) A genomic atlas of mouse hypothalamic development. *Nat Neurosci* 13:767-775.
- Shimomura H, Moriya T, Sudo M, Wakamatsu H, Akiyama M, Miyake Y, Shibata S (2001) Differential daily expression of Per1 and Per2 mRNA in the suprachiasmatic nucleus of fetal and early postnatal mice. *Eur J Neurosci* 13:687-693.
- Silver J (1977) Abnormal development of the suprachiasmatic nuclei of the hypothalamus in a strain of genetically anophthalmic mice. *J Comp Neurol* 176:589-606.

- Silver R, Sookhoo AI, LeSauter J, Stevens P, Jansen HT, Lehman MN (1999) Multiple regulatory elements result in regional specificity in circadian rhythms of neuropeptide expression in mouse SCN. *Neuroreport* 10:3165-3174.
- Sladek M, Sumova A, Kovacikova Z, Bendova Z, Laurinova K, Illnerova H (2004) Insight into molecular core clock mechanism of embryonic and early postnatal rat suprachiasmatic nucleus. *Proc Natl Acad Sci U S A* 101:6231-6236.
- Storch KF, Lipan O, Leykin I, Viswanathan N, Davis FC, Wong WH, Weitz CJ (2002) Extensive and divergent circadian gene expression in liver and heart. *Nature* 417:78-83.
- Strother WN, Norman AB, Lehman MN (1998) D1-dopamine receptor binding and tyrosine hydroxylase-immunoreactivity in the fetal and neonatal hamster suprachiasmatic nucleus. *Brain Res Dev Brain Res* 106:137-144.
- Sumova A, Travnickova Z, Mikkelsen JD, Illnerova H (1998) Spontaneous rhythm in c-Fos immunoreactivity in the dorsomedial part of the rat suprachiasmatic nucleus. *Brain Res* 801:254-258.
- Sumova A, Bendova Z, Sladek M, El-Hennamy R, Laurinova K, Jindrakova Z, Illnerova H (2006) Setting the biological time in central and peripheral clocks during ontogenesis. *FEBS Lett* 580:2836-2842.
- Tokunaga A, Sugita S, Nagai K, Tsutsui K, Ohsawa K (1997) Immunohistochemical characterization of the suprachiasmatic nucleus and the intergeniculate leaflet in the hereditary bilaterally microphthalmic rat. *Neurosci Res* 27:57-63.

- Travnickova Z, Sumova A, Peters R, Schwartz WJ, Illnerova H (1996) Photoperiod-dependent correlation between light-induced SCN c-fos expression and resetting of circadian phase. *Am J Physiol* 271:R825-831.
- Ueda HR, Chen W, Adachi A, Wakamatsu H, Hayashi S, Takasugi T, Nagano M, Nakahama K, Suzuki Y, Sugano S, Iino M, Shigeyoshi Y, Hashimoto S (2002) A transcription factor response element for gene expression during circadian night. *Nature* 418:534-539.
- Viswanathan N, Davis FC (1997) Single prenatal injections of melatonin or the D1-dopamine receptor agonist SKF 38393 to pregnant hamsters sets the offsprings' circadian rhythms to phases 180 degrees apart. *J Comp Physiol A* 180:339-346.
- Vitaterna MH, King DP, Chang AM, Kornhauser JM, Lowrey PL, McDonald JD, Dove WF, Pinto LH, Turek FW, Takahashi JS (1994) Mutagenesis and mapping of a mouse gene, *Clock*, essential for circadian behavior. *Science* 264:719-725.
- Weaver DR, Reppert SM (1995) Definition of the developmental transition from dopaminergic to photic regulation of c-fos gene expression in the rat suprachiasmatic nucleus. *Brain Res Mol Brain Res* 33:136-148.
- Weaver DR, Rivkees SA, Reppert SM (1992) D1-dopamine receptors activate c-fos expression in the fetal suprachiasmatic nuclei. *Proc Natl Acad Sci U S A* 89:9201-9204.

- Wee R, Castrucci AM, Provencio I, Gan L, Van Gelder RN (2002) Loss of photic entrainment and altered free-running circadian rhythms in *math5*^{-/-} mice. *J Neurosci* 22:10427-10433.
- Welsh DK, Logothetis DE, Meister M, Reppert SM (1995) Individual neurons dissociated from rat suprachiasmatic nucleus express independently phased circadian firing rhythms. *Neuron* 14:697-706.
- Yamaguchi S, Isejima H, Matsuo T, Okura R, Yagita K, Kobayashi M, Okamura H (2003) Synchronization of cellular clocks in the suprachiasmatic nucleus. *Science* 302:1408-1412.
- Yan L, Takekida S, Shigeyoshi Y, Okamura H (1999) *Per1* and *Per2* gene expression in the rat suprachiasmatic nucleus: circadian profile and the compartment-specific response to light. *Neuroscience* 94:141-150.
- Yoo SH, Yamazaki S, Lowrey PL, Shimomura K, Ko CH, Buhr ED, Siepkas SM, Hong HK, Oh WJ, Yoo OJ, Menaker M, Takahashi JS (2004) *PERIOD2::LUCIFERASE* real-time reporting of circadian dynamics reveals persistent circadian oscillations in mouse peripheral tissues. *Proc Natl Acad Sci U S A* 101:5339-5346.

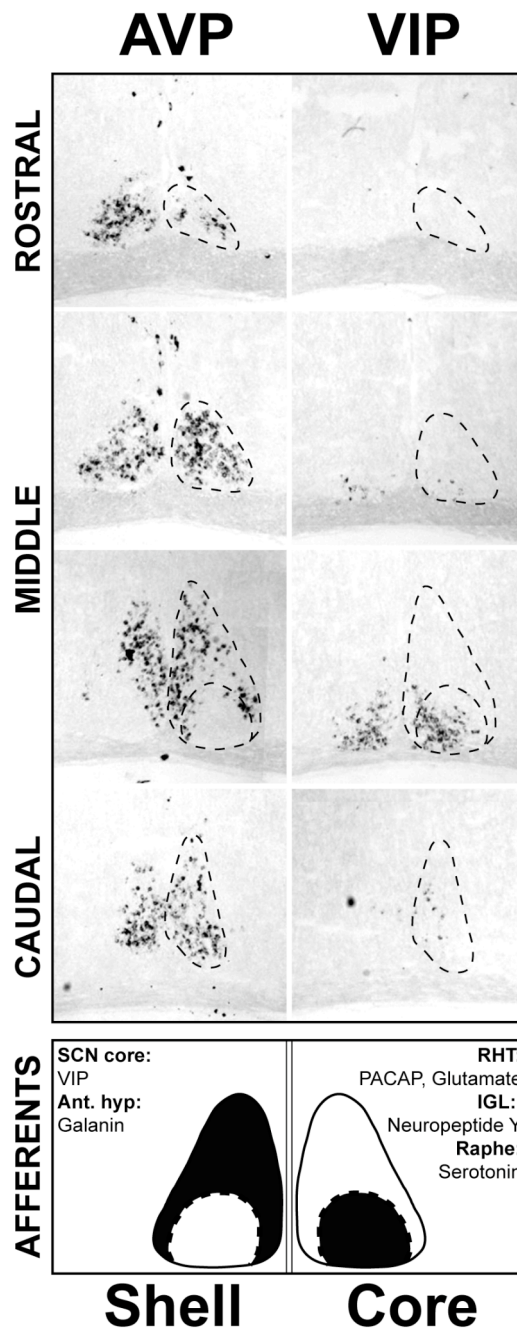


Figure 1. Generalized Suprachiasmatic nuclei organization. Representative *in situ* hybridization images depict expression of arginine vasopressin (AVP) and vasoactive intestinal polypeptide (VIP) mRNA characterizing the SCN shell and core, respectively. Cartoon describes main afferents to each SCN subdivision. (Partially adapted from (Abrahamson and Moore, 2001))

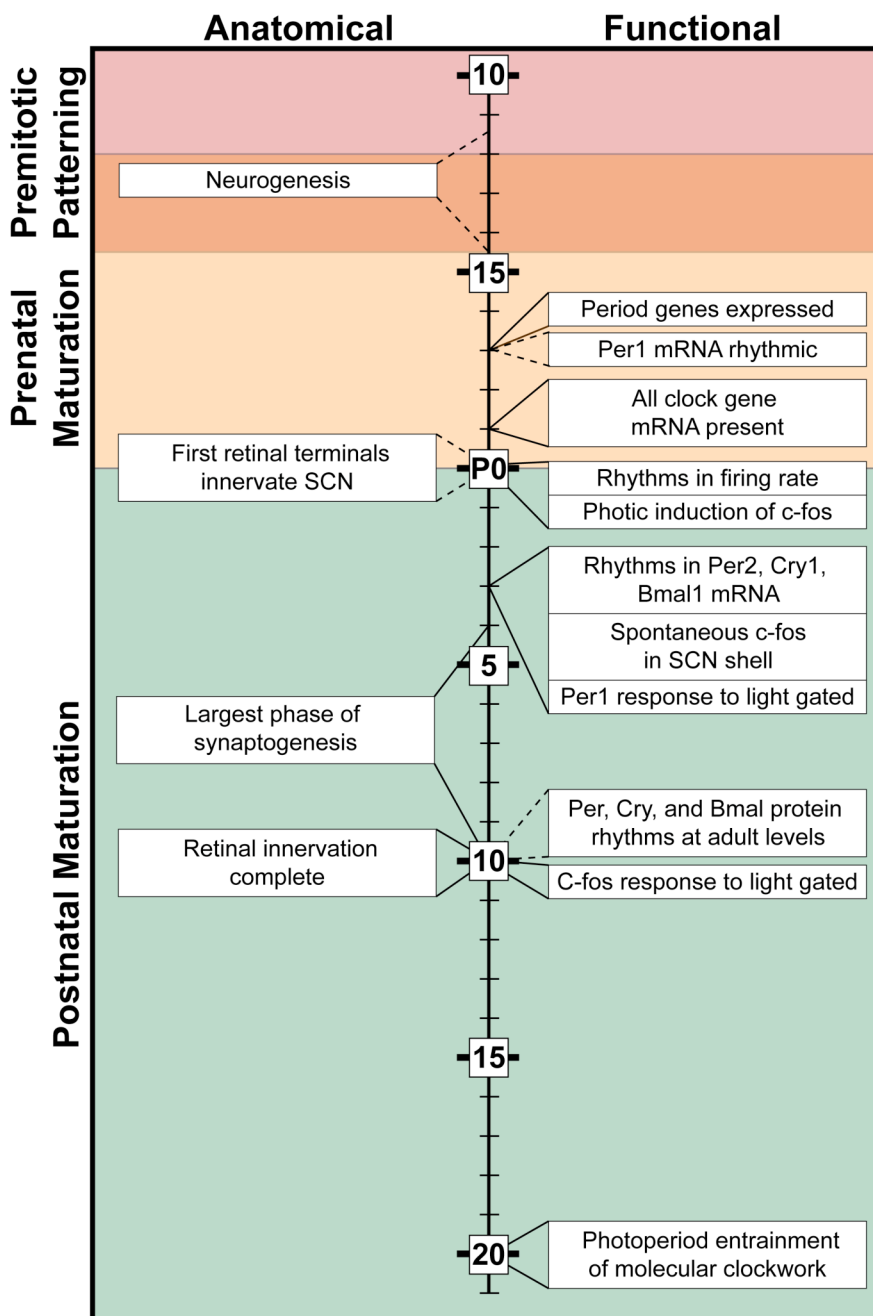


Figure 2. Timeline of Suprachiasmatic nuclei development. Diagram depicts anatomical (left) and functional (right) milestones in SCN development displayed along a timeline divided into periods of premitotic patterning, prenatal maturation, and postnatal maturation. Lines from each milestone indicate data obtained using mouse (dashed lines) or rat models (solid lines).

-CHAPTER 2-
**Development, Maturation, and Necessity of Transcription Factors in the
Mouse Suprachiasmatic Nucleus**

This chapter contains the manuscript:

VanDunk C, Hunter LA, Gray PA (2011) Development, maturation, and necessity of transcription factors in the mouse suprachiasmatic nucleus. *J Neurosci* 31:6457-6467

Abstract

The suprachiasmatic nucleus (SCN) of the hypothalamus is the master mammalian circadian clock. The SCN is highly specialized because it is responsible for generating a near 24 h rhythm, integrating external cues, and translating the rhythm throughout the body. Currently, our understanding of the developmental origin and genetic program involved in the proper specification and maturation of the SCN is limited. Herein, we provide a detailed analysis of transcription factor (TF) (Lein et al., 2007) and developmental-gene expression in the SCN from neurogenesis to adulthood in mice (*Mus musculus*). TF expression within the postmitotic SCN was not static but rather showed specific temporal and spatial changes during prenatal and postnatal development. In addition, we found both global and regional patterns of TF expression extending into the adult. We found the SCN is derived from a distinct region of the neuroepithelium expressing a combination of developmental genes: Six3, Six6, Fzd5, and transient Rx, allowing us to pinpoint the origin of this region within the broader developing telencephalon/diencephalon. We tested the necessity of two TFs in SCN development, ROR α and Six3, which were expressed during SCN development, persisted into adulthood, and showed diurnal rhythmicity. Loss of ROR α function had no effect on SCN peptide expression or localization. In marked contrast, the conditional deletion of Six3 from early neural progenitors completely eliminated the formation of the SCN. Our results provide the first description of the involvement of TFs in the specification and maturation of a neural population necessary for circadian behavior.

Introduction

The suprachiasmatic nucleus (SCN) of the hypothalamus acts as the master mammalian circadian clock generating a near 24 h rhythm through the cyclic expression of key genes, including crucial transcription factors (TFs). The ability of the SCN to integrate external cues and translate rhythms throughout the body reflects a unique specialization of the nucleus and neurons within (Herzog and Schwartz, 2002). Properties underlying the production of 24 h rhythms have been well characterized; however, the genes involved in specification and development of the SCN are unknown.

The SCN is a heterogeneous group of neurons able to generate unified rhythmic output from individual neuronal oscillators (Webb et al., 2009). Expression of arginine vasopressin (AVP) and vasoactive intestinal peptide (VIP) divide the nucleus into two subdivisions, termed dorsomedial/shell, and ventrolateral/core, respectively. Although these gross divisions do not necessarily reflect differences in cellular properties, these areas have been shown to differ in their projection patterns (Leak and Moore, 2001), innervation (Moga and Moore, 1997; Abrahamson and Moore, 2001), and rhythmicity (Hamada et al., 2001; Yan and Okamura, 2002; Bendova et al., 2004; Karatsoreos et al., 2004).

There is an extensive literature describing the birth dating, onset of neurogenesis, and migration of neurons in the SCN of mammals. Initial experiments in rat estimated the SCN is derived from neuroepithelium caudal to the optic recess during the third wave of hypothalamic development (Altman and Bayer, 1986). In addition, studies in mice have

shown that SCN neurogenesis occurs in a ventrolateral to dorsomedial progression approximately 5 d before birth (Shimada and Nakamura, 1973; Okamura et al., 1983; Kabrita and Davis, 2008) consistent with previous findings in rat and hamster (Altman and Bayer, 1978, 1986; Davis et al., 1990; Antle et al., 2005). Additional information regarding the prenatal SCN remains limited, in part because of the difficulty in identifying SCN boundaries beyond cell density estimates before peptide expression. In addition, no single gene has yet been identified that unambiguously distinguishes all SCN neurons from adjacent neural populations.

Individual TFs can distinguish subsets of cells within heterogeneous populations and provide insight into both development and function (Dasen et al., 2005; Gray, 2008). To date, the study of TFs within the SCN has been either in their relation to clock function or as a consequence of focus on neighboring hypothalamic regions. Investigation of TFs specifically within the SCN may provide insight into SCN development, the presence of genetically distinct areas, and relationships between the SCN and other brain regions.

We hypothesized that SCN function is influenced by TF expression and that these genes play a role in both the formation and maturation of SCN rhythmicity. Thus, we provide a detailed spatiotemporal description of TF and developmental-gene expression within the mouse SCN. We find that the SCN undergoes prenatal and postnatal maturation of gene expression. Furthermore, we find that patterns of TF expression reveal a specific gene cascade from which SCN neurons are derived and can be used to identify

the developing SCN before published markers. In addition, we demonstrate a crucial role for an evolutionarily conserved TF in SCN formation.

Materials and Methods

Animals and housing. Male and female wildtype CD1 (Charles River), Six3^{fl^{ox}} (Guillermo Oliver, St. Jude Children's Research Hospital, Memphis, TN), ROR α ^{sg} (002651; The Jackson Laboratory), and Nestin Cre (003771; The Jackson Laboratory) mice were used. Mice were maintained in a normal 12 h light/dark schedule under standard care conditions. Mutant animals were maintained on a C57BL/6 background (Charles River). All experiments were approved by the Animal Studies Committee at Washington University School of Medicine.

Genotyping. Mice were genotyped by PCR for disrupted ROR α gene, Six3 floxed, and/or wild-type alleles as previously described (Liu et al., 2006) or as outlined by The Jackson Laboratory. The presence of Cre was determined by the presence or absence of an amplified band using primers (5' GAGTGAACGAACCTGGTCGAAATCAGTGCG 3') and (5' GCATTACCGGTCGATGCAACGAGTGATGAG 3').

Tissue acquisition. Unless otherwise stated, all collections were done at approximately Zeitgeber time 8 (ZT8). Neonatal pups [postnatal day 0 (P0) to P2] or embryos [embryonic day 10.5 (E10.5) to E18.5] from timed pregnant females (morning of plug was E0.5) were anesthetized on ice and either transcardially perfused (E16.5) or immersion fixed in 4% paraformaldehyde (PFA) in 0.1 M PBS, pH 7.4. Older mice were anesthetized with a ketamine/xylazine mixture before perfusion with 4% PFA. All tissues

were postfixed in 4% PFA overnight at 4°C, cryoprotected in 20% sucrose in PBS, frozen in O.C.T. Compound Embedding Medium (Tissue-Tek), and stored at -75°C. Serial sections (14 or 20 µm) were cut on a Hacker cryostat and thaw mounted on Superfrost Plus slides (Thermo Fisher Scientific). Five adjacent sets of sections were prepared from each embryonic and postnatal age and stored at 20°C.

ZT tissue collection. Tissue was collected as outlined above every 4 h for 24 h from animals (P21-P23) kept in a 12 h light/dark schedule starting at ZT2, two hours after lights on (ZT0). For dark time points, animals were enucleated under red light before perfusion.

Probe synthesis. Plasmids for *in situ* hybridization (ISH) probes were acquired from published sources (Gray et al., 2004; Burns et al., 2008; Zhang et al., 2008) or purchased from Open Biosystems. Gene fragments from verified plasmids were linearized by direct amplification by sequence or vector-specific PCR (gene, GenBank accession number, region, forward primer, reverse primer); AVP, BC051997, GTAATACGACTCACTATAGG (T7), AATTAACCCTCACTAAAGGG (T3); BMP7, BC010771, 281-993, GCCTCTGTTCTTGCTGCGCTCC, CCTGGATGGGCAGAGCATCA; Dlx2, BQ443330, 75-797, CGGGCTCCGCTTCACACCTG, ACGGAGTGTCCTGGGAAAGTGGA; Hmx2, BC023402, T7, ATTTAGGTGACACTATAG (SP6); Per1, BC039768, 532- 1750,

CCCAGAAAGAACTCATGACTG, GCATCTGGTAAAGCACCAGGG; Ptch1, CB723783, T7, T3; ROR α , BC003757, 273-1054, GCCACCTACTCCTGTCCTCG, GCAGGCTCGCTAGAGGTGGTGT; ROR β , BC024842, 331-987, CAGGAACCGTTGCCAACACTGC, CCAGTACGTGGTGGAGTTCGC; Rx, BC024731, 539-1261, CCCGGGATTCGTCCCGGAGT, TTGGCCTTCAGGCGCAGAGC; SHH, BC063087, 51-998, GAGACCCA ACTCCGATGTG, GAAAGCAGAGAACTCCGTGGC. Digoxigenin (DIG)-labeled antisense and sense RNA probes were made using PCR products as template and T7, T3, or SP6 RNA polymerases (Roche). cRNA probes were purified using Quick Spin columns (Roche) and quantified by spectrophotometry. Probes were used at a concentration of 1-2 μ g/ml. Sense counterparts of all probes were tested to ensure probe specificity.

In situ hybridization. Slides were immersed in 4% PFA, permeabilized with proteinase K, and returned to 4% PFA before being washed in 0.1 M triethanolamine-HCl with 0.25% acetic anhydride. Once blocked in hybridization buffer at 65°C slides were incubated in hybridization buffer containing 1-2 μ g/ml DIG-labeled antisense cRNA overnight at 65°C. Slides were then washed in 2X SSC at 62°C, washed in 0.2XSSC at 65°C, blocked with 10% normal horse serum (NHS) in 0.1M PBS, and incubated in alkaline phosphatase-labeled anti-DIG antibody (1:2000 in 10% NHS; Roche) overnight. Sections were washed and color was visualized using nitro blue tetrazolium and 5-Bromo-4-

chloro-3-indolyl phosphate (Roche). Staining was stopped after visual inspection. Sections were washed, fixed in 4% PFA, and coverslipped in 90% glycerol, Vectashield Mounting Medium (Vector Laboratories), or UltraCruz Mounting Media with 4', 6' -diamidino-2-phenylindole (DAPI) (Santa Cruz Biotechnology).

Immunohistochemistry. Sections on slides were dried at room temperature and rinsed in 0.5% Triton X-100 in PBS (PBS-T) before incubating in 10% NHS in PBS-T. Slides were then placed into primary antibody overnight at 4°C. Primary antibodies used include the following: rabbit (Rb) AVP (1:800; Immunostar), Rb Ki67 (1:500; Thermo Fisher Scientific), goat (Gt) Lhx2 (1:500; Santa Cruz Biotechnology), Gt Lhx9 (1:750; Santa Cruz Biotechnology), mouse TuJ1 (1:1000; Covance), and Rb VIP (1:8000; Immunostar). Primary antibodies were removed, and sections were rinsed in PBS-T before incubation in secondary antibodies for 2 h at room temperature. Secondary antibodies used were either the appropriate Alexa Fluor 488 (1:1000; Invitrogen) or cyanine 3 (1:500; Jackson ImmunoResearch). Sections were washed and coverslipped with Ultra-Cruz Mounting Media with DAPI.

Image acquisition. Images were acquired using a Nikon Eclipse 90i microscope, Photometrics Coolsnap HQ2 camera with a Prior Scientific ProScan II motorized translation stage, and acquired in Volocity (PerkinElmer Life and Analytical Sciences) or a Nikon Coolscan V Ed slide scanner with SilverFast SE software (LaserSoft Imaging).

Images were exported as eight-bit JPEG or TIFF files. All images were adjusted for clarity by filtering and/or modifying levels, as necessary, in Photoshop (Adobe Systems).

mRNA quantification and analysis. Percentage of SCN area containing either Lhx1 or ROR α expression was calculated by dividing area expressing mRNA by the total estimated SCN area marked with DAPI, in which area was calculated by outlining regions of interest within NIH Image. Whole SCN quantifications of mRNA expression were performed by quantifying intensity of staining relative to background from 10x ISH images using NIH ImageJ. Margins of the SCN in E17.5 to adult animals were determined by cell density marked with DAPI nuclear stain. For statistical analysis of diurnal variation, one-way ANOVA was applied to relative intensity measurements obtained from ZT2, 6, 10, 14, 18, and ZT22 for Six3, ROR α , and Per1. The differences of mRNA relative intensity between ZT6 and ZT18 were analyzed using Student's *t* test.

Results

Identification of SCN candidate transcription factors

The SCN is a specialized neural structure with an essential behavioral function. We hypothesized that aspects of SCN neurons and SCN function are a direct consequence of the TFs they express and that underlie specification. We set out to identify TFs that might be important for both the development and function of the adult SCN by reexamining a published analysis of nearly 1000 TF and TF-related gene expression patterns in mice at E13.5 and P0 (Gray et al., 2004). Two hundred twenty TFs were previously identified as restricted to populations within the hypothalamus of E13.5 and/or P0 mice. From these data as well as other published work (Rivkees et al., 1992; Schaeren-Wiemers et al., 1997; Jean et al., 1999; Wang and Lufkin, 2000) we identified 72 TFs as possibly expressed in discrete patterns of the postnatal (P0; Supplemental Table 1) and/or prenatal (E13.5; Supplemental Table 2) anterior hypothalamus that includes the SCN. Of these 72 TFs, 28 appeared potentially expressed within the postnatal SCN itself (Supplemental Table 1). We confirmed the perinatal or adult hypothalamic expression of at least 68% of these 28 TFs using data from the Allen Brain Atlas (Lein et al., 2007).

SCN transcription factor expression is diverse and dynamic

Previous large screens of gene expression within the brain, although extremely informative, have generally lacked the spatial and/or temporal precision to determine the

detailed boundaries of expression within the SCN (Gong et al., 2003; Gray et al., 2004; Lein et al., 2007; Shimogori et al., 2010). To directly address the range of TF expression patterns within the early SCN, we selected a subset of nine postnatal TFs (Lhx1, Lhx2, Lhx9, Otp, Pou2f2 (Oct-2), ROR α (Rora), ROR β (Rorb), Six3, and Six6) for detailed ISH or immunohistochemical (IHC) analysis within the P0 mouse SCN. These genes were selected based on their relative levels of expression and specificity within the SCN region and/or previous work, suggesting a possible role in aspects of SCN function (Rivkees et al., 1992; Schaeren-Wiemers et al., 1997; Sato et al., 2004).

We found TFs showed a range of expression patterns suggesting a diverse transcriptional environment (Figure 1). Of the nine postnatal TFs analyzed, six were found specifically expressed in the SCN but not in adjacent hypothalamic nuclei. Compared with a cell density estimate of SCN margins, Six3, Six6, ROR α , and Pou2f2 were expressed throughout the entire SCN, whereas Lhx1 and ROR β both displayed regional specificity within the SCN. Conversely, we found two TFs (Lhx2 and Otp) expressed at lateral and dorsal boundaries but not within the SCN. Lhx9 was neither expressed within the SCN nor served as a boundary marker (data not shown).

To determine whether representative patterns of early postnatal TF expression are modified by postnatal maturation, we examined Six3, Lhx1, and ROR α further for expression at P15, just after eyes open. Six3 retained expression throughout the P15 SCN (Figure 2A). Similar to expression at P0, Lhx1 displayed regionalized specificity within the SCN at P15. Expression of Lhx1 covered $52 \pm 2.6\%$ of the central SCN and partially

overlapped both SCN ventrolateral/core and dorsomedial/shell (Figure 2A). In contrast to expression at P0, ROR α was no longer present throughout the entire SCN; instead, expression was restricted to only the outer $71 \pm 2.2\%$ of the SCN, similar in distribution to AVP and ROR β . ROR α expression did not overlap the VIP-expressing region, seen clearly both in transverse (Figure 2A) and sagittal (Figure 2B) sections through the SCN. We found that expression patterns of Six3, Lhx1, and ROR α at P15 were identical to those at P21 and adult (data not shown).

Six3 and ROR α show diurnal variation

The SCN can entrain to photoperiods (Sumova et al., 2006) and can be considered mature by P21. Also, by this time, the amplitude of circadian changes in expression level of clock genes has reached adult levels (Kovacikova et al., 2006). For clock genes, the differences in phase of expression are a consequence of the interactions in the transcription-translation negative feedback loop that underlie circadian rhythmicity. Much of our understanding of the phasic expression of genes within the SCN has relied on quantitative PCR from whole SCN lysates or radioactive ISH, both of which have limited spatial sensitivity (Sunkin, 2006).

Under standard 12 h light/dark conditions, the mRNA levels of central clock genes Per1, Bmal1, and Cry1 peak and trough at mid-day (ZT6) and mid-night (ZT18) (Oishi et al., 2000; Shearman et al., 2000), with Bmal1 and Cry1 in anti-phase of the mid-day peak of Per1. We tested with nonradioactive ISH whether Per1, Lhx1, ROR α ,

and Six3 mRNA displayed variations at these time points. We found that changes in Six3 and Per1 were significantly different between mid-day and mid-night ($p= 0.00064$ and 0.028 respectively, Student's t test), while ROR α and Lhx1 levels were not ($p=0.055$ and 0.1065 , respectively).

The spatial localization of ROR α at ZT8 in the mature SCN suggested that any change in phase of expression might correspond to changes in spatial localization as well as abundance. We tested the expression of Six3 and ROR α for changes in mRNA intensity and localization of mRNA over a diurnal period ($n=3$ for each time point). We found ROR α displayed temporal variation within the SCN (one-way ANOVA, $F_{(5,47)}= 6.64$, $p=0.0001$), with peak at ZT6 and trough at ZT22, in phase with Per1 (one-way ANOVA, $F_{(5,21)}= 4.56$, $p=0.0089$) (Figure 3A, B), consistent with previous PCR-based analyses (Sato et al., 2004). ROR α was never expressed within the VIP-expressing region, which indicated a previously unrecognized spatial localization. Six3 also showed diurnal variations in expression with peak at ZT6 and trough at ZT18 (one-way ANOVA, $F_{(5,47)}= 10.55$, $p<0.0001$) (Figure 3A, B).

Transcription factors identify the prenatal SCN

Although the SCN is not functionally mature until postnatal stages, early components of rhythmicity are present in late embryonic life. Some of the earliest rhythms were seen in day/night variations in metabolic activity as early as E19 in the rat (Reppert and Schwartz, 1984) as well as individual rhythmically firing neurons at E22 in

the rat (Shibata and Moore, 1987), which corresponds to approximately E16.5 and E19.5 in mouse, respectively. The expression of *Six3*, *Lhx1*, and *ROR α* in both the early postnatal and mature SCN suggested that these same genes might provide insight into the development of the SCN during the prenatal stage in which cellular rhythmicity emerges.

To clearly identify the perinatal SCN, we determined the onset and localization of AVP and VIP by ISH and IHC. Consistent with previous work in other rodents (Romero and Silver, 1990; Isobe et al., 1995; Ban et al., 1997), we found both AVP and VIP mRNA expression prenatally but protein-labeled cell bodies only at postnatal stages (data not shown). AVP mRNA expression was present in the SCN by E17.5 (two of three animals), while already strongly expressed in the supraoptic nuclei (SON) at this time (data not shown). VIP mRNA expression was present in the SCN by E18.5 (three of five animals) (data not shown). Within the SCN, both peptides were expressed in spatially restricted regions similar to that seen in the adult from their onset, suggesting specification of peptidergic identity occurs before E17.5. The global expression of *Six3* and *ROR α* in the SCN at P0 led us to theorize that their expression would identify the boundaries of the SCN during prenatal maturation. Thus, we analyzed the expression of *Six3*, *Lhx1*, and *ROR α* between the end of neurogenesis at E14.5 and birth (P0).

At E14.5, *Six3* was expressed within a portion of the early hypothalamus in both the presumptive SCN region as well as dorsal areas. In contrast, *Lhx1* was present in discrete bilateral regions distal to the third ventricle within the broader *Six3* domain (Figure 4). A small subset of the ventral most *Lhx1/Six3* region was found to express

ROR α in two of five animals examined, suggesting that the onset of ROR α (Figure 4) occurs at this time point. At E15.5, prior to the onset of VIP or AVP mRNA expression, there was an increase in the area and approximate number of cells expressing Lhx1 and ROR α . Additionally, nuclear staining with DAPI revealed the first signs of aggregation into a cell dense nucleus at this stage (Figure 4, white arrow). However, both Lhx1 and ROR α expression extended beyond the newly forming, cell-dense area, which would be consistent with the presence of neurons that will become the SCN before the onset of clustering. We hypothesized that these genes could be used as prenatal genetic markers to define cells of the SCN more precisely than cell density estimates. By E17.5, ROR α expression encompassed the entire SCN and completely overlapped with Six3, whereas Lhx1 expression was reduced to a central portion of the SCN (Figure 4). Six3 expression, however, also marked cells more dorsal and lateral to the SCN (data not shown). Postnatally, these dorsal populations retained their Six3 expression and comprised the anterior paraventricular nucleus (aPV) and subparaventricular regions of the hypothalamus (data not shown). By P0, Six3 and ROR α expression completely overlapped cell density estimates of SCN margins, whereas Lhx1 continued to remain centralized (Figure 4).

These data suggest that TFs can be used to identify the prenatal SCN before the onset of peptide markers, dense clustering of cells, and onset of rhythmic activity. The data further suggest that the onset of ROR α expression occurs after SCN neurogenesis is complete, consistent with literature describing the delayed onset of ROR α expression

within other brain regions (Nakagawa and O'Leary, 2003). In addition, these data indicate that the SCN is not fully specified by the end of neurogenesis and that SCN maturation occurs in stages both prenatally and postnatally.

ROR α does not specify postnatal SCN structure

In a molecular model of the circadian clock, ROR α positively regulates Bmal1, thereby aiding in the stability of the core rhythm (Sato et al., 2004). Knock-outs of ROR α show slight behavioral abnormalities in circadian rhythms, leading to a shortened circadian period (Sato et al., 2004). To date, it is unknown whether the change in circadian period is attributable solely to the interaction of ROR α with Bmal1 or whether there is an anatomical change within the SCN. Therefore, we investigated the role of ROR α in the development of the SCN by comparing the localization of SCN markers in wild-type mice with *staggerer* mice (ROR $\alpha^{sg/sg}$) containing a deletion of the fifth exon in the ROR α gene that causes formation of a premature stop codon and a functionally null protein (Hamilton et al., 1996).

We found the expression of SCN markers in ROR $\alpha^{sg/sg}$ mice were normal. The spatial mRNA expression patterns of AVP and VIP within the SCN as well as that of SCN boundary marker Otp in the hypothalamus (data not shown) remained unaltered in all P15 sg/sg mutants (four of four) compared with wild-type littermates (Figure 5). Thus, although we found that the postnatal expression of ROR α anatomically distinguished the

core of the SCN from its shell, *ROR α* expression was not necessary for the differentiation, presence, or segregation of peptidergic cells within the SCN.

Identification of the SCN neuroepithelium

The ability of *Six3* and *Lhx1* to delineate the prenatal, postmitotic SCN suggested that they might also precisely define the suprachiasmatic neuroepithelium within the early telencephalon/diencephalon boundary zone beyond previous anatomical estimates (Altman and Bayer, 1986). Therefore, we assessed the expression of these genes just before neurogenesis, at E10.5 and during neurogenesis (E11.5 – E13.5) in mice. Specifically, we examined the region from the rostral eye fields extending caudally to the developing pituitary to identify the exact spatial origin of the SCN.

At E10.5, *Six3* marked a broad dorsoventral and rostrocaudal region of the developing floor plate (Figure 6A and data not shown), consistent with previous reports (Oliver et al., 1995). At E11.5, *Six3* was restricted to more ventral regions of the early telencephalon/diencephalon but remained expressed within the developing hypothalamus and pituitary (Figure 6A, D). *Lhx1* expression began at E11.5 in a very small band of cells at the ventral edge of the *Six3*-expressing zone (Figure 6A, arrow), allowing for the identification of the early SCN within the telencephalon/diencephalon boundary region (Figure 6D). Both a dorsal and rostrocaudal expansion in the number of cells expressing *Lhx1* occurred from E12.5 to E13.5, whereas *Six3* expression became more restricted but still surrounded the base of the third ventricle (Figure 6A). The coincident onset of and

increase in *Lhx1* expression during the period of SCN neurogenesis suggests *Lhx1* is one of the first TFs to be expressed in fully postmitotic SCN neurons.

Relationship of early SCN to developmental transcription factors

Identification of the suprachiasmatic neuroepithelium suggested the SCN was derived from a highly discrete region of the developing neural plate. Our initial reanalysis of brain TF expression identified 58 TFs with discrete expression in the area of the E13.5 anterior hypothalamus (Supplemental Table 2). We confirmed the embryonic hypothalamic expression of at least 66% of these 58 TFs using data from Genepaint and Eurexpress expression databases (Visel et al., 2004; Diez-Roux et al., 2011). These TFs included early forebrain genes *Six6* and *Dlx2*. In addition, reduction in the amount of *Rx* (*Rax*) present in early neuroepithelium has been shown to disrupt SCN location and cell number by an unknown mechanism (Silver, 1977; Tucker et al., 2001). To clarify the origins of the SCN within the developing telencephalon/diencephalon, we compared the expression of *Six3* and *Lhx1* with that of early forebrain genes *Six6*, *Dlx2*, and *Rx*.

At E10.5, *Rx* expression overlapped that of *Six3* in the early ventral floor plate (Figure 6B) from the early eye fields through the early developing pituitary (data not shown) consistent with a previous analysis (Bailey et al., 2004). At E11.5, a rostrocaudal gap was evident in *Rx* expression. *Rx* persisted within the eye itself and in ventral floor plate just rostral to the developing pituitary (data not shown). *Six6* expression was first seen at E11.5 in a ventrally restricted but overlapping pattern with *Six3* within the entire

rostrocaudal region examined, including within this Rx-negative gap (Figure 6B, D). Dlx2 expression was first seen in a small band of ventral cells within the Six3/Six6-expressing and Rx-negative domain (Figure 6B, D). Lhx1 was expressed in a subset of the Dlx2-expressing domain (Figure 6D).

By E12.5 and E13.5 as Six3/Six6 expression continued, the Dlx2-expressing region expanded rostrocaudally (Figure 6D) and dorsally both beneath as well as along the lateral aspects of the third ventricle stratifying the region surrounding the base of the early third ventricle into three subregions (Figure 6B). The ventral-most portions of Dlx2 expression overlapped with Lhx1 expression. The mid region retained only Six3/Six6/Dlx2, and the most dorsal aspects lacked Dlx2 (Figure 6B). The overlap between Dlx2 and Lhx1 in the most ventral regions suggested that this combination marked newly postmitotic neurons of the SCN, consistent with findings in embryonic rat. The presence of an Lhx1-negative, Dlx2-positive region suggested that Dlx2 might be expressed during the transition period of cells during the last stages of mitosis to early stages of differentiation similar to its expression within the ventral thalamus (Andrews et al., 2003).

The absence of a single TF specific to the SCN suggested that SCN development might also rely on extrinsic morphogens and other signaling peptides to provide key regionalization signals (Burns et al., 2008; Liu et al., 2010). The expression of Six3, Six6, and Dlx2 in the presumptive suprachiasmatic neuroepithelium can be used to identify the immature SCN within the complex early signaling environment of the developing

telencephalon/diencephalon. We found that, at E10.5, the Six3/Rx region also expressed Frizzled5 (Fzd5), a Wnt receptor, in a region surrounding the base of the third ventricle (Figure 6C). This broad dorsal to ventral Six3/Rx/Fzd5 region was further demarcated by the expression of SHH. Six3/Rx/Fzd5 regions lateral to the ventricle expressed SHH, although it remained absent from the most ventral medial region at the base of the third ventricle (Figure 6C). Unlike Rx, Fzd5 expression continued to overlap with Six3/Six6 at E11.5, further defining the SCN proliferative zone in both the dorsoventral (Figure 6C) and rostrocaudal dimensions (Figure 6D). Fzd5 expression at E12.5 and E13.5 was still present beneath the third ventricle but was restricted to the dorsal region overlapping with the Six3/Six6 region only (Figure 6C, D). Fzd5 expression did not overlap with the region containing postmitotic Lhx1 cells and Dlx2, which suggested the expression of Fzd5 likely marked regions of active proliferation. We found that, at E12.5, the most ventral Dlx2- and Lhx1-expressing regions overlapped with TuJ1, a marker of postmitotic neurons, while the more dorsal Dlx2-negative region expressed Ki67, a marker of proliferating cells (data not shown). Throughout this period of neurogenesis, the early SCN was completely devoid of bone morphogenetic protein 7 and lacked the common SHH receptor Patched1 (data not shown).

Our data suggest that the SCN is derived from a proliferative region expressing Six3, Six6, Fzd5, and transient Rx. Furthermore, early postmitotic cells of the SCN express Six3, Six6, Lhx1, and transiently express Dlx2. Figure 7 shows a summary of the relative patterns of developmental-gene expression during SCN development.

Six3 is required for SCN formation

In the present study, we found that Six3 was continually expressed in the SCN and its progenitors from before neurogenesis to adult when expression was diurnal. This suggested that Six3 has an important role in the SCN and its development. Therefore, we tested whether Six3 is necessary for the formation and maturation of the SCN using a Nestin-cre transgenic to eliminate Six3 ($Six3^{flox/flox}$) (Liu et al., 2006) specifically in progenitors within the neural plate before to specification.

We analyzed the anatomy and expression of Six3 mRNA in $Six3^{flox/flox}/Nestin-cre^+$ mutants (n=5), $Six3^{flox/flox}/Nestin-cre^-$ (n=3), and $Six3^{flox/+}/Nestin-cre^+$ (n=2) littermate controls at E18.5-19.5. We found the Nestin-cre transgenic exhibited a range of Six3 loss in the developing mouse brain, from complete loss to no loss (Figure 8), likely as a result of variation in the onset and duration of cre-recombinase expression. $Six3^{flox/flox}/Nestin-cre^+$ mice with complete Six3 deletion (n=4 of 5) showed holoprosencephaly and a noticeable enlargement and/or merger of the lateral and third ventricles not seen in littermate controls (data not shown). Furthermore, Six3 ablations lead to loss of the pituitary (Figure 8B). In contrast, retina and optic nerves remained intact (data not shown).

$Six3^{flox/flox}/Nestin-cre^+$ E18.5 and E19.5 animals with complete bilateral loss of Six3 expression showed no expression of ROR α or AVP in the ventral anterior hypothalamus (Figure 8A, asterisks). Importantly, loss of Six3 did not lead to the displacement of the SCN because no ectopic nuclei were present along the ventral surface

either rostral or caudal to the optic chiasm, as assessed through a DAPI nuclear stain (data not shown). Loss of ROR α and AVP was SCN specific because the aPV and SON of *Six3*^{flox/flox}/*Nestin-cre*⁺ mice retained AVP expression and the dorsal lateral geniculate (dLG) and ventroposterior medial (VPM) nuclei in both E18.5 and E19.5 mutants continued to express ROR α (Figure 8B). In addition, in all mutants tested, the zona incerta (ZI), which normally expresses Six3, was unaffected (Figure 8B).

To assess whether absence of SCN at E18.5 and E19.5 was attributable to dissolution of the SCN nucleus after cells became postmitotic or the complete disruption of neurogenesis, we analyzed *Six3*^{flox/flox}/*Nestin-cre*⁺ mice at E15.5 (n=5) for early postmitotic SCN markers Lhx1 and ROR α as well as for dense cell clusters. We found that loss of Six3 leads to absence of both early postmitotic genes, consistent with a disruption in specification. E15.5 *Six3*^{flox/flox}/*Nestin-cre*⁺ mice displaying partial Six3 deletion showed a loss of ROR α and Lhx1 only in regions lacking Six3 (Figure 8C). *Six3*^{flox/flox}/*Nestin-cre*⁺ mice that retained expression of Six3 showed prominent expression of both ROR α and Lhx1 (Figure 8C). Together, these results show the necessity of a TF for proper SCN formation and development.

Discussion

Recently, several groups have directly analyzed the expression of large numbers of genes (>1000) within the developing and/or mature hypothalamus by *in situ* hybridization (Gray et al., 2004; Lein et al., 2007; Shimogori et al., 2010) looking for patterns of localization capable of defining small populations of neurons that may correspond to unique functional classes. All of these analyses have shown broad genetic distinctions between hypothalamic nuclei. Other studies have also provided detailed analyses of the roles of several developmental genes in hypothalamic and pituitary ontogeny (Sladek et al., 2004; Davis et al., 2010). However, large anatomical screens, because of their breadth, often lack the spatial detail necessary for a more thorough analysis of specific brain regions. Here we provide a detailed analysis of developmental gene expression in the SCN, describe a specific gene cascade from which SCN neurons are derived, and identify a highly conserved transcription factor necessary for SCN formation.

Altman and Bayer (1986) hypothesized that the early suprachiasmatic neuroepithelium formed from a region just caudal to the optic recess. Our data narrow this description showing that the SCN is derived from a distinct region of neuroepithelium expressing a combination of the developmental genes *Six3*, *Six6*, *Fzd5*, and transient *Rx*, allowing us to pinpoint the suprachiasmatic neuroepithelium within the broader developing telencephalon/diencephalon (for summary, refer to Figure 7 A-C).

ZRDCT anophthalmic mice have decreased expression of Rx protein, and 30% of mutant mice show defects in SCN anatomy and function (Silver, 1977; Tucker et al., 2001). The defects vary widely with respect to disruptions in location and/or cell number, but dense clusters of cells are always seen, indicating formation of nuclei. These data along with our observation of transient Rx before SCN neurogenesis (Figures 6D, 7A, B) suggests that Rx is not necessary for specification of SCN neurons but that loss may disrupt early progenitor domains (Liu et al., 2010).

Altman and Bayer further hypothesized that the suprachiasmatic neuroepithelium was divided into two regions, dorsal and ventral, from which the corresponding dorsomedial/shell and ventrolateral/core were derived. Our data are not consistent with the presence of two genetically distinct regions contained within the suprachiasmatic neuroepithelium. We suggest that the proposed regions outlined by Altman and Bayer are a consequence of temporal proliferation or differential response to non-cell-autonomous cues, such as morphogens or other early-signaling gradients, rather than distinct genetic differences in progenitor type.

We demonstrated that the onset of *Dlx2* and *Lhx1* expression at E11.5 is coincident with the documented onset of SCN neurogenesis (Kabrita and Davis, 2008). This suggests *Dlx2* and *Lhx1* mark neurons as they exit the proliferative zone that will form the SCN. At E12.5/E13.5, the region that gives rise to the SCN contains both proliferating and postmitotic neurons. We demonstrate three zones of overlapping gene expression in the SCN at this age and propose that these distinct TF-expressing zones

represent phases of SCN neuronal development: (I) dorsal Six3/Six6/Fzd5: premitotic/proliferative, (II) mid Six3/Six6/Dlx2: late-mitotic/early-postmitotic, and (III) ventral Six3/Six6/Dlx2/Lhx1: postmitotic (for summary, refer to Figure 7D). Our proposed late-mitotic/early-postmitotic Six3/Six6/Dlx2 zone is similar to the region of migratory “late-forming neurons” outlined by Altman and Bayer (Altman and Bayer, 1986). In addition, our data support the notion of a ventrodorsal gradient in SCN neurogenesis (Kabrita and Davis, 2008) because the expression of Lhx1, a postmitotic marker, was first seen at the most ventral aspects of the early SCN and progressively expanded dorsally as neurogenesis proceeded.

We found that TF expression within the postmitotic SCN was not static but rather showed specific temporal and spatial changes during both prenatal development and postnatal maturation. This was indicated by dynamic expression of Lhx1 prenatally and ROR α postnatally, in which expression of both genes spanned the entire SCN at early stages but became differentially regionalized through development. We propose that changes in localization of gene expression may indicate underlying structural or functional maturation of the SCN. This is supported by the central regionalization of Lhx1 around E17.5, coincident with the perinatal onset of peptide expression. Furthermore, dorsomedial/shell localization of ROR α , evident by P15, is concurrent with the proposed termination of retinal fibers into the SCN (Takatsuji et al., 1995) and onset of photoperiodic entrainment of clock genes (Kovacikova et al., 2005). It would be reasonable to presume that neurons or areas within the SCN may undergo further

specification or specialization as external innervation into the nucleus, such as postnatal retinal innervation (McNeill et al., 2011) and synaptogenesis progress. The identification of TFs with discrete localization within the SCN may reflect additional subdivisions and/or subsets of neurons with distinct functions.

Regional specificity of gene expression, similar to $ROR\alpha$, has also been reported for *Period1* and *Period2*, with expression mainly limited to the dorsomedial/ shell during subjective day in rat and hamster (Hamada et al., 2001). Interestingly, some evidence suggests functional division of the SCN into regions of endogenous rhythmicity (dorsomedial/shell) or induced rhythms (ventrolateral/core) (Sumova et al., 1998; Guido et al., 1999; Hamada et al., 2001; Yan and Okamura, 2002; Hamada et al., 2004; Ramanathan et al., 2006). Given the role of $ROR\alpha$ in stability aspects of the clock through regulation of *Bmal1*, it may be advantageous for the clock to lack stabilizing elements in an inducible region. Furthermore, the pan-SCN expression of *Six3* in phase with *Per1* may suggest a role for *Six3* in maintenance of clock gene expression or underlying circadian rhythmicity.

$ROR\alpha$ is one member of related orphan nuclear receptors that serve not only in the differentiation and development of multiple tissue types, including the cerebellum and thalamus (Becker-Andre et al., 1993; Carlberg et al., 1994; Hamilton et al., 1996; Matysiak-Scholze and Nehls, 1997; Nakagawa et al., 1997; Dussault et al., 1998; Nakagawa et al., 1998; Vogel et al., 2000; Sato et al., 2004), but also in circadian function (Schaeren-Wiemers et al., 1997; Sumi et al., 2002). We found that loss of $ROR\alpha$

had no effect on either the presence or location of AVP and VIP neurons, indicating that it was not necessary for peptide expression or development of peptidergic segregation.

The role of Six3 in eye development is highly conserved across vertebrates and in *Drosophila* (Simeone et al., 1994; Seo et al., 1999). Six3 has been proposed to play a role in proliferation of retinal precursors (Del Bene et al., 2004), lens formation (Liu et al., 2006), neuroretina specification (Liu et al., 2010), regulation of rhodopsin expression (Manavathi et al., 2007), and early anterior patterning (Kobayashi et al., 2002; Lagutin et al., 2003; Gestri et al., 2005; Lavado et al., 2008). Six3 has been shown widely expressed throughout the anterior brain at early stages, narrowing expression over time and remaining transient for many neuronal populations. We found that Six3 was expressed within the suprachiasmatic neuroepithelium before the onset of neurogenesis into adulthood, suggesting an important role for Six3 in the SCN. Moreover, expression of Six3 in adult mice displayed diurnal variation. Although our data cannot discriminate between whether this variation is a response to rhythmic photic input or reveals an underlying circadian rhythm in Six3 expression, they suggest a link between Six3 and day/night changes.

We demonstrated that Six3 is crucial to the development of the SCN. Using a Nestin-cre transgene to limit loss of Six3 to neural progenitors, we tested the role of Six3 in SCN specification. We showed the loss of Six3 during development leads to elimination of ROR α and AVP expression as well as the absence of dense cell clustering perinatally, consistent with the elimination of the SCN. In contrast, extra-SCN structures,

including hypothalamic SON and aPV, as well as thalamic VPM and Six3 expressing ZI, were still present. This suggests that Six3 may not be acting solely in global early patterning but may have an additional role in specification of the SCN. We propose that the absence of gene expression is a consequence of the failure to form the SCN initially and not a role for Six3 in the maintenance of SCN cell survival, because SCN-specific Lhx1 expression and cell density were also absent at E15.5. These data suggest a necessary role for Six3 in SCN development and that Lhx1 and ROR α represent lineage-specific SCN genes.

Overall, these data demonstrate that TF expression can provide insight into both the specification and development of the SCN. We find that TF expression can describe the early suprachiasmatic neuroepithelium and demonstrate that the SCN undergoes maturation both prenatally and postnatally. Maturation is evident by the changes in localization of gene expression within the SCN over time. It is currently unclear whether the specific loss of gene expression in distinct areas of the SCN is necessary for proper circadian function. However, we find that disruption of at least one TF, Six3, can have large-scale effects on SCN development. Profiling of genes with SCN-specific expression for spatial and temporal onset allows researchers, for the first time, to begin to understand the roles of these genes in the anatomical and functional development of this complex nucleus.

References:

- Abrahamson EE, Moore RY (2001) Suprachiasmatic nucleus in the mouse: retinal innervation, intrinsic organization and efferent projections. *Brain Res* 916:172-191.
- Altman J, Bayer SA (1978) Development of the diencephalon in the rat. I. Autoradiographic study of the time of origin and settling patterns of neurons of the hypothalamus. *J Comp Neurol* 182:945-971.
- Altman J, Bayer SA (1986) The development of the rat hypothalamus. *Adv Anat Embryol Cell Biol* 100:1-178.
- Andrews GL, Yun K, Rubenstein JL, Mastick GS (2003) Dlx transcription factors regulate differentiation of dopaminergic neurons of the ventral thalamus. *Mol Cell Neurosci* 23:107-120.
- Antle MC, LeSauter J, Silver R (2005) Neurogenesis and ontogeny of specific cell phenotypes within the hamster suprachiasmatic nucleus. *Brain Res Dev Brain Res* 157:8-18.
- Bailey TJ, El-Hodiri H, Zhang L, Shah R, Mathers PH, Jamrich M (2004) Regulation of vertebrate eye development by Rx genes. *Int J Dev Biol* 48:761-770.
- Ban Y, Shigeyoshi Y, Okamura H (1997) Development of vasoactive intestinal peptide mRNA rhythm in the rat suprachiasmatic nucleus. *J Neurosci* 17:3920-3931.

- Becker-Andre M, Andre E, DeLamarter JF (1993) Identification of nuclear receptor mRNAs by RT-PCR amplification of conserved zinc-finger motif sequences. *Biochem Biophys Res Commun* 194:1371-1379.
- Bendova Z, Sumova A, Illnerova H (2004) Development of circadian rhythmicity and photoperiodic response in subdivisions of the rat suprachiasmatic nucleus. *Brain Res Dev Brain Res* 148:105-112.
- Burns CJ, Zhang J, Brown EC, Van Bibber AM, Van Es J, Clevers H, Ishikawa TO, Taketo MM, Vetter ML, Fuhrmann S (2008) Investigation of Frizzled-5 during embryonic neural development in mouse. *Dev Dyn* 237:1614-1626.
- Carlberg C, Hooft van Huijsduijnen R, Staple JK, DeLamarter JF, Becker-Andre M (1994) RZR_s, a new family of retinoid-related orphan receptors that function as both monomers and homodimers. *Mol Endocrinol* 8:757-770.
- Dasen JS, Tice BC, Brenner-Morton S, Jessell TM (2005) A Hox regulatory network establishes motor neuron pool identity and target-muscle connectivity. *Cell* 123:477-491.
- Davis FC, Boada R, LeDeaux J (1990) Neurogenesis of the hamster suprachiasmatic nucleus. *Brain Res* 519:192-199.
- Davis SW, Castinetti F, Carvalho LR, Ellsworth BS, Potok MA, Lyons RH, Brinkmeier ML, Raetzman LT, Carninci P, Mortensen AH, Hayashizaki Y, Arnhold IJ, Mendonca BB, Brue T, Camper SA (2010) Molecular mechanisms of pituitary

- organogenesis: In search of novel regulatory genes. *Mol Cell Endocrinol* 323:4-19.
- Del Bene F, Tessmar-Raible K, Wittbrodt J (2004) Direct interaction of geminin and Six3 in eye development. *Nature* 427:745-749.
- Diez-Roux G, Banfi S, Sultan M, Geffers L, Anand S, Rozado D, Magen A, Canidio E, Pagani M, Peluso I, Lin-Marq N, Koch M, Bilio M, Cantiello I, Verde R, De Masi C, Bianchi SA, Cicchini J, Perroud E, Mehmeti S, et al. (2011) A high-resolution anatomical atlas of the transcriptome in the mouse embryo. *PLoS Biol* 9:e1000582.
- Dussault I, Fawcett D, Matthyssen A, Bader JA, Giguere V (1998) Orphan nuclear receptor ROR alpha-deficient mice display the cerebellar defects of staggerer. *Mech Dev* 70:147-153.
- Gestri G, Carl M, Appolloni I, Wilson SW, Barsacchi G, Andreazzoli M (2005) Six3 functions in anterior neural plate specification by promoting cell proliferation and inhibiting Bmp4 expression. *Development* 132:2401-2413.
- Gong S, Zheng C, Doughty ML, Losos K, Didkovsky N, Schambra UB, Nowak NJ, Joyner A, Leblanc G, Hatten ME, Heintz N (2003) A gene expression atlas of the central nervous system based on bacterial artificial chromosomes. *Nature* 425:917-925.
- Gray PA (2008) Transcription factors and the genetic organization of brain stem respiratory neurons. *J Appl Physiol* 104:1513-1521.

- Gray PA, Fu H, Luo P, Zhao Q, Yu J, Ferrari A, Tenzen T, Yuk DI, Tsung EF, Cai Z, Alberta JA, Cheng LP, Liu Y, Stenman JM, Valerius MT, Billings N, Kim HA, Greenberg ME, McMahon AP, Rowitch DH, Stiles CD, Ma Q (2004) Mouse brain organization revealed through direct genome-scale TF expression analysis. *Science* 306:2255-2257.
- Guido ME, de Guido LB, Goguen D, Robertson HA, Rusak B (1999) Daily rhythm of spontaneous immediate-early gene expression in the rat suprachiasmatic nucleus. *J Biol Rhythms* 14:275-280.
- Hamada T, Antle MC, Silver R (2004) Temporal and spatial expression patterns of canonical clock genes and clock-controlled genes in the suprachiasmatic nucleus. *Eur J Neurosci* 19:1741-1748.
- Hamada T, LeSauter J, Venuti JM, Silver R (2001) Expression of Period genes: rhythmic and nonrhythmic compartments of the suprachiasmatic nucleus pacemaker. *J Neurosci* 21:7742-7750.
- Hamilton BA, Frankel WN, Kerrebrock AW, Hawkins TL, FitzHugh W, Kusumi K, Russell LB, Mueller KL, van Berkel V, Birren BW, Kruglyak L, Lander ES (1996) Disruption of the nuclear hormone receptor RORalpha in staggerer mice. *Nature* 379:736-739.
- Herzog ED, Schwartz WJ (2002) A neural clockwork for encoding circadian time. *J Appl Physiol* 92:401-408.

- Isobe Y, Nakajima K, Nishino H (1995) Arg-vasopressin content in the suprachiasmatic nucleus of rat pups: circadian rhythm and its development. *Brain Res Dev Brain Res* 85:58-63.
- Jean D, Bernier G, Gruss P (1999) Six6 (Otx2) is a novel murine Six3-related homeobox gene that demarcates the presumptive pituitary/hypothalamic axis and the ventral optic stalk. *Mech Dev* 84:31-40.
- Kabrita CS, Davis FC (2008) Development of the mouse suprachiasmatic nucleus: Determination of time of cell origin and spatial arrangements within the nucleus. *Brain Res* 1195:20-27.
- Karatsoreos IN, Yan L, LeSauter J, Silver R (2004) Phenotype matters: identification of light-responsive cells in the mouse suprachiasmatic nucleus. *J Neurosci* 24:68-75.
- Kobayashi D, Kobayashi M, Matsumoto K, Ogura T, Nakafuku M, Shimamura K (2002) Early subdivisions in the neural plate define distinct competence for inductive signals. *Development* 129:83-93.
- Kovacikova Z, Sladek M, Bendova Z, Illnerova H, Sumova A (2006) Expression of clock and clock-driven genes in the rat suprachiasmatic nucleus during late fetal and early postnatal development. *J Biol Rhythms* 21:140-148.
- Kovacikova Z, Sladek M, Laurinova K, Bendova Z, Illnerova H, Sumova A (2005) Ontogenesis of photoperiodic entrainment of the molecular core clockwork in the rat suprachiasmatic nucleus. *Brain Res* 1064:83-89.

- Lagutin OV, Zhu CC, Kobayashi D, Topczewski J, Shimamura K, Puellas L, Russell HR, McKinnon PJ, Solnica-Krezel L, Oliver G (2003) Six3 repression of Wnt signaling in the anterior neuroectoderm is essential for vertebrate forebrain development. *Genes Dev* 17:368-379.
- Lavado A, Lagutin OV, Oliver G (2008) Six3 inactivation causes progressive caudalization and aberrant patterning of the mammalian diencephalon. *Development* 135:441-450.
- Leak RK, Moore RY (2001) Topographic organization of suprachiasmatic nucleus projection neurons. *J Comp Neurol* 433:312-334.
- Lein ES, Hawrylycz MJ, Ao N, Ayres M, Bensinger A, Bernard A, Boe AF, Boguski MS, Brockway KS, Byrnes EJ, Chen L, Chen L, Chen TM, Chin MC, Chong J, Crook BE, Czaplinska A, Dang CN, Datta S, Dee NR, et al. (2007) Genome-wide atlas of gene expression in the adult mouse brain. *Nature* 445:168-176.
- Liu W, Lagutin OV, Mende M, Streit A, Oliver G (2006) Six3 activation of Pax6 expression is essential for mammalian lens induction and specification. *Embo J* 25:5383-5395.
- Liu W, Lagutin O, Swindell E, Jamrich M, Oliver G (2010) Neuroretina specification in mouse embryos requires Six3-mediated suppression of Wnt8b in the anterior neural plate. *J Clin Invest* 120:3568-3577.

- Manavathi B, Peng S, Rayala SK, Talukder AH, Wang MH, Wang RA, Balasenthil S, Agarwal N, Frishman LJ, Kumar R (2007) Repression of Six3 by a corepressor regulates rhodopsin expression. *Proc Natl Acad Sci U S A* 104:13128-13133.
- Matysiak-Scholze U, Nehls M (1997) The structural integrity of ROR alpha isoforms is mutated in staggerer mice: cerebellar coexpression of ROR alpha1 and ROR alpha4. *Genomics* 43:78-84.
- McNeill DS, Sheely CJ, Ecker JL, Badea TC, Morhardt WG, Hattar S (2011) Development of melanopsin-based irradiance detecting circuitry. *Neural Development* IN PRESS.
- Moga MM, Moore RY (1997) Organization of neural inputs to the suprachiasmatic nucleus in the rat. *J Comp Neurol* 389:508-534.
- Nakagawa S, Watanabe M, Inoue Y (1997) Prominent expression of nuclear hormone receptor ROR alpha in Purkinje cells from early development. *Neurosci Res* 28:177-184.
- Nakagawa S, Watanabe M, Isobe T, Kondo H, Inoue Y (1998) Cytological compartmentalization in the staggerer cerebellum, as revealed by calbindin immunohistochemistry for Purkinje cells. *J Comp Neurol* 395:112-120.
- Nakagawa Y, O'Leary DD (2003) Dynamic patterned expression of orphan nuclear receptor genes RORalpha and RORbeta in developing mouse forebrain. *Dev Neurosci* 25:234-244.

- Oishi K, Fukui H, Ishida N (2000) Rhythmic expression of BMAL1 mRNA is altered in Clock mutant mice: differential regulation in the suprachiasmatic nucleus and peripheral tissues. *Biochem Biophys Res Commun* 268:164-171.
- Okamura H, Fukui K, Koyama E, Tsutou HL, Tsutou T, Terubayashi H, Fujisawa H, Ibata Y (1983) Time of vasopressin neuron origin in the mouse hypothalamus: examination by combined technique of immunocytochemistry and [3H]thymidine autoradiography. *Brain Res* 285:223-226.
- Oliver G, Mailhos A, Wehr R, Copeland NG, Jenkins NA, Gruss P (1995) Six3, a murine homologue of the sine oculis gene, demarcates the most anterior border of the developing neural plate and is expressed during eye development. *Development* 121:4045-4055.
- Ramanathan C, Nunez AA, Martinez GS, Schwartz MD, Smale L (2006) Temporal and spatial distribution of immunoreactive PER1 and PER2 proteins in the suprachiasmatic nucleus and peri-suprachiasmatic region of the diurnal grass rat (*Arvicanthis niloticus*). *Brain Res* 1073-1074:348-358.
- Reppert SM, Schwartz WJ (1984) The suprachiasmatic nuclei of the fetal rat: characterization of a functional circadian clock using ¹⁴C-labeled deoxyglucose. *J Neurosci* 4:1677-1682.
- Rivkees SA, Weaver DR, Reppert SM (1992) Circadian and developmental regulation of Oct-2 gene expression in the suprachiasmatic nuclei. *Brain Res* 598:332-336.

- Romero MT, Silver R (1990) Time Course of peptidergic expression in fetal suprachiasmatic nucleus transplanted into adult hamster. *Level Brain Research* 57:1-6.
- Sato TK, Panda S, Miraglia LJ, Reyes TM, Rudic RD, McNamara P, Naik KA, FitzGerald GA, Kay SA, Hogenesch JB (2004) A functional genomics strategy reveals Rora as a component of the mammalian circadian clock. *Neuron* 43:527-537.
- Schaeren-Wiemers N, Andre E, Kapfhammer JP, Becker-Andre M (1997) The expression pattern of the orphan nuclear receptor RORbeta in the developing and adult rat nervous system suggests a role in the processing of sensory information and in circadian rhythm. *Eur J Neurosci* 9:2687-2701.
- Seo HC, Curtiss J, Mlodzik M, Fjose A (1999) Six class homeobox genes in drosophila belong to three distinct families and are involved in head development. *Mech Dev* 83:127-139.
- Shearman LP, Sriram S, Weaver DR, Maywood ES, Chaves I, Zheng B, Kume K, Lee CC, van der Horst GT, Hastings MH, Reppert SM (2000) Interacting molecular loops in the mammalian circadian clock. *Science* 288:1013-1019.
- Shibata S, Moore RY (1987) Development of neuronal activity in the rat suprachiasmatic nucleus. *Brain Res* 431:311-315.
- Shimada M, Nakamura T (1973) Time of neuron origin in mouse hypothalamic nuclei. *Exp Neurol* 41:163-173.

- Shimogori T, Lee DA, Miranda-Angulo A, Yang Y, Wang H, Jiang L, Yoshida AC, Kataoka A, Mashiko H, Avetisyan M, Qi L, Qian J, Blackshaw S (2010) A genomic atlas of mouse hypothalamic development. *Nat Neurosci* 13:767-775.
- Silver J (1977) Abnormal development of the suprachiasmatic nuclei of the hypothalamus in a strain of genetically anophthalmic mice. *J Comp Neurol* 176:589-606.
- Simeone A, D'Apice MR, Nigro V, Casanova J, Graziani F, Acampora D, Avantaggiato V (1994) Orthopedia, a novel homeobox-containing gene expressed in the developing CNS of both mouse and Drosophila. *Neuron* 13:83-101.
- Sladek M, Sumova A, Kovacikova Z, Bendova Z, Laurinova K, Illnerova H (2004) Insight into molecular core clock mechanism of embryonic and early postnatal rat suprachiasmatic nucleus. *Proc Natl Acad Sci U S A* 101:6231-6236.
- Sumi Y, Yagita K, Yamaguchi S, Ishida Y, Kuroda Y, Okamura H (2002) Rhythmic expression of ROR beta mRNA in the mice suprachiasmatic nucleus. *Neurosci Lett* 320:13-16.
- Sumova A, Travnickova Z, Mikkelsen JD, Illnerova H (1998) Spontaneous rhythm in c-Fos immunoreactivity in the dorsomedial part of the rat suprachiasmatic nucleus. *Brain Res* 801:254-258.
- Sumova A, Bendova Z, Sladek M, El-Hennamy R, Laurinova K, Jindrakova Z, Illnerova H (2006) Setting the biological time in central and peripheral clocks during ontogenesis. *FEBS Lett* 580:2836-2842.

- Sunkin SM (2006) Towards the integration of spatially and temporally resolved murine gene expression databases. *Trends Genet* 22:211-217.
- Takatsuji K, Senba E, Mantyh PW, Tohyama M (1995) A relationship between substance P receptor and retinal fibers in the rat suprachiasmatic nucleus. *Brain Res* 698:53-61.
- Tucker P, Laemle L, Munson A, Kanekar S, Oliver ER, Brown N, Schlecht H, Vetter M, Glaser T (2001) The eyeless mouse mutation (*ey1*) removes an alternative start codon from the *Rx/rax* homeobox gene. *Genesis* 31:43-53.
- Visel A, Thaller C, Eichele G (2004) GenePaint.org: an atlas of gene expression patterns in the mouse embryo. *Nucleic Acids Res* 32:D552-556.
- Vogel MW, Sinclair M, Qiu D, Fan H (2000) Purkinje cell fate in staggerer mutants: agenesis versus cell death. *J Neurobiol* 42:323-337.
- Wang W, Lufkin T (2000) The murine *Otp* homeobox gene plays an essential role in the specification of neuronal cell lineages in the developing hypothalamus. *Dev Biol* 227:432-449.
- Webb AB, Angelo N, Huettner JE, Herzog ED (2009) Intrinsic, nondeterministic circadian rhythm generation in identified mammalian neurons. *Proc Natl Acad Sci U S A* 106:16493-16498.
- Yan L, Okamura H (2002) Gradients in the circadian expression of *Per1* and *Per2* genes in the rat suprachiasmatic nucleus. *Eur J Neurosci* 15:1153-1162.

Zhang J, Fuhrmann S, Vetter ML (2008) A nonautonomous role for retinal frizzled-5 in regulating hyaloid vitreous vasculature development. *Invest Ophthalmol Vis Sci* 49:5561-5567.

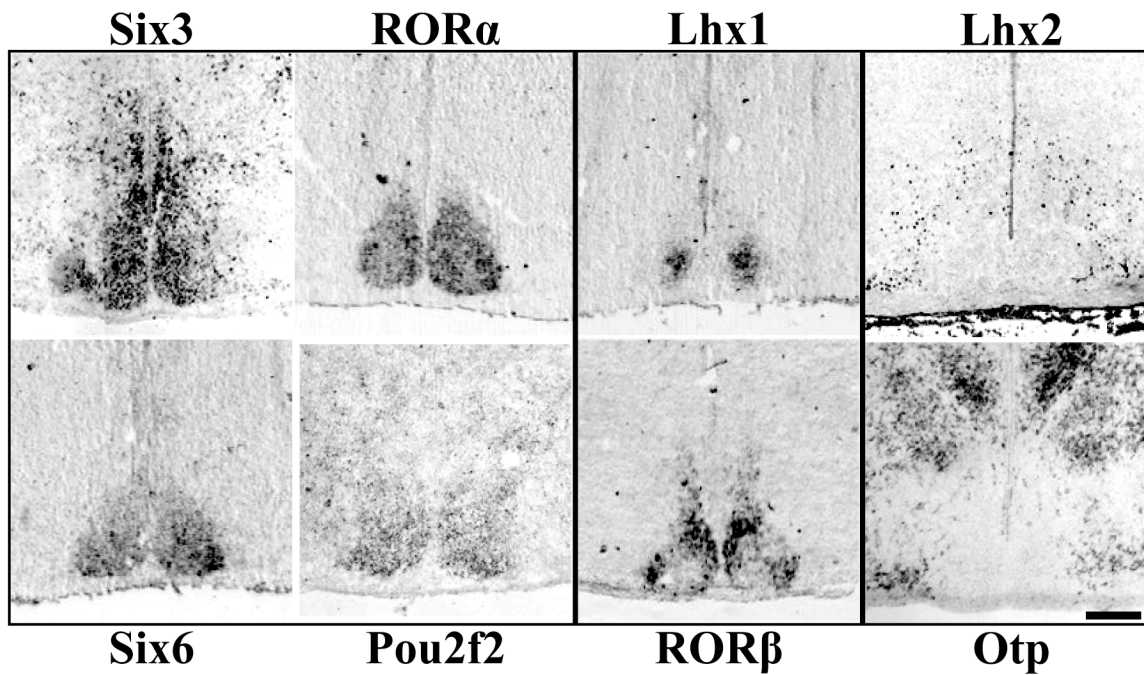


Figure 1. Diverse patterns of transcription factor expression in P0 mouse SCN. Representative ISH and IHC images of mid-SCN coronal sections showing specific expression throughout the entire SCN but not adjacent hypothalamus for Six3, ROR α , Six6, and Pou2f2, but restricted localization within the SCN for Lhx1 and ROR β . Lhx2 and Otp are expressed outside the SCN, indicating a transcription factor boundary. Scale bar, 250 μ m.

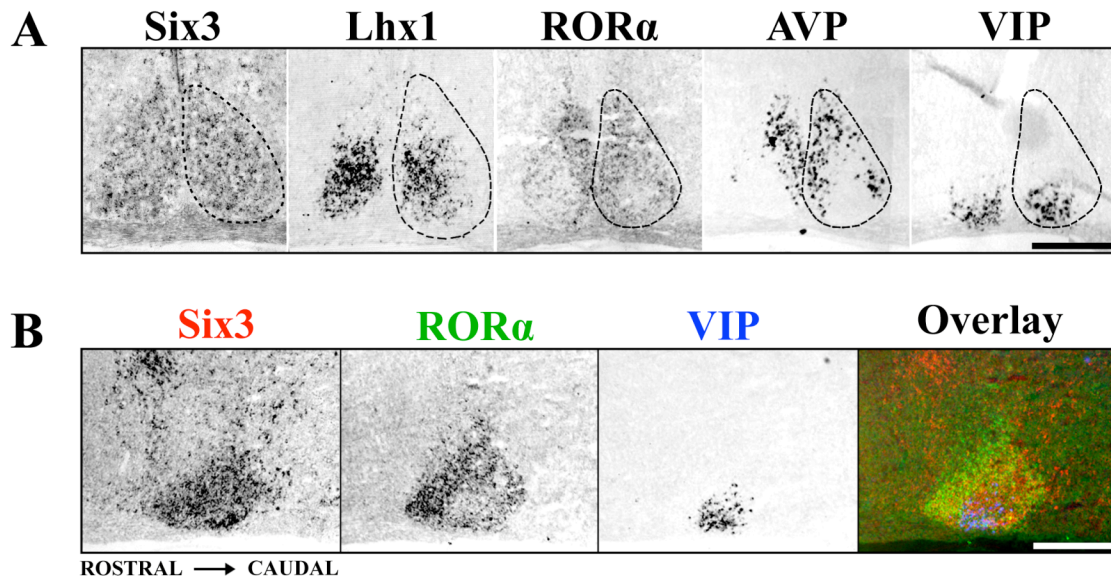


Figure 2. The adolescent mouse SCN shows discrete patterns of transcription factor expression. **A**, Representative ISH images showing localization of *Six3*, *Lhx1*, and *ROR α* expression within coronal sections of mid-SCN at P15. Note the discrete localization of *ROR α* to a region overlapping *AVP* but not *VIP* expression, whereas *Lhx1* overlaps both. Dotted lines indicate the margins of the SCN. **B**, ISH images from adjacent sagittal sections of *Six3* (red), *ROR α* (green), and *VIP* (blue) are overlaid in pseudocolor, showing the full rostral to caudal expression of *Six3* throughout the SCN and the localized absence of *ROR α* from the *VIP*-expressing region. Scale bars, 250 μ m.

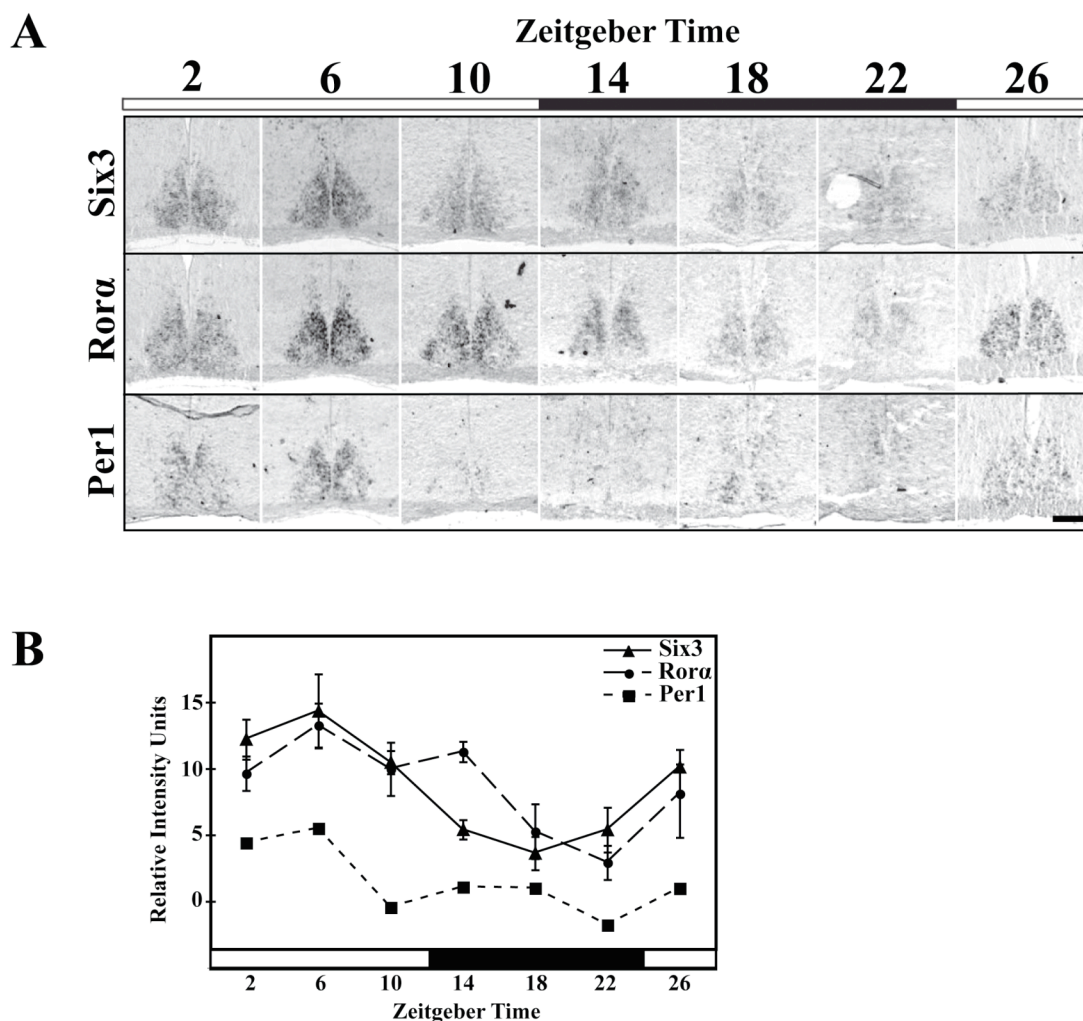


Figure 3. Six3 and ROR α show diurnal variation in expression. **A**, Representative ISH images showing expression of Six3, ROR α , and Per1 mRNA in the coronal mid-SCN in P21–P23 mice raised under a 12 h light/dark cycle and sampled every 4 h (ZT0 indicates lights on). In contrast to Per1 and Six3, ROR α is expressed only in the outer shell region. **B**, Quantification of averaged relative mRNA intensity in arbitrary units for Six3, ROR α , and Per1 over the same 24 h time period, showing diurnal variation for Six3 (one-way ANOVA, $F_{(5,47)} = 10.55$, $p < 0.0001$), ROR α (one-way ANOVA, $F_{(5,47)} = 6.64$, $p = 0.0001$), and Per1 (one-way ANOVA, $F_{(5,21)} = 4.56$, $p = 0.0089$), with peak at ZT6 and trough at ZT22 for ROR α and Per1 and ZT18 for Six3 ($n = 3$). Black bars indicate 12 h of dark. Error bars show SEM. Scale bar, 250 μm .

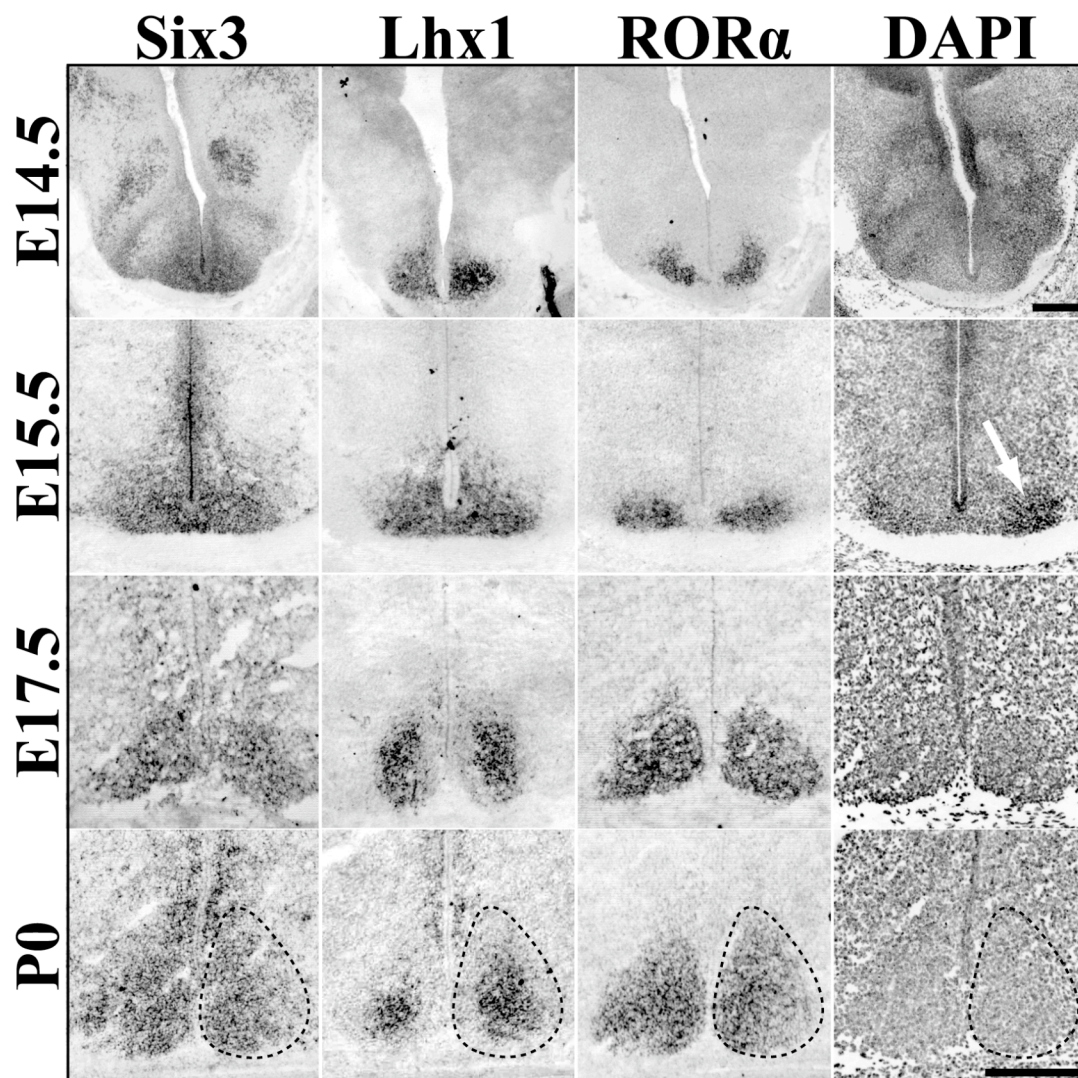


Figure 4. Dynamic transcription factor expression during SCN prenatal maturation. Representative ISH images of *Six3*, *Lhx1*, and *RORα* mRNA expression in the embryonic mouse SCN (E14.5 to P0), showing spatial specificity and prenatal maturation of transcription factor expression. Dotted lines indicate margins of SCN estimated from the cell density marker DAPI (example shown in rightmost panels). White arrow at E15.5 indicates onset of visible clustering of cells. Note change in *Lhx1* pattern from global to centrally restricted between E15.5 and P0. E17.5 *Lhx1* image was obtained from tissue cut at a different angle and thus the appearance of larger SCN compared with *Six3* and *RORα*. Scale bar, 250 μ m.

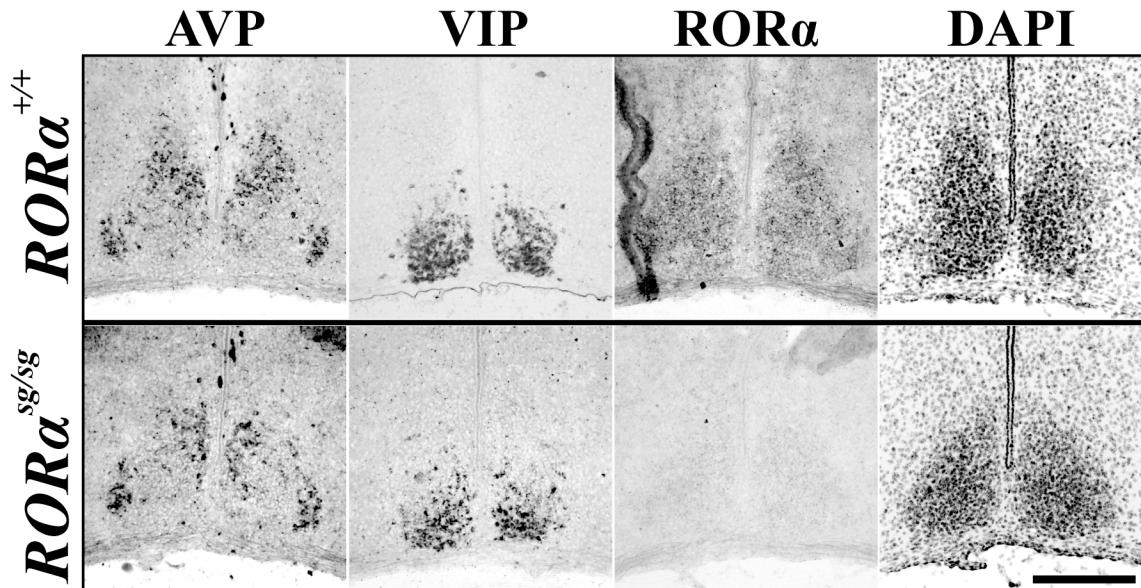


Figure 5. *ROR α* is not necessary for normal SCN peptide localization. Representative ISH images of AVP and VIP mRNA expression, markers of SCN subdivisions, as well as transcription factor *ROR α* and inverted DAPI nuclear stain in P15 *ROR α* mutant (*sg/sg*, bottom) and wild-type littermate (*+/+*, top) mice. Note that segregation of peptidergic expression patterns was similar to littermate control. Scale bar, 250 μ m.

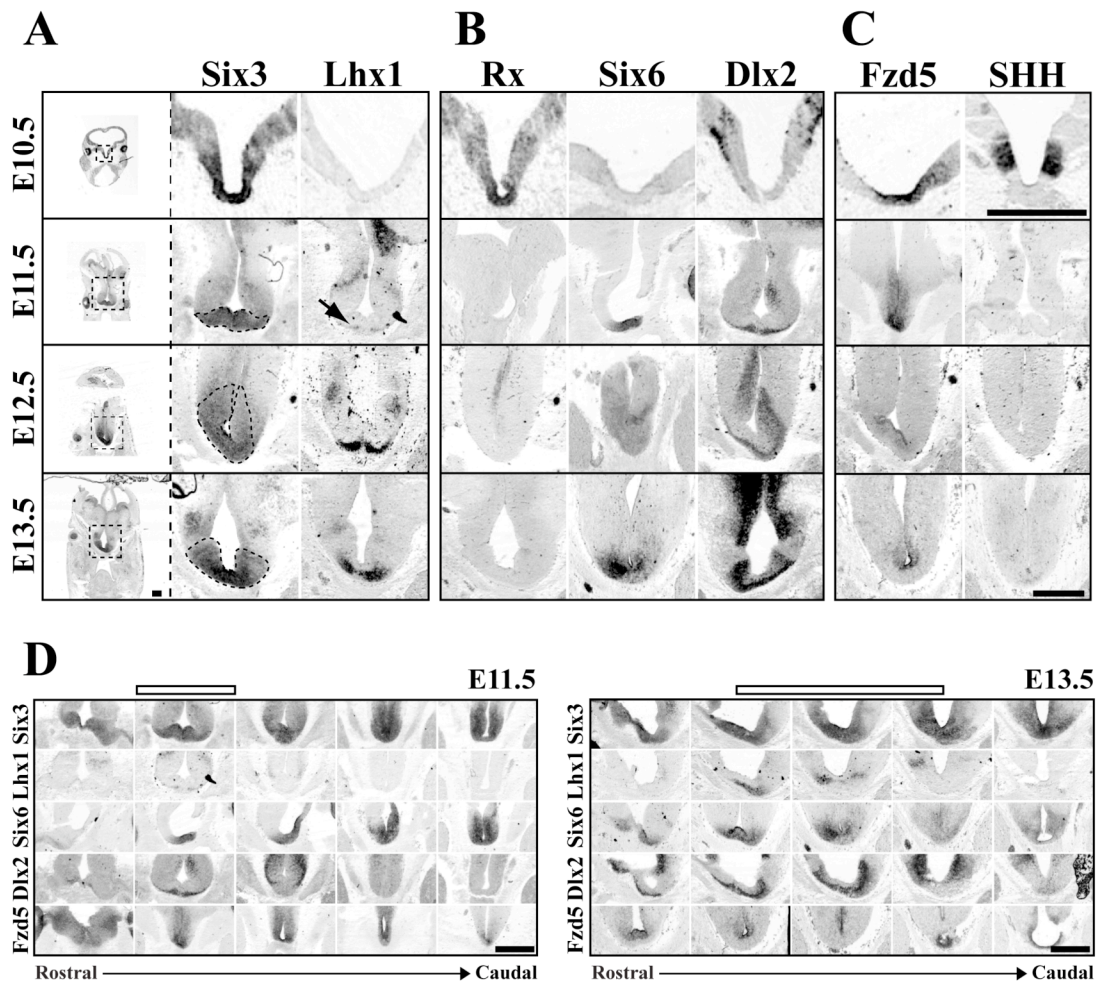


FIGURE 6

Figure 6. SCN is derived from a distinct progenitor domain. Representative images of Six3 and Lhx1 (*A*), Rx, Six6, and Dlx2 (*B*), and Fzd5 and SHH (*C*) mRNA expression (columns) in SCN progenitor domain from E10.5 to E13.5 (rows). Leftmost column shows entire coronal section, with dotted box indicating approximate region of enlarged images in corresponding row to the right. Dotted black lines in enlarged Six3 images indicate hypothesized early SCN margins outlined by Six3 expression from E11.5 to E13.5. Note at E10.5 that the region that will give rise to SCN neurons expresses a combination of Six3, Rx, and Fzd5. By E11.5, Rx expression is lost and Six6 expression begins. Also note the E11.5 onset of Lhx1 (black arrow) and Dlx2 on the most ventral aspects of tissue beneath the third ventricle. Scale bar, 500 μm . *D*, Rostrocaudal location of SCN progenitor domain. ISH images depict patterns of Six3, Lhx1, Six6, Dlx2, and Fzd5 mRNA expression (rows) in transverse plane from rostral eye fields to caudal developing pituitary at E11.5 and E13.5. Open bars above indicate the developing SCN within the rostrocaudal axis. Note that, although expression of Six3 and Six6 is consistent along the ventral surface from rostral eye fields to the early pituitary, Lhx1 and Dlx2 mark discrete zones within this region at both E11.5 and E13.5. Please note in *D* that E11.5 depicts same transverse images as shown in *A–C*, and E13.5 shows the same Six6 and Fzd5 images shown in *A–C* now within the rostrocaudal context of the developing brain. Scale bar, 500 μm .

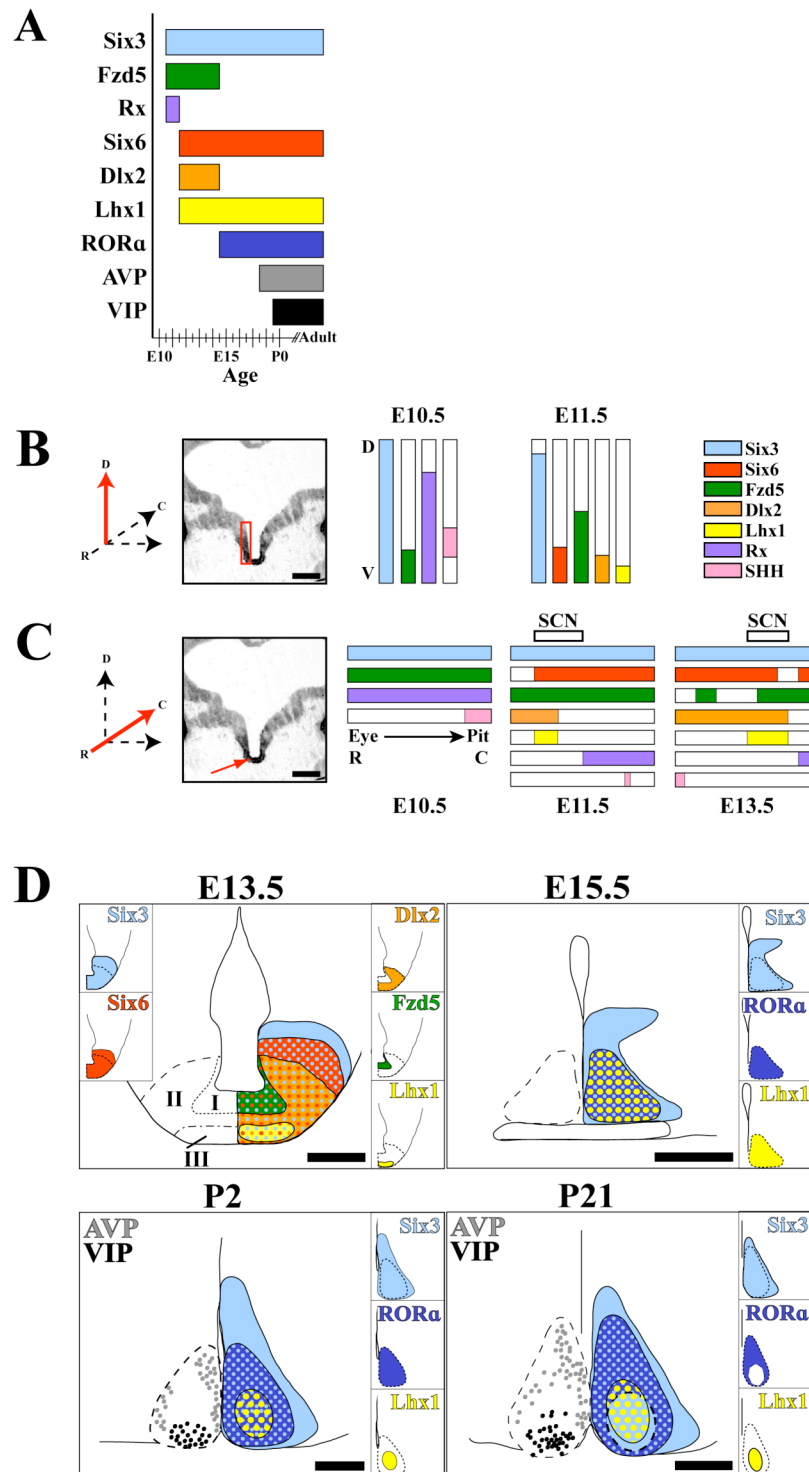


FIGURE 7

Figure 7. Summary of SCN development. **A**, Bar graph indicates onset and duration of transcription factor and peptide mRNA expression from E10.5 to adult in the mouse SCN. **B**, **C**, Diagrams summarize dorsoventral and rostrocaudal extent of developmental gene expression within the early telencephalon/diencephalon containing the hypothesized early SCN. Red arrows on orientation axes show directionality of diagram in relation to indicated red regions. **B**, Summary of dorsoventral (D–V) extent of mRNA expression (colored bars) within the same region of anterior hypothalamus, indicated by red box in image showing *Six3* expression, at E10.5 (left) and E11.5 (middle). Scale bar, 250 μm . Colors correspond to genes in legend (right). Note the absence of *SHH* but presence of *Fzd5* within the ventral most domains, i.e., putative early SCN. **C**, Summary of rostrocaudal (R–C) extent of mRNA expression within the midline (red arrow) of the ventral developing telencephalon/diencephalon at E10.5 (left), E11.5 (middle), and E13.5 (right). Scale bar, 250 μm . The most rostral point is marked by the retina (Eye) and caudal by the developing pituitary (Pit). Colors correspond to genes in legend in **B**. Open top bars at E11.5 and E13.5 indicate rostrocaudal extent of putative SCN progenitor domain within larger developing brain. **D**, Diagrams of SCN transcription factor localization indicate expression during neurogenesis (E13.5), within the prenatal postmitotic (E15.5), early postnatal (P2), and functionally mature SCN (P21). Dotted lines on left indicate the margins of the SCN. Insets indicate expression pattern of individual transcription factors. Colored dots indicate regions of coexpression. Note hypothesized zones of developing SCN at E13.5: I, premitotic/proliferative; II, late-mitotic/early-postmitotic; III, postmitotic. Also note the changes in localization of both *Lhx1* and *ROR α* over time. Scale bars, 250 μm .

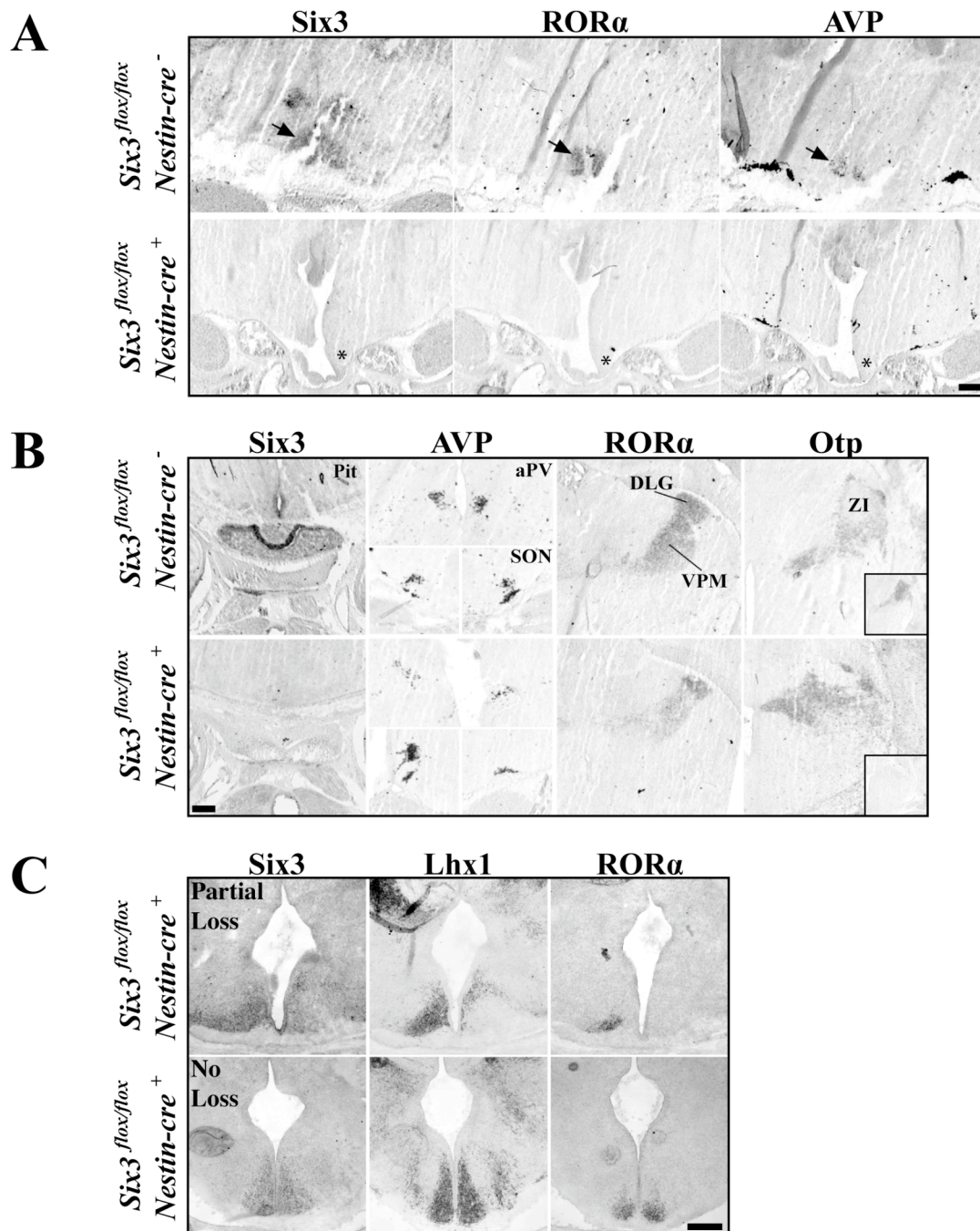


FIGURE 8

Figure 8. Six3 is necessary for SCN formation. Expression of Six3, ROR α , AVP, and Otp in *Six3^{flox/flox}/Nestin-cre⁺* compared with *Six3^{flox/flox}/Nestin-cre⁻* littermate controls. **A**, Expression of Six3, ROR α , and AVP in SCN (arrows in top) are completely eliminated in conditional Six3 knock-outs, shown at E18.5 (asterisks). **B**, Marker analysis of the pituitary, hypothalamic (aPV and SON), and thalamic (dLG, VPM, and ZI) nuclei show that complete disruption of Six3 leads to loss of the pituitary, whereas nuclei surrounding the SCN remain intact in *Six3^{flox/flox}/Nestin-cre⁺* experimental animals. Bottom right inset in Otp column represents adjacent section for Six3 expression. **C**, Variability in the targeted elimination of floxed Six3 in E15.5 mice. Expression of Six3, Lhx1, and ROR α in *Six3^{flox/flox}/Nestin-cre⁺* mice that showed either partial loss (top) or no loss (bottom) of Six3. Top, Unilateral Six3 deletions lead to unilateral loss of ROR α and Lhx1. Bottom, Mice that retain Six3 expression still express both Lhx1 and ROR α . Scale bars, 250 μ m.

Supplemental Table 1. Transcription factors with discrete expression within the mouse SCN at P0.

Gene	Entrez Gene ID	Family	SCN	Potentially in SCN	Boundary	In Situ Verified	Source	ABA E18 Expression Confirmation	ABA Adult Expression Confirmation
Sox2	20674	HMG	X					X	X
Sox5	20678	HMG	X						
Zfhx3	11906	Homeobox	X					X	X
Hmx3	15373	Homeobox	X						
Lhx1	16869	Homeobox	X			X		X	X
Six3	20473	Homeobox	X			X		X	
Six6*	20476	Homeobox	X			X	Jean et al., 1999		
Vax1	22326	Homeobox	X						X
Rora	19883	Nucrec	X			X		X	X
Rorb*	225998	Nucrec	X			X	Schaeren-Wiemers et al., 1997	X	X
Nr4a1	15370	Nucrec	X					X	X
Pou2f2*	18987	Pou	X			X	Rivkees et al., 1992	X	
Peg3	18616	ZN C2H2	X						
Tef12	21406	bHLH		X					
Olig2	50913	bHLH		X					
Sox14	20669	HMG		X					
Dlx2	13392	Homeobox		X				X	X
Dlx5	13395	Homeobox		X					
Lhx9	16876	Homeobox		X					
Sox4	20677	HMG			X			X	
Dlx1	13390	Homeobox			X			X	
Isl1	16392	Homeobox			X			X	X
Lhx2*	16870	Homeobox				X	Menger et al., 2005	X	
Lhx5	16873	Homeobox			X			X	
Lhx8	16875	Homeobox			X			X	
Otp	18420	Homeobox			X	X		X	
Pbx3	18516	Homeobox			X			X	
Nr2f2	11819	Nucrec			X			X	

List of 28 transcription factors identified as within, potentially within, or directly adjacent to the postnatal mouse SCN obtained from re-examination of a genome-scale transcription factor expression database (Gray et al., 2004) and other published work (*Rivkees et al., 1992; Schaeren-Wiemers et al., 1997; Jean et al., 1999; Menger et al., 2005). Genes highlighted in grey were further assessed for precise expression within the SCN region. The last two columns represent those genes whose expression was further confirmed in the Allen Brain Atlas either E18 (ABA E18) or Adult (ABA Adult) (Lein et al., 2007). bHLH – basic helix-loop-helix, HMG – high mobility group, Nucrec – nuclear receptor, ZN-Zinc finger type C2H2.

Supplemental Table 2. Transcription factors with discrete mRNA expression within the mouse anterior hypothalamus at E13.5.

Gene	Entrez Gene ID	Family	Anterior Hypothalamus	Boundary	In Situ Verified	Source	Database Expression Confirmation
Npas1	18142	bHLH	X				
Olig2	50913	bHLH	X				X
Baz2a	116848	Bromo	X				X
Baz2b	227940	Bromo	X				
Smarcc1	20588	Bromo	X				
Smarcd3	66993	Bromo	X				
FoxD3	15221	Forkhead	X				
FoxO1	56458	Forkhead	X				
Foxp4	74123	Forkhead	X				X
Hmgb1	15289	HMG	X				X
Hmgb2	97165	HMG	X				X
Sox21	223227	HMG	X				X
Sox4	20677	HMG	X				
Sox5	20678	HMG	X				X
Tef712	21416	HMG	X				X
Atbf1	11906	Homeobox	X				X
Dlx1	13390	Homeobox	X				X
Dlx2	13392	Homeobox	X		X		X
Dlx5	13395	Homeobox	X				X
Hes1	15205	Homeobox	X				X
Hmx2*	15372	Homeobox	X			Wang and Lufkin, 2000	X
Hmx3	15373	Homeobox	X				
HoxD3	15434	Homeobox	X				
Lhx1	16869	Homeobox	X		X		X
Lhx2	16870	Homeobox	X				X
Lhx4	16872	Homeobox	X				
Nkx2.1	21869	Homeobox	X				X
Six3	20473	Homeobox	X		X		X
Six6*	20476	Homeobox	X		X	Jean et al., 1999	X

Supplemental Table 2 (Con't). Transcription factors with discrete mRNA expression within the mouse anterior hypothalamus at E13.5.

Gene	Entrez Gene ID	Family	Anterior Hypothalamus	Boundary	In Situ Verified	Source	Database Expression Confirmation
Tcf2	21410	Homeobox	X				
Vax1	22326	Homeobox	X				X
Crip2	68337	LIM	X				X
Csrp2	13008	LIM	X				
Lmo4	16911	LIM	X				X
Zyx	22793	LIM	X				
Nr1h2	22260	Nucrec	X				X
Rxra	20181	Nucrec	X				
Nr2e1	21907	Nucrec	X				X
Pou2f2	18987	Pou	X		X		X
Rfx3	19726	RFX	X				X
Peg3	18616	ZN C2H2	X				X
Zic3	22773	ZN C2H2	X				X
Zic4	22774	ZN C2H2	X				
Chd4	107932	ZN PHD	X				
Sim1	20464	bHLH		X			
Baz1b	22385	Bromo		X			X
Cited1	12705	Cited		X			X
Dlx6	13396	Homeobox		X			X
Isl1	16392	Homeobox		X			X
Lhx5	16873	Homeobox		X			X
Otp	18420	Homeobox		X	X		X
Lmo1	109594	LIM		X			X
Rxrg	20183	Nucrec		X			
Nr2f2	11819	Nucrec		X			X
Pou3f1	18991	Pou		X			X
Pou3f2	18992	Pou		X			
Stat5A	20850	Stat		X			
Zdhhc2	70546	ZN DHHC		X			X

List of 58 transcription factors identified as within or directly adjacent to the SCN obtained from re-examination of a genome-scale transcription factor expression database (Gray et al., 2004) and other published work (*Jean et al., 1999; Wang and Lufkin, 2000). Genes highlighted in grey were further assessed for precise expression within the SCN region. The last column represents those genes whose expression was further confirmed using either Genepaint (Visel et al., 2004) or Eurexpress (Diez-Roux et al., 2011). bHLH – basic helix-loop-helix, Bromo - Bromodomain, CITED – CREB-binding protein/p300-interacting transactivator with ED-rich tail HMG – high mobility group, Forkhead – Forkhead box, Nucrec – nuclear receptor, RFX – Regulatory factor X, STAT – signal transducer and activator of transcription, ZN C2H2 – Zinc finger type C2H2, ZN DHHC – Zinc finger DHHC domain-containing.

-CHAPTER 3-

**Role of retinal innervation and vasoactive intestinal polypeptide
signaling in mouse suprachiasmatic nuclei development**

Abstract

The suprachiasmatic nuclei (SCN) can be both anatomically and functionally subdivided. It is unknown whether these subdivisions represent intrinsic genetic differences within cells or if they are induced through SCN maturation. Herein, we utilize mouse models that lack either *Atoh7*, necessary for retinal ganglion cell development, functional vasoactive intestinal polypeptide (VIP), or VIP receptor 2 (VPAC₂, *Vipr2*) to test for the affects of two salient aspects of the circadian system in shaping SCN development. We found the size and location of the SCN to be unaffected by the absence of retinal innervation. In addition, animals lacking retinal innervation maintain localization in expression of *Six3*, *Lhx1*, and *Rora*, three transcription factors that mark the SCN. We found loss of VIP/VPAC₂ signaling had minimal effects on SCN size. Further, localization and expression levels of both *Six3* and *Lhx1* are maintained within animals kept under 12 h light/dark, while the expression of *Rora* became more consistent between SCN subdivisions. VIP and VPAC₂ mutant animals kept in constant darkness displayed greatly reduced levels of *Rora* while maintaining levels of *Six3* expression as compared to C57BL/6 controls. Despite reductions in the total levels of *Rora*, differences in expression between dorsal and ventral regions of the SCN remained, albeit to a lesser extent. The absolute difference between levels of *Rora* in SCN subdivisions does not correlate with behavioral rhythmicity in animals lacking VIP/VPAC₂ signaling. We conclude that maturational changes in the localization of transcription factors within the SCN occur independent of retinal innervation and VIP signaling and may reflect more intrinsic differences in subsets of neurons within the nuclei.

Introduction

Activity in the form of sensory stimuli, spontaneous activity, and neurotransmitter signaling has been shown to shape brain development (for review (Gu, 2002; Grubb and Thompson, 2004; Huberman et al., 2008; Butz et al., 2009). In the circadian system, ~20,000 neurons comprise the suprachiasmatic nuclei (SCN) that are responsible for producing and coordinating near 24 h rhythms for the entire body and entraining these rhythms to external stimuli. Two of the most salient aspects of the circadian system are retinal input, for daily and seasonal entrainment, and vasoactive intestinal polypeptide (VIP) signaling, for synchronization of individually oscillating cells (Aton et al., 2005). How these activity signals contribute to shaping the anatomical and functional development of the SCN is unknown.

The SCN undergoes modifications and refinements of its gene expression through development. Peptides, whose expression is known to distinguish two classic subdivisions of the SCN, core and shell, are localized to their corresponding regions from their onset (VanDunk et al., 2011). Unlike peptide expression, the adult localization of transcription factor (TF) expression occurs gradually and loosely correlates with SCN maturational time points. Specifically, *Lhx1* (Lim homeobox protein 1) expression becomes centralized within the SCN during the same perinatal period as peptide mRNA expression begins, approximately embryonic day 17.5 (E17.5) (VanDunk et al., 2011). In addition, expression of *Rora* (Retinoic orphan receptor alpha) becomes regionalized to the SCN shell concurrent with the increase in retinal innervation within the SCN as well

as an increase in the number of cells expressing VIP (approximately postnatal day seven to twenty-one (P7-P21)). The temporal expression patterns of immediate early genes *c-fos* and *pERK*, and well studied clock genes *Per1* and *Per2* in several species have pointed to at least two functionally distinct regions within the SCN: one of endogenous rhythmicity (shell) roughly correlating with areas of vasopressin expression and one of induced rhythms (core) roughly correlating with areas expressing VIP, gastrin-releasing peptide, or calbindin (mouse, rat: (Sumova et al., 1998; Guido et al., 1999; Hamada et al., 2001; Yan and Okamura, 2002; Ramanathan et al., 2006); hamsters: (Silver et al., 1996; Hamada et al., 2004)). The gradual localization of gene expression along with the presence of functionally distinct SCN subdivisions leads to questions of whether these changes and differential subdivision functions are intrinsic to the cells themselves or if they are induced.

Through sensory experience and early spontaneous waves of neural firing, retinal innervation and activity have been shown to shape adult patterns of connectivity and patterning in the formation of ocular dominance columns and lateral geniculate nucleus layer segregation, respectively (for review (Sengpiel and Kind, 2002; Del Rio and Feller, 2006)). Furthermore, neurotransmitters such as acetylcholine and serotonin aid in neurodevelopment by promoting cortical plasticity (for review (Gu, 2002)). Both modulation of sensory experience, loss of retinal inputs, and loss of VIP have been shown to impact circadian function. Light information entering the retina is processed by retinal ganglion cells which then transmit the photic and non-photoc information to several brain

regions, including the SCN by way of the retinohypothalamic tract. Both unilateral and bilateral enucleation in adult rats can lead to changes in the number of cells in the SCN expressing VIP (Holtzman et al., 1989; Okamoto et al., 1990; Laemle and Rusa, 1992; Denis et al., 1993). Moreover, enucleation in both rats and hamsters has revealed retinal innervation necessary for oscillations in pERK normally found within the core of the SCN (Lee et al., 2003). In addition, rearing animals under various photoperiods has a direct consequence on the establishment of free-running period both at the single cell and behavioral level (Ohta et al., 2006; Ciarleglio et al., 2011). In the circadian system loss of a principal neurotransmitter, VIP, leads to desynchronization of the individually oscillating cells (Aton et al., 2005). Thus, animals deficient in either VIP or VPAC₂ display altered behavioral rhythms, with most animals unable to maintain a normal single statistically significant circadian period (Harmar et al., 2002; Colwell et al., 2003). Currently, it is unknown whether retinal innervation or peptide signaling have a role in shaping SCN gene expression and/or cellular functioning.

Herein, we utilize complimentary genetic models to investigate the role of two critical circadian components in shaping the development of the SCN. Specifically, we monitor the localization of TF expression in mouse models that lack either *Atoh7*, necessary for retinal ganglion cell development, or functional VIP peptide or VIP receptor 2 (VPAC₂, *Vipr2*). Understanding if retinal activity or signaling pathways contribute to changes in expression of SCN-specific TFs will help us gain insight into how functional subdivisions and ultimately the functional SCN network is formed.

Materials and Methods

Animals and housing. Male and female wild-type C57BL/6 (Charles River), Vip^{-/-} (Colwell et al., 2003) (founders provided by Dr. Chris Colwell, UCLA), Vipr2^{-/-} (Harmar et al., 2002) (founders provided by Chris Colwell, UCLA), and Atoh7Cre (Yang et al., 2003) (Susan Culican, Washington University in St. Louis) mice were used. Mice were maintained in a normal 12 h light/dark schedule under standard care conditions. Mutant animals were maintained on a C57BL/6 background (Charles River). All experiments were approved by the Animal Studies Committee at Washington University and followed NIH guidelines.

Genotyping: Mice were genotyped by PCR for presence of Atoh7, Vip, Vipr2 and/or wild-type alleles as previously described (Wee et al., 2002; Colwell et al., 2003), or as outlined by The Jackson Laboratory. The presence of Cre was determined by the presence or absence of an amplified band as previously described (VanDunk et al., 2011).

Tissue acquisition. Unless otherwise stated, all collections were done at approximately zeitgeber time (ZT) 8. Neonatal pups (P0-P2) from timed pregnant females (morning of plug = E0.5) were anesthetized on ice and transcardially perfused with 4% paraformaldehyde (PFA) in 0.1 M PBS, pH 7.4. Older mice were anesthetized with a ketamine/xylazine mixture before perfusion with 0.9% saline followed by 4% PFA. All tissues were post fixed in 4% PFA overnight at 4°C, cryoprotected in 20% sucrose in

PBS, frozen in O.C.T. Compound Embedding Medium (Tissue-Tek), and stored at -75°C. Serial sections (20µm) were cut on a Hacker cryostat and thaw mounted on Superfrost Plus slides (Thermo Fisher Scientific). Five adjacent sets of sections were prepared from each postnatal age and stored at -20°C.

Probe synthesis. Plasmids for *in situ* hybridization probes were acquired from published sources (Gray et al., 2004; Burns et al., 2008; Zhang et al., 2008) or purchased from Open Biosystems. Gene fragments from verified plasmids were linearized by direct amplification by sequence or vector-specific PCR. Digoxigenin (DIG)-labeled anti-sense and sense RNA probes were made using PCR products as template and T7, T3, or SP6 RNA polymerases (Roche). cRNA probes were purified using Quick Spin columns (Roche) and quantified by spectrophotometry. Probes were used at a concentration of 1-2 µg/ml. Sense counterparts of all probes were tested to ensure probe specificity.

In situ hybridization. Slides were immersed in 4% PFA, permeabilized with proteinase K, returned to 4% PFA before being washed in 0.1 M triethanolamine-HCl with 0.25% acetic anhydride. Once blocked in hybridization buffer at 65°C slides were incubated in hybridization buffer containing 1-2 µg/ml DIG-labeled anti-sense cRNA overnight at 65°C. Slides were then washed in 2XSSC buffer at 62°C, washed in 0.2XSSC at 65°C, blocked with 10% normal horse serum (NHS) in 0.1M PBS, and incubated in alkaline phosphatase labeled anti-DIG antibody (1:2000 in 10% NHS; Roche) overnight. Sections

were washed and color was visualized using Nitro blue tetrazolium and 5-Bromo-4-chloro-3-indolyl phosphate (Roche). Staining was stopped after visual inspection. Sections were washed, fixed in 4% PFA, and coverslipped in 90% glycerol, Vectashield Mounting Medium (Vector Laboratories), or UltraCruz Mounting Media with DAPI (Santa Cruz Biotechnology).

Image acquisition. Images were acquired using a Nikon Eclipse 90i microscope, Photometrics Coolsnap HQ2 camera with a Prior Scientific ProScan II motorized translation stage, and acquired in Volocity (PerkinElmer Life and Analytical Sciences). Images were exported as 8bit JPEG or TIFF files. All images were adjusted for clarity by filtering and/or modifying levels, as necessary, in Photoshop (Adobe Systems). To improve aesthetics of images, non-tissue backgrounds were processed to exclude debris.

mRNA quantification and analysis. The most mid-SCN coronal section for each brain was selected for gene expression quantifications by assessing rostral to caudal location as well as section with the greatest area. Percentage of SCN area containing gene expression was calculated by dividing area expressing mRNA by the total estimated SCN area marked with DAPI, where area was calculated by outlining regions of interest within NIH ImageJ. Whole SCN quantifications of mRNA expression were performed by quantifying intensity of staining relative to background from 10x ISH images using NIH ImageJ and are reported in arbitrary intensity units (AIUs). Margins of the SCN were determined by

cell density marked with DAPI nuclear stain. Subdivision specific measurements were made by first outlining the total SCN area as marked by DAPI stain. Areas within the dorsal or ventral SCN were sampled as representative of either shell or core subdivisions, respectively. The sample for ventral SCN was obtained from an area representing the bottom 1/3 and middle half of each individual nucleus. Within NIH ImageJ a ROI ellipse was drawn within the ventrally isolated region and measured, the same ROI circle was then placed within the dorsal SCN and a representative shell measurement was taken. Absolute intensity differences between SCN subdivisions were calculated by taking dorsal values minus ventral values. For all statistics and values listed in tables, left and right SCN nuclei from each animal were tested as individual samples, thus one brain produced two samples. The differences were analyzed using Student's unpaired *t* test.

General SCN morphology was assessed by obtaining outlines drawn based on cellular density marked with nuclear DAPI stain and measuring individual nuclei for mid-SCN width, area, and cell density. Rostral to caudal length of the nuclei was calculated by counting the number of sections containing Rora staining and estimating length based on section thickness.

Behavioral recording. Adult (P30+) *Vipr2*^{-/-} (n=9), *Vip*^{-/-} (n=9), and C57BL/6 mice (n=4) were housed individually in cages equipped with running wheels and maintained in light-tight chambers illuminated with fluorescent bulbs ($2.4 \pm 0.5 \times 10^{18}$ photons s⁻¹ m⁻²; General Electric). Running wheel activity was recorded in 6 min bins (Clocklab,

Actimetrics) during 6 days in 12 h light/dark and then during 9 days in constant darkness. Animals were collected at a projected CT6/8 based on individual locomotor periodicities. All animals were enucleated under red light before perfusion.

Analysis of Behavioral Rhythmicity. Behavioral rhythmicity was analyzed as described by Aton and colleagues (Aton et al., 2005). Designations for rhythmic behavioral categories were made in the following manner: rhythmic (single statistically significant period), polyrhythmic (two or more significant periods), or arrhythmic (no significant period).

Results

Effects of retinal innervation on SCN transcription factor expression

Morphological Analysis

Several methods have been used in the past to address the role of retinal activity in the development of the SCN. Enucleation and use of a naturally occurring anophthalmic mouse have produced varying effects on gross anatomical SCN development ranging from rostral displacement of nuclei (bilateral enucleation, (Nagai et al., 1992)), to severe loss in cell numbers and unilateral loss of nuclei (anophthalmic, (Silver, 1977); microphthalmic, (Tokunaga et al., 1997)). However, anophthalmic mice have a mutation in the early patterning gene, *Rx*, necessary for the formation of not only the eye but also components of forebrain (Mathers et al., 1997) which may produce additional effects leading to morphological changes. In order to understand the developmental role of retinal innervation in shaping the SCN we took advantage of a mouse deficient in a key TF expressed almost exclusively in the retina and necessary for ganglion cell development, *Atoh7* (also termed *Math5*) (Wang et al., 2001). *Atoh7* knock-out (*Atoh7*^{-/-}) mice lack ~80% of retinal ganglion cells and fail to form both the optic and retinohypothalamic tracts (RHT). Lack of retinal input renders these animals unable to entrain to light and to have a slightly increased circadian period (Wee et al., 2002). *Atoh7* knock-outs and heterozygous littermates were kept on a 12 h light/dark cycle (LD) and sampled at mid-day on postnatal days two (P2; *Atoh7*^{+/-} (n=2), *Atoh7*^{-/-} (n=3)) and 21-25

(P21-P25; *Atoh7*^{+/-} (n=4), *Atoh7*^{-/-} (n=8)). In this manner both initial formation of the SCN, the subsequent increase in nuclei size, and general morphology could be assessed.

The SCN was easily recognized as bilateral densely packed clusters of cells on either side of the third ventricle in all animals assessed (Figure 1). Further, general rostrocaudal location (data not shown), coronal mid-SCN area, and rostral to caudal length of the SCN were similar between *Atoh7*^{+/-} and *Atoh7*^{-/-} animals at both P2 and P21-P25 (Table 1). In addition, density of cells within the P21-P25 mid-coronal SCN of *Atoh7*^{-/-} animals was similar to *Atoh7*^{+/-} littermates (Table 1). In summary, we find retinal innervation is not necessary for SCN localization, proliferation, or rostral to caudal nucleus expansion.

In situ hybridization Analysis

To examine the effects of retinal innervation on maturation of the SCN, *Atoh7*^{+/-} and *Atoh7*^{-/-} mice at both P2 and P21-P25 were assessed for whole SCN expression and localization of *Six3*, *Lhx1*, and *Rora*. Overall, we found maturation of *Lhx1* and *Rora* patterns of expression within the SCN occur independent of retinal innervation (Figure 2). The pan-SCN localization and level of *Six3* expression was maintained in P2 and P21-P25 *Atoh7*^{-/-} mice as compared to *Atoh7*^{+/-} and was not statistically different (P2: *Atoh7*^{+/-}, 29.6 ± 0.95 AIU, *Atoh7*^{-/-}, 36.6 ± 4.25 AIU; $p=0.164$; P21-P25: *Atoh7*^{+/-}, 28.92 ± 2.77 AIU, *Atoh7*^{-/-}, 25.18 ± 2.07 AIU; $p=0.299$) (P2, Figure 2A; P21-P25, Figure 2B).

Localization of Lhx1 to the central SCN was seen in *Atoh7* knock-out animals at both P2 and P21-P25, but the percentage of SCN expressing Lhx1 was reduced in comparison to *Atoh7* heterozygotes (P2: *Atoh7*^{+/-}, 33.04 ± 1.9%, *Atoh7*^{-/-}, 24.358 ± 4.03%; *p*=0.022; P21-P25: *Atoh7*^{+/-}, 34.84 ± 1.96%, *Atoh7*^{-/-} 29.09 ± 2.88%; *p*=0.029) (P2, Figure 2A; P21-P25, Figure 2B). Whole SCN levels of Lhx1 remained similar between *Atoh7*^{+/-} and *Atoh7*^{-/-} animals (P2: *Atoh7*^{+/-}, 13.36 ± 3.06 AIU, *Atoh7*^{-/-} 6.63 ± 3.93 AIU; *p*=0.09; P21-P25: *Atoh7*^{+/-}, 9.48 ± 1.38 AIU, *Atoh7*^{-/-} 6.91 ± 2.25 AIU; *p*=0.18).

Whole SCN levels of *Rora* expression in P2 *Atoh7*^{-/-} mice were consistent with *Atoh7*^{+/-} mice (*Atoh7*^{+/-}, 17.6 ± 0.68 AIU, *Atoh7*^{-/-} 21.75 ± 3.6 AIU; *p*=0.306). However, at P21-P25 *Atoh7* knock-outs displayed a reduction in whole SCN levels of *Rora* (*Atoh7*^{+/-}, 33.07 ± 2.00 AIU, *Atoh7*^{-/-} 19.52 ± 2.70 AIU; *p*=0.001) (P2, Figure 2A; P21-P25, Figure 2B). To specifically address the localization of *Rora* to the SCN shell the absolute intensity difference between dorsal and ventral SCN were quantified and compared between *Atoh7*^{+/-} and *Atoh7*^{-/-} mice (see methods). We find that the absolute intensity differences between dorsal and ventral levels of *Rora* are comparable to heterozygous controls for two of eight *Atoh7* knock-outs tested (Figure 2B). This suggests that in the absence of retinal innervation the localization of *Rora* and Lhx1 mRNA can be achieved.

Effects of VIP/VPAC₂ signaling on SCN transcription factor expression

Disassociated SCN cultures from mice lacking VIP show that individual cells become desynchronized with one another and can re-synchronize with bath application of a *Vipr2* agonist (Aton et al., 2005). Further, animals deficient in VIP or VPAC₂ and kept in constant darkness (DD) display a range of behavioral phenotypes. The behavioral inconsistencies are thought to be a consequence of lower coherence of individually oscillating cells leading to lower amplitude network oscillations (Ciarleglio et al., 2009). It is not known whether VIP/ VPAC₂ signaling plays a role in the development of the SCN in addition to acting as a synchronizing agent. Recent research suggests VIP and VPAC₂ may have a role in the regulation of gating of cellular response to light. The absence of VIP and VPAC₂ shifts the time of day in which cells of the SCN can respond to a light pulse, from being gated only during subjective night periods to responding to light pulses given both during subjective day and subjective night (Hughes et al., 2004; Dragich et al., 2010). Thus, it is possible that the onset of VIP expression or VIP signaling may elicit changes in single cells altering cellular properties and ultimately changing functionality or inducing expression of specific TFs.

Morphological Analysis

We find that the SCN remain present as bilateral nuclei and in similar rostrocaudal locations in animals either lacking VIP or VPAC₂ when compared to C57BL/6 (Wt) controls. *Vip*^{-/-} and *Vipr2*^{-/-} animals displayed similar rostral to caudal

SCN length, mid-SCN width, and cell density; however a reduction in mid-SCN area was observed in both $Vip^{-/-}$ and $Vipr2^{-/-}$ animals when compared to Wt (Figure 3, Table 2).

In situ hybridization Analysis

The role of intrinsic peptide activity in SCN development was assessed by examination of $Vip^{-/-}$ and $Vipr2^{-/-}$ mice under LD (collected at ZT8) and DD (collected at projected CT6) conditions. Tissue was examined for the expression and localization of *Rora* and *Six3* under both light conditions, and *Lhx1* under LD.

LD

$Vip^{-/-}$ (n=5) animals maintained in LD show levels of *Six3* gene expression similar to that of $Vip^{+/-}$ littermates (n=2) (12.658 ± 1.039 and 13.53 ± 1.481 respectively, $p=0.201$) (Figure 4A). In addition, there were no changes in the whole SCN level of *Lhx1* expression or percentage of SCN expressing *Lhx1* (Figure 4A). Whole SCN levels of *Rora* were also found comparable between $Vip^{-/-}$ and $Vip^{+/-}$ ($Vip^{-/-}$, 14.222 ± 1.246 ; $Vip^{+/-}$, 20.324 ± 3.72 ; $p=0.638$) animals. The absolute intensity difference between *Rora* levels in the dorsal and ventral SCN were reduced in both $Vip^{+/-}$ and $Vip^{-/-}$ mice as compared to values obtained from Wt animals kept in LD (Previous observations). No difference was seen in the absolute intensity differences of *Rora* in SCN subdivisions between $Vip^{+/-}$ and $Vip^{-/-}$ animals (Figure 4A).

DD

Expression of *Six3* was unaffected in VIP/VPAC₂ signaling mutants kept in DD when compared to Wt, (Wt, 19.93 ± 1.18 AIU; *Vip*^{-/-}, 19.36 ± 1.03 AIU, $p=0.788$; *Vipr2*^{-/-}, 19.18 ± 0.92 AIU, $p=0.875$). However, *Vip*^{-/-} and *Vipr2*^{-/-} animals displayed significantly reduced whole SCN levels of *Rora* (Wt, 25.47 ± 1.77 AIU; *Vip*^{-/-}, 15.36 ± 0.58 AIU, $p=0.005$; *Vipr2*^{-/-}, 15.47 ± 0.92 AIU, $p=0.008$). There were no significant differences between levels of whole SCN *Rora* in *Vip*^{-/-} compared to *Vipr2*^{-/-} mice, suggesting that either method of disrupting signaling reduces the total expression of *Rora* at CT6/8.

Wild-type animals displayed large absolute intensity differences in expression of *Rora* between SCN subdivisions (10.73 ± 2.2 AID). Reduced whole SCN levels of *Rora* represented reductions in both ventral and dorsal levels in both VIP and VPAC₂ mutants. Despite these reductions, differences between levels of *Rora* in dorsal and ventral regions of the SCN remained with higher levels in the dorsal SCN maintained, albeit to a lesser extent (*Vip*^{-/-}, 2.4 ± 0.5 AID; *Vipr2*^{-/-}, 6.66 ± 1.4 AID).

It is currently unknown whether the regionalization of *Rora* to the shell of the SCN, leading to higher levels of *Rora* in the dorsal than in the ventral SCN, is necessary for behavioral rhythmicity. *Vip*^{-/-} and *Vipr2*^{-/-} animals kept in DD show variability in their ability to produce free-running locomotor rhythms. Behavioral variations include animals with a single, slightly shortened locomotor circadian period, presence of two or more circadian periods, and some mice which are completely arrhythmic (Harmar et al., 2002;

Colwell et al., 2003; Hughes and Piggins, 2008). It is currently unknown whether there are intrinsic differences between animals deficient in either VIP or VPAC₂ that are able to retain a single period and those that are incapable of producing a single stable rhythm.

To address whether localization or abundance of Rora expression and behavioral phenotype were correlated we analyzed behaviorally segregated Vip^{-/-} and Vipr2^{-/-} animals. Free-running behavior was observed over a period of nine days in DD after which each animal was assigned as rhythmic (single statistically significant period), polyrhythmic (two or more significant periods), or arrhythmic (no significant period). Behavioral segregation yielded Vip^{-/-} and Vipr2^{-/-} animals within each category (Vip^{-/-}: 4 Rhythmic, 1 Polyrhythmic, 3 Arrhythmic; Vipr2^{-/-}: 1 Rhythmic, 3 Polyrhythmic, 4 Arrhythmic) (Vip^{-/-} Figure 5A, Vipr2^{-/-} Figure 5B). We found that regardless of their behavioral rhythmicity, all VIP and VPAC₂ mutant groups differed significantly from Wt in whole SCN levels of Rora. There was no correlation between the animals with the highest whole SCN Rora levels and behavioral status. In addition, there was no correlation between the animals with the highest absolute intensity differences between SCN subdivisions and behavioral rhythmicity, although Vipr2^{-/-} animals displayed consistently higher subdivision differences in Rora than Vip^{-/-} animals (Vip^{-/-} Figure 5A, Vipr2^{-/-} Figure 5B). It remains unclear whether there is a connection between the retained ventral vs. dorsal distinctions in Rora expression and rhythmicity or if the variations are merely a consequence of random desynchrony.

Discussion:

Proper development of complex neural systems involves the coordination of both intrinsic genetic factors and extrinsic signals (Gu, 2002; Grubb and Thompson, 2004; Huberman et al., 2008; Butz et al., 2009). Within the circadian system two key elements, retinal input, and VIP signaling are crucial for proper system function. However, the roles for these elements in the appropriate development of the SCN are unknown. Herein, we show that maturational changes in localization of gene expression occur independent of retinal innervation or VIP signaling, suggesting that these changes may reflect more intrinsic differences within subsets of SCN neurons.

Atoh7 knock-outs, due to a loss of retinal ganglion cells, do not transmit light information to the SCN and animals lose their abilities to entrain to light cycles. We found that *Atoh7* mutant mice show no changes in SCN structure or location. Further, we found no changes in the centralization of *Lhx1* or the pan-SCN expression of *Rora* and *Six3* at P2. The collection of P21-P25 free-running mice at a single ZT offers a pseudo-randomized sampling of animals throughout a circadian time frame. Sampling animals with free running molecular clocks means that while *Rora* is expressed in a circadian fashion (Sato et al., 2004) individual animals may be at different points within mRNA oscillations. If retinal innervation was necessary for variations in subdivision specific *Rora* expression we would expect there to never be changes in expression between the subdivisions, expressed either as pan-SCN *Rora* expression or low levels of *Rora* throughout the nuclei. We found that distinctions are still present between ventral and

dorsal levels of *Rora* in a subset of *Atoh7* mutant animals. In addition, we found centralization of *Lhx1* and the pan-SCN expression of *Six3* are retained at this later postnatal stage.

While *Lhx1* expression remained centralized in *Atoh7* knock-out animals at both P2 and P21-P25 the area of SCN expressing *Lhx1* was reduced. Interestingly, whole SCN levels of *Lhx1* remained, suggesting a smaller number of cells expressing higher levels of *Lhx1* in the absence of retinal innervation. It is currently unclear why maintaining total levels of *Lhx1* expression may be important for the SCN.

VIP signaling mutants showed no changes in the location or presence of SCN nuclei. We found that while rostral to caudal SCN length and mid-SCN width remained similar, there was a significant difference in mid-SCN area of *Vip*^{-/-} and *Vipr2*^{-/-} mice compared to wild-type controls. Further investigations will need to be carried out in order to see if this represents a true change in the absence of VIP signaling or is a consequence of uncontrollable variations in section angle from sample to sample.

It has been well established that animals lacking VIP/ VPAC₂ signaling maintain behavioral rhythmicity in the presence of 12 h light/dark cycles by processes of negative and positive masking (Harmar et al., 2002; Colwell et al., 2003). The mechanisms of how light directly influences locomotor activities are unknown. Regardless of their behavioral abilities in response to light, several groups have shown reduced clock gene expression in VIP/ VPAC₂ signaling mutants kept under both LD and DD conditions. Levels of clock gene expression in *Vipr2*^{-/-} mice and SCN slice preparations show reductions in levels of

clock genes *Per1*, *Per2*, and *Bmal1* in *Vip*^{-/-} (Loh et al., 2011) and *Per1*, *Per2* in *Vipr2*^{-/-} mice (Harmar et al., 2002). Generally, the reductions in clock gene expression in animals kept without light cues are thought to reflect desynchrony among individual cellular oscillators throughout the SCN and possibly also the loss of a small number of rhythmically active cells (Aton et al., 2005). We find that VIP mutants kept in DD display severely reduced levels of *Rora*, but retain similar levels of expression as heterozygotes when under an LD cycle. This suggests that the masking effects may not be acting completely indirectly, but that there may be some connection between the mechanism of masking and the ability to coordinate rhythms within the SCN on a cellular level. However, we must take into account that VIP heterozygous animals have been shown to display an intermediate phenotype in disruption of period and phasing of neuronal activity rhythms (Brown et al., 2007). This may indicate that there is an intermediate effect on the number of cells synchronized or the level of synchronization that may lead to a reduction in total levels of *Rora* expression seen at one given time.

Similar to VIP mutants, we find VPAC₂ mutant animals also show reduced levels of *Rora* within whole, ventral, and dorsal SCN measurements in DD as compared to wild-type. Interestingly, the absolute differences in *Rora* expression between dorsal and ventral SCN in VPAC₂ mutants were statistically similar to wild-type animals, while VIP mutants show statistically significant differences when compared to both wild-type and VPAC₂ animals.

Surprisingly, no differences were found between the expression of *Six3* in VIP heterozygous and homozygous mutants kept in LD or homozygous VIP and VPAC₂ mutants kept in DD as compared to wild-type animals. The absence of reduction in whole SCN expression of *Six3* in VIP and VPAC₂ mutants kept in DD suggests that either expression of *Six3* is independent of the molecular oscillations of the clock or that regulation of *Six3* expression is mediated by light input and is not circadianly regulated.

Not all VIP and VPAC₂ mutants are behaviorally arrhythmic. A subset of these animals are able to maintain a single circadian period, although shortened (Colwell et al., 2003). It is not known whether this ability to maintain rhythmicity reflects unique properties of the network changed with loss of VIP, compensation from an additional signaling element, random coherence, or maintenance of aspects of functional subdivisions. In wild-type animals *Rora* is expressed at significantly higher levels in the shell than in the core. It is not known if this pattern has behavioral relevance. We found that rhythmic, arrhythmic, and polyrhythmic VIP and VPAC₂ mutants had reduced levels of *Rora* expression in the ventral and dorsal SCN, with higher levels of *Rora* in the dorsal SCN maintained in most animals. There was no correlation between either the total levels of *Rora* expression or the amount of absolute difference in *Rora* expression between subdivisions and behavioral locomotor outcome. Thus, it is likely that these changes are merely a consequence of non-uniform desynchrony occurring within SCN nuclei of individual animals.

Overall, we found that the localization of TFs within the SCN, namely centralization of *Lhx1* and the shell regionalization of *Rora*, occur independent of retinal innervation and VIP signaling. This may provide evidence of more intrinsic differences between specific subsets of SCN neurons. However, it is possible that changes in TF localization may still indicate functional time points induced by means other than those tested here such as progression of synaptogenesis, gliogenesis, etc. Future work will need to be done to continue finding and understanding the ways in which the SCN progresses and matures to form functional subdivisions and a functional nucleus.

References

- Aton SJ, Colwell CS, Harmar AJ, Waschek J, Herzog ED (2005) Vasoactive intestinal polypeptide mediates circadian rhythmicity and synchrony in mammalian clock neurons. *Nat Neurosci* 8:476-483.
- Brown TM, Colwell CS, Waschek JA, Piggins HD (2007) Disrupted neuronal activity rhythms in the suprachiasmatic nuclei of vasoactive intestinal polypeptide-deficient mice. *J Neurophysiol* 97:2553-2558.
- Burns CJ, Zhang J, Brown EC, Van Bibber AM, Van Es J, Clevers H, Ishikawa TO, Taketo MM, Vetter ML, Fuhrmann S (2008) Investigation of Frizzled-5 during embryonic neural development in mouse. *Dev Dyn* 237:1614-1626.
- Butz M, Worgotter F, van Ooyen A (2009) Activity-dependent structural plasticity. *Brain Res Rev* 60:287-305.
- Card JP, Moore RY (1984) The suprachiasmatic nucleus of the golden hamster: immunohistochemical analysis of cell and fiber distribution. *Neuroscience* 13:415-431.
- Ciarleglio CM, Axley JC, Strauss BR, Gamble KL, McMahon DG (2011) Perinatal photoperiod imprints the circadian clock. *Nat Neurosci* 14:25-27.
- Ciarleglio CM, Gamble KL, Axley JC, Strauss BR, Cohen JY, Colwell CS, McMahon DG (2009) Population encoding by circadian clock neurons organizes circadian behavior. *J Neurosci* 29:1670-1676.

- Colwell CS, Michel S, Itri J, Rodriguez W, Tam J, Lelievre V, Hu Z, Liu X, Waschek JA (2003) Disrupted circadian rhythms in VIP- and PHI-deficient mice. *Am J Physiol Regul Integr Comp Physiol* 285:R939-949.
- Del Rio T, Feller MB (2006) Early retinal activity and visual circuit development. *Neuron* 52:221-222.
- Denis P, Dussailant M, Nordmann JP, Berod A, Saraux H, Rostene W (1993) Vasoactive intestinal peptide/peptide histidine isoleucine mRNA in the eye and suprachiasmatic nucleus of normal and monocularly enucleated rats. *Graefes Arch Clin Exp Ophthalmol* 231:541-545.
- Dragich JM, Loh DH, Wang LM, Vosko AM, Kudo T, Nakamura TJ, Odom IH, Tateyama S, Hagopian A, Waschek JA, Colwell CS (2010) The role of the neuropeptides PACAP and VIP in the photic regulation of gene expression in the suprachiasmatic nucleus. *Eur J Neurosci* 31:864-875.
- Gray PA, Fu H, Luo P, Zhao Q, Yu J, Ferrari A, Tenzen T, Yuk DI, Tsung EF, Cai Z, Alberta JA, Cheng LP, Liu Y, Stenman JM, Valerius MT, Billings N, Kim HA, Greenberg ME, McMahon AP, Rowitch DH, Stiles CD, Ma Q (2004) Mouse brain organization revealed through direct genome-scale TF expression analysis. *Science* 306:2255-2257.
- Grubb MS, Thompson ID (2004) The influence of early experience on the development of sensory systems. *Curr Opin Neurobiol* 14:503-512.

- Gu Q (2002) Neuromodulatory transmitter systems in the cortex and their role in cortical plasticity. *Neuroscience* 111:815-835.
- Guido ME, de Guido LB, Goguen D, Robertson HA, Rusak B (1999) Daily rhythm of spontaneous immediate-early gene expression in the rat suprachiasmatic nucleus. *J Biol Rhythms* 14:275-280.
- Hamada T, Antle MC, Silver R (2004) Temporal and spatial expression patterns of canonical clock genes and clock-controlled genes in the suprachiasmatic nucleus. *Eur J Neurosci* 19:1741-1748.
- Hamada T, LeSauter J, Venuti JM, Silver R (2001) Expression of Period genes: rhythmic and nonrhythmic compartments of the suprachiasmatic nucleus pacemaker. *J Neurosci* 21:7742-7750.
- Harmar AJ, Marston HM, Shen S, Spratt C, West KM, Sheward WJ, Morrison CF, Dorin JR, Piggins HD, Reubi JC, Kelly JS, Maywood ES, Hastings MH (2002) The VPAC(2) receptor is essential for circadian function in the mouse suprachiasmatic nuclei. *Cell* 109:497-508.
- Holtzman RL, Malach R, Gozes I (1989) Disruption of the optic pathway during development affects vasoactive intestinal peptide mRNA expression. *New Biol* 1:215-221.
- Huberman AD, Feller MB, Chapman B (2008) Mechanisms underlying development of visual maps and receptive fields. *Annu Rev Neurosci* 31:479-509.

- Hughes AT, Piggins HD (2008) Behavioral responses of *Vipr2*^{-/-} mice to light. *J Biol Rhythms* 23:211-219.
- Hughes AT, Fahey B, Cutler DJ, Coogan AN, Piggins HD (2004) Aberrant gating of photic input to the suprachiasmatic circadian pacemaker of mice lacking the VPAC2 receptor. *J Neurosci* 24:3522-3526.
- Laemle LK, Rusa R (1992) VIP-like immunoreactivity in the suprachiasmatic nuclei of a mutant anophthalmic mouse. *Brain Res* 589:124-128.
- Lee HS, Nelms JL, Nguyen M, Silver R, Lehman MN (2003) The eye is necessary for a circadian rhythm in the suprachiasmatic nucleus. *Nat Neurosci* 6:111-112.
- Loh DH, Dragich JM, Kudo T, Schroeder AM, Nakamura TJ, Waschek JA, Block GD, Colwell CS (2011) Effects of vasoactive intestinal Peptide genotype on circadian gene expression in the suprachiasmatic nucleus and peripheral organs. *J Biol Rhythms* 26:200-209.
- Mathers PH, Grinberg A, Mahon KA, Jamrich M (1997) The *Rx* homeobox gene is essential for vertebrate eye development. *Nature* 387:603-607.
- Nagai N, Nagai K, Nakagawa H (1992) Effect of orbital enucleation on glucose homeostasis and morphology of the suprachiasmatic nucleus. *Brain Res* 589:243-252.
- Ohta H, Mitchell AC, McMahon DG (2006) Constant light disrupts the developing mouse biological clock. *Pediatr Res* 60:304-308.

- Okamoto S, Okamura H, Takahashi Y, Akagi Y, Yanaihara N, Ibata Y (1990) Contrary effect of eye enucleation on VIP-immunoreactive neurons in the suprachiasmatic nucleus and the superior colliculus of the rat. *Neurosci Lett* 112:137-142.
- Ramanathan C, Nunez AA, Martinez GS, Schwartz MD, Smale L (2006) Temporal and spatial distribution of immunoreactive PER1 and PER2 proteins in the suprachiasmatic nucleus and peri-suprachiasmatic region of the diurnal grass rat (*Arvicanthis niloticus*). *Brain Res* 1073-1074:348-358.
- Sato TK, Panda S, Miraglia LJ, Reyes TM, Rudic RD, McNamara P, Naik KA, FitzGerald GA, Kay SA, Hogenesch JB (2004) A functional genomics strategy reveals Rora as a component of the mammalian circadian clock. *Neuron* 43:527-537.
- Sengpiel F, Kind PC (2002) The role of activity in development of the visual system. *Curr Biol* 12:R818-826.
- Silver J (1977) Abnormal development of the suprachiasmatic nuclei of the hypothalamus in a strain of genetically anophthalmic mice. *J Comp Neurol* 176:589-606.
- Silver R, Romero MT, Besmer HR, Leak R, Nunez JM, LeSauter J (1996) Calbindin-D28K cells in the hamster SCN express light-induced Fos. *Neuroreport* 7:1224-1228.

- Sumova A, Travnickova Z, Mikkelsen JD, Illnerova H (1998) Spontaneous rhythm in c-Fos immunoreactivity in the dorsomedial part of the rat suprachiasmatic nucleus. *Brain Res* 801:254-258.
- Tokunaga A, Sugita S, Nagai K, Tsutsui K, Ohsawa K (1997) Immunohistochemical characterization of the suprachiasmatic nucleus and the intergeniculate leaflet in the hereditary bilaterally microphthalmic rat. *Neurosci Res* 27:57-63.
- VanDunk C, Hunter LA, Gray PA (2011) Development, maturation, and necessity of transcription factors in the mouse suprachiasmatic nucleus. *J Neurosci* 31:6457-6467.
- Wang SW, Kim BS, Ding K, Wang H, Sun D, Johnson RL, Klein WH, Gan L (2001) Requirement for *math5* in the development of retinal ganglion cells. *Genes Dev* 15:24-29.
- Wee R, Castrucci AM, Provencio I, Gan L, Van Gelder RN (2002) Loss of photic entrainment and altered free-running circadian rhythms in *math5*^{-/-} mice. *J Neurosci* 22:10427-10433.
- Yan L, Okamura H (2002) Gradients in the circadian expression of *Per1* and *Per2* genes in the rat suprachiasmatic nucleus. *Eur J Neurosci* 15:1153-1162.
- Yang Z, Ding K, Pan L, Deng M, Gan L (2003) *Math5* determines the competence state of retinal ganglion cell progenitors. *Dev Biol* 264:240-254.

Zhang J, Fuhrmann S, Vetter ML (2008) A nonautonomous role for retinal frizzled-5 in regulating hyaloid vitreous vasculature development. *Invest Ophthalmol Vis Sci* 49:5561-5567.

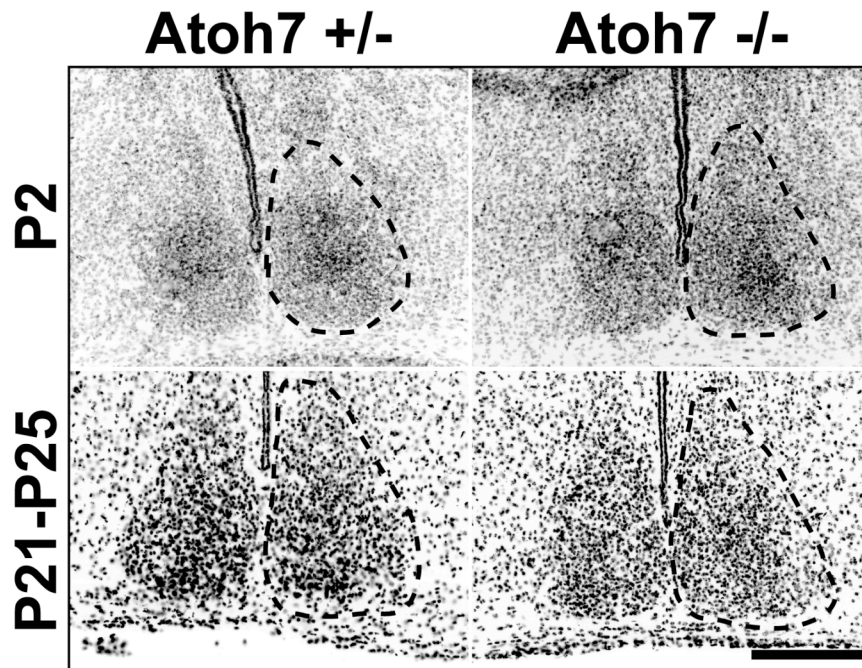


Figure 1. SCN presence and location are unaffected by absence of retinal innervation. Inverted fluorescent DAPI stain of coronal mid-SCN at P2 and P21-P25 for *Atoh7*^{+/-} and *Atoh7*^{-/-} mice showing cellular density. Dotted lines indicate boundaries of the nuclei based off of DAPI stain. Scale bar, 250 μ m. Distinct bilateral nuclei representing the SCN are present along the ventral surface of the brain in *Atoh7* heterozygotes that possess an intact retinohypothalamic tract and *Atoh7* knock-outs lacking retinal innervation to the SCN.

Table 1. SCN area and length are maintained in the absence of retinal innervation.

Age, Genotype, n	Average mid-SCN Area (square micron)	Rostral to Caudal Length (um)	mid-SCN width (um)	Whole mid-SCN density (nuclei/ square micron)
P2, Atoh7 +/-, (4)	84,332 ± 4,283	320 ± 0.0	316.82 ± 14.99	-----
P2, Atoh7 -/-, (6)	76,617 ± 4,986 <i>p</i> =0.275	270 ± 50.00 <i>p</i> =0.500	331.77 ± 8.94 <i>p</i> =0.430	-----
P21-P25, Atoh7 +/-, (8)	87,663 ± 9,477	445 ± 47.87	284.59 ± 11.44	0.00886 ± 0.000530
P21-P25, Atoh7 -/-, (16)	99,271 ± 3,600 <i>p</i> =0.293	345 ± 16.37 <i>p</i> =0.125	326.54 ± 7.02 <i>p</i> =0.012	0.00792 ± 0.000278 <i>p</i> =0.160

Table displays mid-SCN area (calculated by averaging measurements of right and left nuclei for each animal), rostral to caudal length, mid-SCN width, and mid-SCN density measurements of SCN nuclei (\pm s.e.m.), showing no overall changes in SCN size in the absence of retinal innervation.

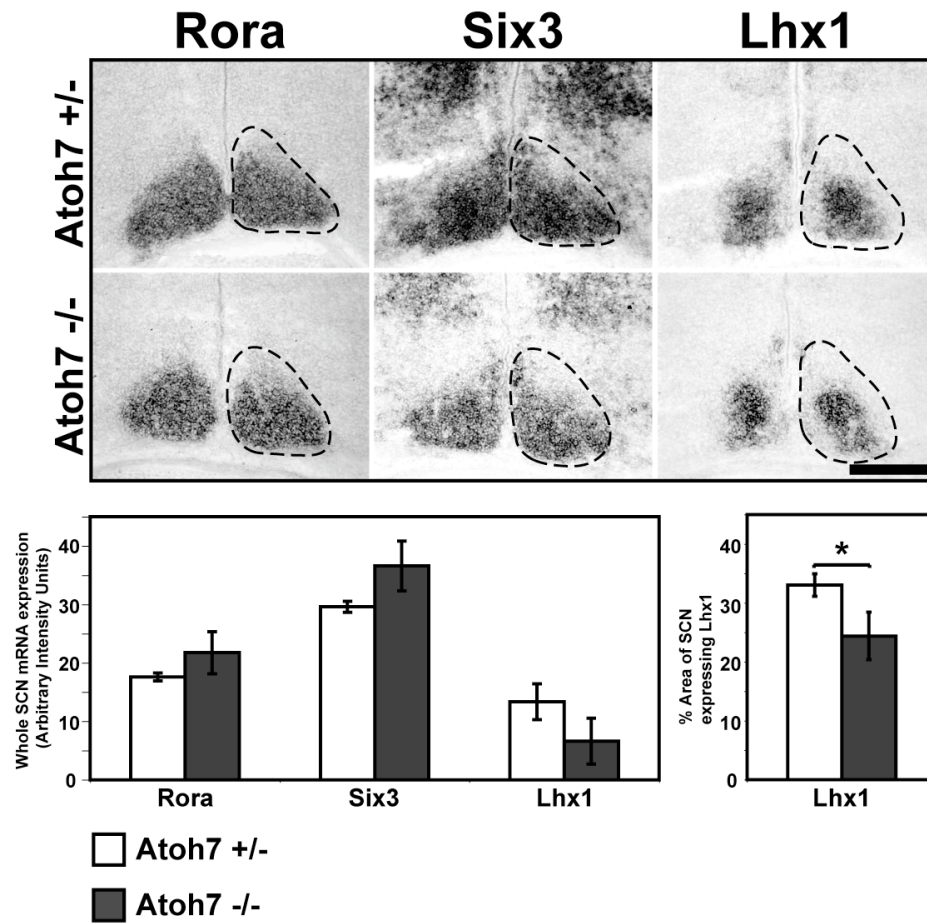


FIGURE 2A

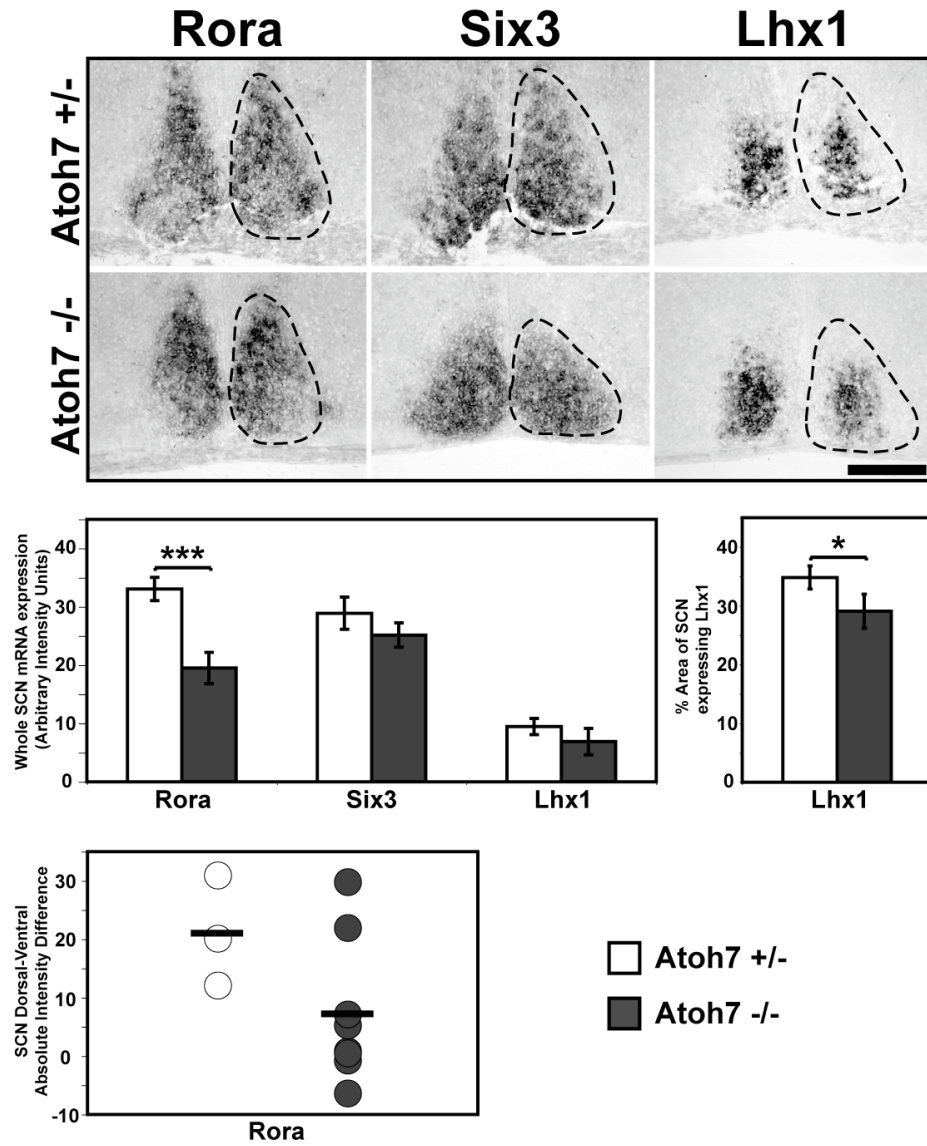


FIGURE 2B

Figure 2. Progressive localization of transcription factor expression is maintained in *Atoh7* knock-outs. *In situ* hybridization (ISH) of coronal mid-SCN expressing *Rora*, *Six3*, or *Lhx1* mRNA in P2 (**A**) and P21-P25 (**B**) *Atoh7*^{+/-} and *Atoh7*^{-/-} mice. Dashed lines indicate SCN outline based on DAPI nuclear stain. **A**, *top*, Representative images show pan-SCN expression of *Rora* and *Six3* as well as centralization of *Lhx1* maintained in *Atoh7* knock-out animals. *Bottom*, bar graphs show maintained whole SCN expression levels of *Rora*, *Six3*, and *Lhx1* measured in arbitrary intensity units (AIUs) (left) while percentage of SCN expressing *Lhx1* is reduced (right). **B**, *top*, ISH images depict maintained ability of *Atoh7* knock-outs to localize expression of *Rora* to the shell and *Lhx1* to the central SCN while conserving *Six3* expression throughout the nuclei. *Middle*, bar graph, indicates a significant reduction in *Atoh7* knock-out whole SCN levels of *Rora* as compared to *Atoh7* heterozygotes (left) and reduction in percentage of SCN expressing *Lhx1* (right). *Bottom*, scatter plot shows the absolute intensity difference in expression levels of *Rora* between SCN subdivisions and indicates no change between *Atoh7* knock-outs and heterozygotes. Wide black bars indicate average values. Scale bar, 250 μ m. Asterisks indicate significance based on un-paired *t* test (*, $p \leq 0.05$; **, $p \leq 0.01$, ***, $p \leq 0.005$).

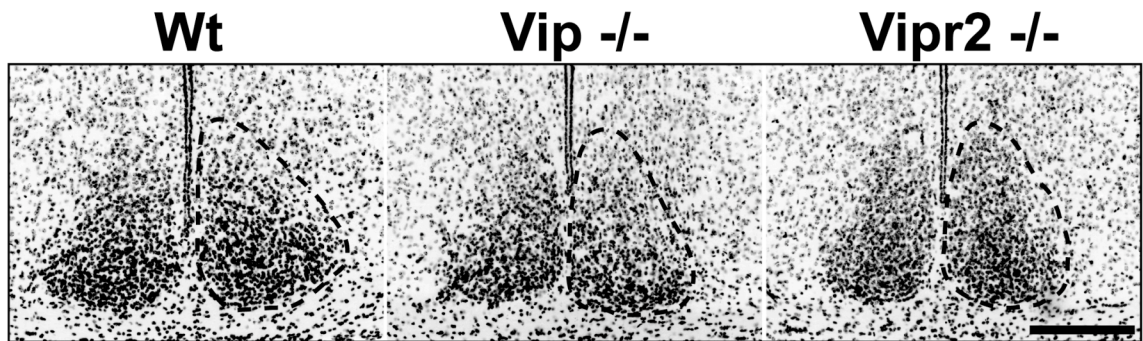


Figure 3. SCN presence and location are unaffected by absence of VIP/ VPAC₂ signaling. Inverted fluorescent DAPI nuclear stain of coronal mid-SCN for C57BL/6 (Wt), *Vip*^{-/-}, and *Vipr2*^{-/-} show clear bilateral nuclei. Dotted lines indicate boundaries of the nucleus based off of DAPI stain. Scale bar, 250 μ m.

Table 2. SCN location and morphology are maintained in VIP/ VPAC₂ signaling mutants.

Age, Genotype, n	Average mid-SCN Area (square microns)	Rostral to Caudal Length (um)	mid-SCN width (um)	Whole mid-SCN density (nuclei/ square micron)
P21+, Wt, (8)	106,693 ± 4,264	470 ± 28.87	303.07 ± 9.09	0.00774 ± 0.00364
P21+, Vip ^{-/-} , (18)	91,413 ± 2,061 <i>p</i> =0.008	387 ± 16.67 <i>p</i> =0.053	301.80 ± 3.74 <i>p</i> =0.914	0.00779 ± 0.000184 <i>p</i> =0.898
P21+, Vipr2 ^{-/-} , (18)	90,873 ± 3,975 <i>p</i> =0.013	445 ± 25.00 <i>p</i> =0.532	294.68 ± 10.53 <i>p</i> =0.553	0.00816 ± 0.000235 <i>p</i> =0.353

Table displays mid-SCN area (calculated by averaging measurements of right and left nuclei for each animal), rostral to caudal length and mid-SCN width measurements of SCN nuclei (\pm s.e.m.). No changes were seen in rostral to caudal SCN length, SCN width, or mid-SCN cell density; however a slight difference was found in the mid-SCN area of Vip^{-/-} and Vipr2^{-/-} animals as compared to controls.

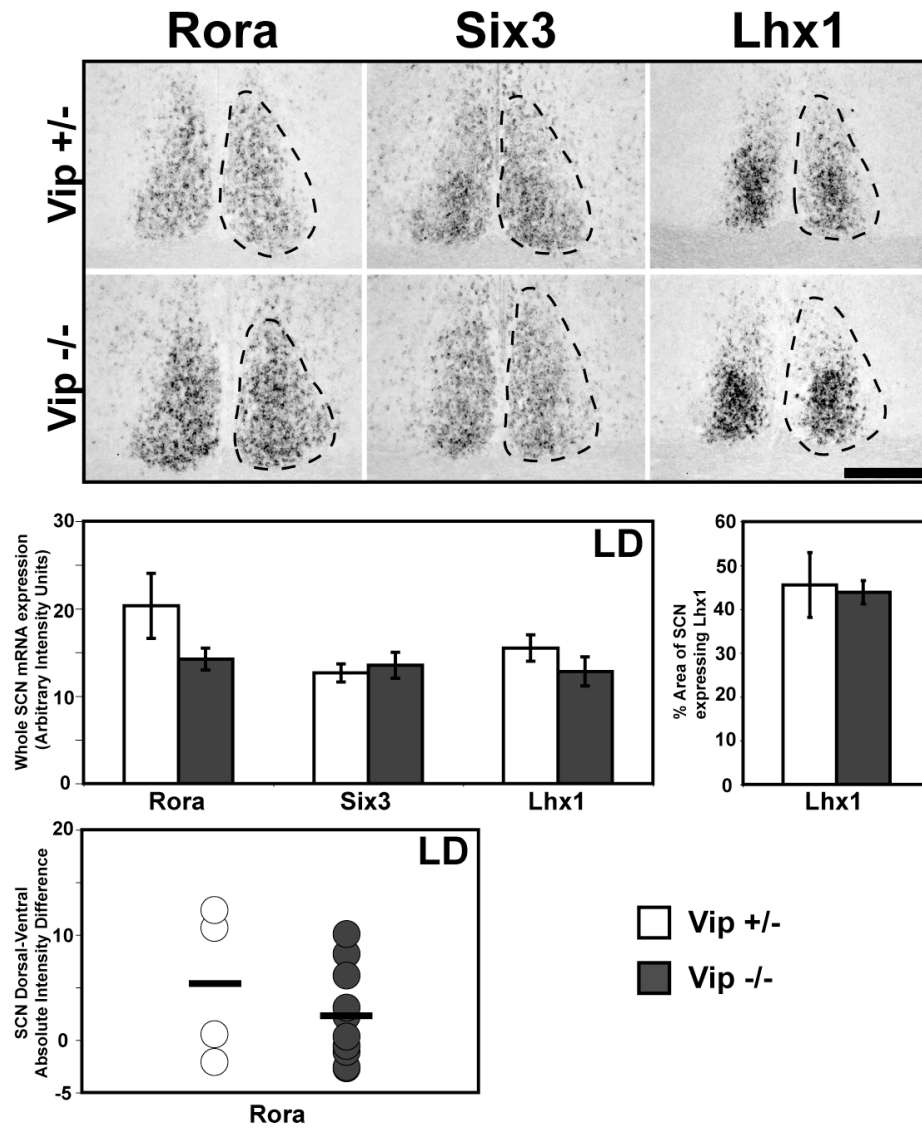


FIGURE 4A

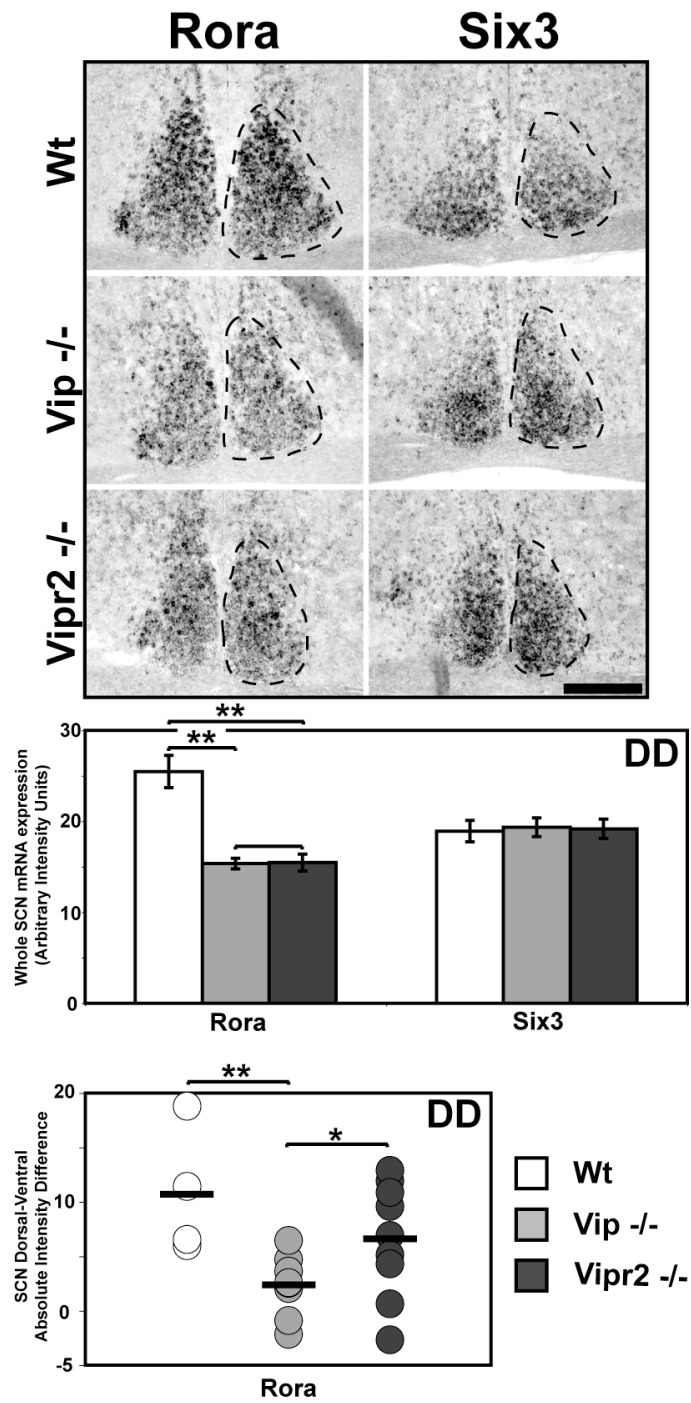


FIGURE 4B

Figure 4. Abundance of Rora expression is reduced in VIP and VPAC₂ mutants kept in constant darkness but not under 12 h light/dark. *In situ* hybridization (ISH) of coronal mid-SCN tissue from VIP and/or VPAC₂ knock-out animals and C57BL/6 (Wt) controls kept under 12 h light/dark (LD) (**A**) or constant darkness (DD) (**B**). **A**, *top*, ISH images depict maintained centralization of Lhx1 in *Vip*^{-/-} animals. *Middle*, bar graphs indicate no differences between whole SCN expression of Rora, Six3, Lhx1 (left) and no change in the percentage of SCN expressing Lhx1 (right). *Bottom*, scatter plot shows no change in absolute intensity differences in Rora between SCN subdivisions. Wide black lines in scatter plots indicate average values. **B**, *top*, ISH images show lack of differential Rora expression between SCN subdivisions in VIP/VPAC₂ signaling mutants. *Middle*, bar graph shows reduced expression of Rora in *Vip*^{-/-} and *Vipr2*^{-/-} animals. *Bottom*, Scatter plot depicts reductions in Rora absolute intensity differences between SCN subdivisions. Scale bars, 250 μm. Asterisks indicate significance based on un-paired *t* test (*, $p \leq 0.05$; **, $p \leq 0.01$, ***, $p \leq 0.005$).

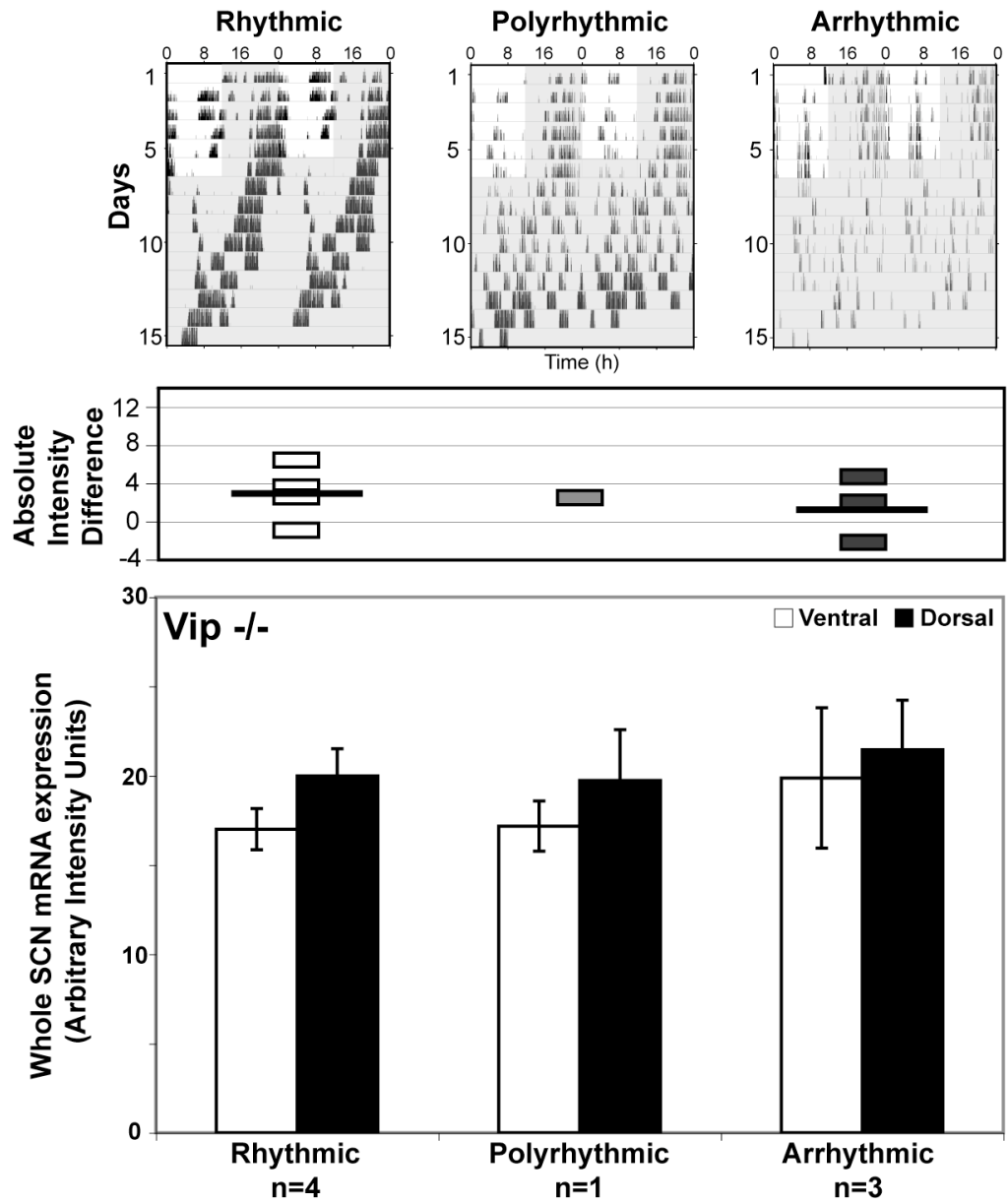


FIGURE 5A

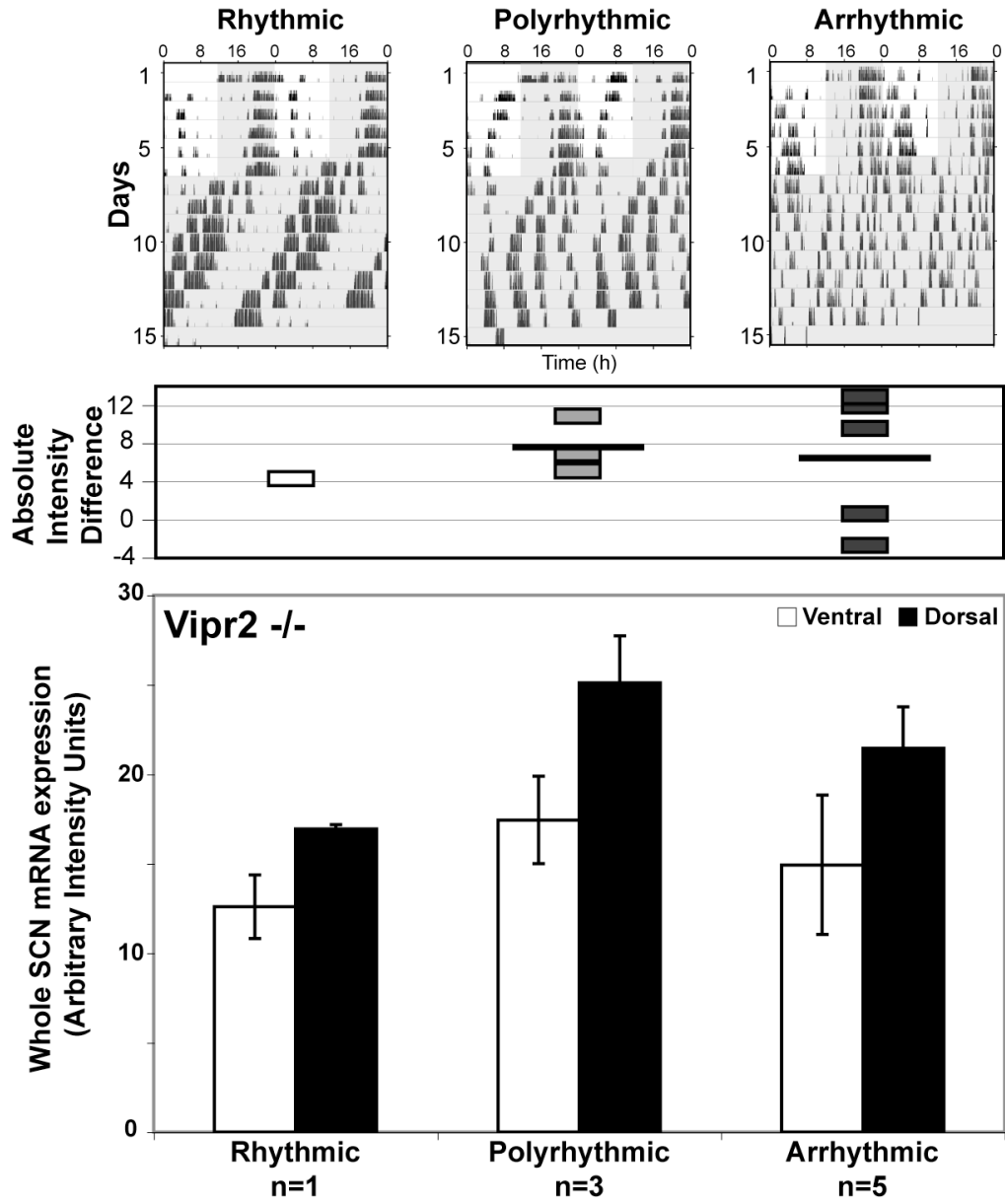


FIGURE 5B

Figure 5. Abundance and localization of Rora expression does not correlate with behavioral rhythmicity. **Top**, double-plotted actograms show wheel-running activity from either *Vip*^{-/-} (**A**) or *Vipr2*^{-/-} (**B**) animals maintained on a 12 h light/dark schedule for six days before being transferred to nine days in constant darkness. Grayed hours indicate periods of darkness. Animals were classified as behaviorally rhythmic, polyrhythmic, or arrhythmic based on their free-running rhythms. **Middle**, scatter plots display absolute intensity differences in the expression of Rora between SCN subdivisions. Wide black lines in scatter plots indicate average values. **Bottom**, bar graphs show average mRNA intensity of Rora in the ventral and dorsal SCN of behaviorally segregated mutants. Note that higher levels of Rora in the shell were maintained in all groups tested, but there is no correlation between levels of Rora and locomotor phenotype.

-CHAPTER 4-

**Roles of homeobox protein Six3 in postmitotic GABA-ergic
populations of *Mus musculus***

Abstract

The suprachiasmatic nuclei (SCN) act as principal mammalian circadian pacemakers regulating many biological processes including hormone secretion, body temperature regulation, and sleep/wake activity. Remarkably, the genes and transcription factors (TFs) necessary for the specification and maturation of the SCN have not been well defined. The TF, Six3, has recently been identified as expressed within SCN neurons from before initial specification to adult. The extended expression of Six3 in the SCN is not unique; rather Six3 remains expressed in several hypothalamic and thalamic nuclei even in adult mice. The postmitotic role for Six3 in neurons is unknown. Herein, we examine the effects of deletion of Six3 postmitotically in mice with emphasis on the SCN, by targeting deletion from postmitotic GABA-ergic populations. Within the SCN, successful Six3 deletion did not effect the expression and localization of TFs *Rora*, *Lhx1*, and *Per1* or the peptides vasoactive intestinal polypeptide or arginine vasopressin. *Six3^{flox/flox}/Gad2-cre(+)* knock-outs displayed a severe growth deficit evident by postnatal day ten and leading to early lethality shortly after weaning. Six3 expression is unchanged in the pituitary gland but is completely eliminated from several GABA-ergic hormone-regulating nuclei including the arcuate and the substantia nigra pars reticulata. We conclude that the postmitotic deletion of Six3 from SCN neurons does not affect the phenotypic specification and localization of several SCN TFs or peptides, but may control the specification or function of nuclei responsible for key growth signals.

Introduction

The embryonic telencephalon/diencephalon gives rise to key structures regulating biological homeostasis and arousal as well as structures relaying and processing sensory information (McCormick and Bal, 1994; Williams et al., 2001). Currently, the molecular pathways controlling the development and function of these vital brain regions are not well understood. In order to elucidate the roles specific genes play in the development of behaviorally important structures, several groups have performed large-scale transcription factor screens, identifying genes expressed in relatively discrete populations of cells throughout the brain (Gray et al., 2004; Lein et al., 2007; Shimogori et al., 2010).

The SCN, central circadian pacemakers for the mammalian system, are just one of the many nuclei derived from the telencephalon/diencephalon. They are responsible for creating and maintaining near 24 h rhythms, which regulate essential homeostatic processes such as temperature and energy regulation (for review (Ko and Takahashi, 2006)). The SCN are heterogeneous nuclei comprised of equally rhythmogenic neurons, which vary in neuropeptide content, TF expression, response to stimuli, and other respects. Currently, the TFs that contribute to the specification of rhythmic neurons or cellular subtypes are unknown. Screens for TF expression have been successful in identifying genes expressed within the SCN at several points in development. Among them is the highly conserved TF, Six3. Interestingly, Six3 was shown expressed within the early SCN neuroepithelium and continued to be expressed in all SCN neurons

through adult stages, where expression within the nuclei was found to cycle between periods of light and dark (VanDunk et al., 2011).

Six3 is known to act at several stages in cellular development. Through interactions with Wnt signaling pathways, Pax6, and Geminin (Kobayashi et al., 2002; Lagutin et al., 2003; Gestri et al., 2005; Lavado et al., 2008), Six3 plays an essential role in patterning the mammalian forebrain. In addition, Six3 has been shown to be critical in cellular proliferation (Del Bene et al., 2004), specification of neuronal subtypes (Liu et al., 2010), regulation of gene expression (Manavathi et al., 2007), and lens formation (Liu et al., 2006) during eye development. Recently, Six3 was additionally found necessary for the formation of the SCN (VanDunk et al., 2011). We demonstrated that deletion of Six3 specifically from neural progenitors not only eliminated the presence of dense cell clusters along the ventral anterior forebrain, but also the expression of several SCN-genes including the TFs Lhx1 and Rora, and the peptide arginine vasopressin (AVP).

The SCN are not the only nuclei with Six3 expression into adult stages. Cell types within the retina and several nuclei derived from the telencephalon and diencephalon also retain Six3 expression (Conte et al., 2005). The continued expression of Six3 within the SCN and other brain regions as well as its known roles within eye development suggests this gene may be playing additional roles postmitotically. Herein, we examine the effects of deletion of Six3 postmitotically in mice with emphasis on the SCN, by targeting deletion from GABA-ergic populations, as most, if not all, neurons of the SCN express GABA (Okamura et al., 1990). Specifically, we investigated the role of postmitotic

expression of Six3 in the specification or maintenance of SCN neuronal subtypes, with focus on neurons expressing TFs Rora, Lhx1, Per1 or the neuropeptides AVP or vasoactive intestinal polypeptide (VIP). We find that Six3 is not necessary for proper expression or localization of postnatal TF or peptide mRNA. However, we demonstrate that postmitotic expression of Six3 has a profound impact on animal growth, suggesting a role for Six3 in nuclei regulating growth hormones, appetite, or motivation.

Materials and Methods

Animals and housing. Male and female wild-type C57BL/6 (Charles River), *Six3flox* (Liu et al., 2006) (Guillermo Oliver, St. Jude Children's Research Hospital, Memphis, TN), *Gad2-cre* (010802; (Taniguchi et al., 2011) The Jackson Laboratory), and *Rosa26-tdTomato* (007909; (Madisen et al., 2010), The Jackson Laboratory) were used. Mice were maintained in a normal 12 h light/dark schedule under standard care conditions. Mutant animals were maintained on a C57BL/6 background (Charles River). All experiments were approved by the Animal Studies Committee at Washington University and followed NIH guidelines.

Genotyping. Mice were genotyped by PCR for *Gad2-cre*, *Six3* floxed, and/or wild-type alleles as described previously (Liu et al., 2006) or as outlined by The Jackson Laboratory. The presence of Cre was determined by the presence or absence of an amplified band as previously described (VanDunk et al., 2011).

Tissue acquisition. Unless otherwise stated, all collections were done at approximately zeitgeber time (ZT) 8. Neonatal pups [postnatal day 0 (P0) to P2] or embryos [embryonic day 10.5 (E10.5) to E18.5] from timed pregnant females (morning of plug was E0.5) were anesthetized on ice and either transcardially perfused (\geq E16.5) or immersion fixed in 4% paraformaldehyde (PFA) in 0.1 M PBS, pH 7.4. Older mice were anesthetized with a ketamine/xylazine mixture before perfusion with 0.9% saline followed by 4% PFA. All

tissues were post fixed in 4% PFA overnight at 4°C, cryoprotected in 20% sucrose in PBS, frozen in O.C.T. Compound Embedding Medium (Tissue-Tek), and stored at -75°C. Serial sections (20µm) were cut on a Hacker cryostat and thaw mounted on Superfrost Plus slides (Thermo Fisher Scientific). Five adjacent sets of sections were prepared from each postnatal age and stored at -20°C.

Probe synthesis. Plasmids for *in situ* hybridization probes were acquired as previously described (VanDunk et al., 2011). Gene fragments from verified plasmids were linearized by direct amplification by sequence or vector-specific PCR. Digoxigenin (DIG)-labeled anti-sense and sense RNA probes were made using PCR products as template and T7, T3, or SP6 RNA polymerases (Roche). cRNA probes were purified using Quick Spin columns (Roche) and quantified by spectrophotometry. Probes were used at a concentration of 1-2 µg/ml. Sense counterparts of all probes were tested to ensure probe specificity.

In situ hybridization. Slides were immersed in 4% PFA, permeabilized with proteinase K, returned to 4% PFA before being washed in 0.1 M triethanolamine-HCl with 0.25% acetic anhydride. Once blocked in hybridization buffer at 65°C slides were incubated in hybridization buffer containing 1-2 µg/ml DIG-labeled anti-sense cRNA overnight at 65°C. Slides were then washed in 2XSSC buffer at 62°C, washed in 0.2XSSC at 65°C, blocked with 10% normal horse serum (NHS) in 0.1M PBS, and incubated in alkaline

phosphatase labeled anti-DIG antibody (1:2000 in 10% NHS; Roche) overnight. Sections were washed and color was visualized using Nitro blue tetrazolium and 5-Bromo-4-chloro-3-indolyl phosphate (Roche). Staining was stopped after visual inspection. Sections were washed, fixed in 4% PFA, and coverslipped in 90% glycerol, Vectashield Mounting Medium (Vector Laboratories), or UltraCruz Mounting Media with DAPI (Santa Cruz Biotechnology).

Image acquisition. Images were acquired using a Nikon Eclipse 90i microscope, Photometrics Coolsnap HQ2 camera with a Prior Scientific ProScan II motorized translation stage, and acquired in Volocity (PerkinElmer Life and Analytical Sciences). Images were exported as 8bit JPEG or TIFF files. All images were adjusted for clarity by filtering and/or modifying levels, as necessary, in Photoshop (Adobe Systems).

Analysis. General SCN morphology was assessed by obtaining outlines drawn based on cellular density marked with nuclear DAPI stain and measuring individual nuclei for mid-SCN width, area, and cell density. Rostral to caudal length of the nuclei was calculated by counting the number of sections containing Rora staining and estimating length based on section thickness. Growth was measured by measuring weight every two to three days.

Results

Onset of *Gad2*-cre expression in the SCN

The onset of *Gad2*-cre recombination in the early SCN was assessed by crossing *Gad2*-cre expressing mice with reporter mice containing the *Rosa26* locus with loxP flanked STOP cassettes followed by red fluorescent protein (tdTomato). In this manner, tdTomato was expressed following cre-mediated recombination in mice containing both transgenes. We found that while cre recombinase was present within the early SCN by E12.5, as marked by the overlap of *Six3* and *Lhx1*, cre-mediated expression of tdTomato was not present until E13.5 (Figure 1). These data suggest successful recombination and consequent reporter protein expression events require approximately two days after cells of the SCN become postmitotic to be visualized.

Gad2-cre driven conditional knock-out of *Six3* leads to growth deficiencies

Crossing *Six3^{lox/+}/Gad2-cre(+)* males x *Six3^{lox/lox}* females yielded homozygous (*Six3^{lox/lox}/Gad2-cre(+)*) and heterozygous (*Six3^{lox/+}/Gad2-cre(+)*) mutants as well as homozygous and heterozygous *Six3 Gad2-cre(-)* controls in normal Mendelian numbers. We found P2 homozygous and heterozygous mutants and control littermates were similar in weight and disposition. However, *Six3^{lox/lox}/Gad2-cre(+)* homozygous mutants did not undergo normal weight gain and growth as they developed, evident by P10 (Figure 2), which led to lethality around P21. Prior to death these animals displayed mild ataxic gate

and appeared hypoactive. No growth or disposition deficits were observed in *Six3^{flox/+}* *Gad2-cre(+)* heterozygous mutant animals.

Role of Six3 in postmitotic specification of SCN neurons

To test whether Six3 was necessary for the postmitotic specification of SCN neurons and neuronal subtypes we analyzed *Six3^{flox/flox}/Gad2-cre(+)* and *Six3^{flox}/Gad2-cre(-)* littermate controls for expression of TF and peptide mRNA and general SCN anatomy. Animals were observed at postnatal days 2 (P2, n=2) and 21 (P21, n=2). We found that Six3 was successfully eliminated from the SCN of P2 experimental mice while expression remained present in regions not expressing GABA, such as the pituitary gland (Figure 3).

Deletion of Six3 from postmitotic SCN neurons did not have any adverse effects on the general morphology of neural tissues in animals at P2 (data not shown). Through assessment of nuclear DAPI stain, indicating cellular density, we found the relative rostrocaudal positioning, size, and morphology of SCN nuclei remained intact following postmitotic Six3 deletion (Table 1). *In situ* hybridization for the expression of SCN TFs revealed that the whole SCN expression of Rora was maintained in these animals, as well as the expression and centralized localization of Lhx1. In addition, we found that the expression of AVP mRNA was maintained within the SCN shell (Figure 3).

Analysis of *Six3^{flox/flox}/Gad2-cre(+)* P21 mice showed that although these animals displayed severe growth deficits, no gross morphological defects were present within the

neural tissue (data not shown). Further, general morphology and size of the SCN were maintained (Table 1). We found Six3 was almost completely eliminated in *Six3^{flox/flox}/Gad2-cre(+)* homozygous mutants (Figure 4). Remaining low levels may indicate either background expression, inefficiency in recombination, or expression of Six3 in non-GABAergic cells. In the absence of Six3 we found that mRNA expression levels and localization of the TFs Rora and Per1, as well as the peptide VIP, were maintained. In addition, the localization of Rora to the SCN shell, characteristic of mature SCN anatomy (VanDunk et al., 2011), and VIP to the core SCN remained. Together, these data suggest postmitotic Six3 is not necessary for the specification of peptidergic neurons within the SCN or their anatomical localization. In addition, the presence of Six3 postmitotically does not appear to influence TF expression or maturational changes in localization.

Gad2-cre conditional deletion of Six3 may affect extra-SCN structures

By analyzing the full rostral to caudal expression of Gad1 and Six3 mRNA within P2 neural tissue we found that co-expression was not unique to the SCN. At least six additional regions were found to contain strong overlap (Figure 5). These regions include: Amacrine cells of the inner nuclear layer of the retina, reticular hypothalamic nuclei, lateral arcuate nuclei, posterior pretectal/ olivary pretectal nuclei, substantia nigra pars reticulata (SNpr), and the medial terminal nucleus of the accessory optic tract (a full list of regions of potential overlap can be found in Supplemental Table 1). We find that

Six3^{flox/flox}/Gad2-cre(+) mice successfully lose expression of Six3 in each of these areas (Figure 5B).

Discussion:

We have previously demonstrated that premitotic Six3 plays a critical role in the formation and specification of cells that will become the SCN (VanDunk et al., 2011). In the current study we found that Six3 is not necessary to shape SCN cell identity postmitotically. We found the presence and localization of SCN-expressed TFs Rora, Lhx1, and Per1 were maintained in Six3 knock-outs sampled at neonatal (P2) and functionally mature stages (P21). In addition, Six3 expression was not necessary for the onset or the localization of cells expressing AVP or VIP mRNA. These findings suggest development of TF and peptidergic subtypes within the SCN occur independent of postmitotic Six3 or, alternatively, that these regions are specified premitotically and are unaffected by the postmitotic loss of Six3. Successful recombination using Gad2-cre was first evident by E13.5, approximately two days after neurons of the SCN became postmitotic. This delayed recombination indicates SCN neurons may have already begun expressing postmitotic markers, such as Lhx1, before Six3 is functionally removed. Lhx1 is one of the first TFs expressed by postmitotic SCN neurons (VanDunk et al., 2011) and its early deletion has been suggested to influence peptidergic specification (Blackshaw et al., 2010). Therefore, it may not be surprising that Six3 loss after the onset of Lhx1 would not affect peptide expression in the SCN.

Although expression and localization of established TFs and peptides persisted following the postmitotic deletion of Six3, it is unknown whether the expression of Six3 during this period may aid in maintenance of clock gene rhythms or greater circadian

function. The severe growth impairment and early lethality seen in *Six3^{lox/lox}/Gad2-cre(+)* experimental mice make it impossible to look for effects on circadian function using the standard assessment of locomotor rhythms through wheel-running behavior. However, other measures such as recording neuronal rhythmicity in the intact slice or dispersed cultures, which utilize tissues from younger animals, may be useful options. Alternatively, previous reports have shown that reductions in functional Six3 protein, by single-allele deletions, can lead to the failed activation of downstream targets such as Sonic hedgehog and Nkx2.1 (Geng et al., 2008). This suggests that single-allele deletions may be enough to show changes in normal Six3 function. While *Six3^{lox/+}/Gad2-cre(+)* heterozygous mutant animals did not display abnormal growth patterns, these animals could be used as an alternative way to assess the effects of postmitotic Six3 deletion on circadian function.

The severe runting phenotype displayed by Six3 postmitotic knock-outs was surprising given the normal development of the pituitary gland, the main producer of hormones regulating growth and development (Sam and Frohman, 2008). It is likely then that the deletions of Six3 from extra-SCN regions showing co-localization with Gad1 are contributing to the failure of normal growth in these animals. The progressive nature of this phenotype closely resembles the effects seen in animals with highly reduced levels of dopamine. Szczyпка and colleagues (1999) demonstrated that animals, lacking normal levels of circulating dopamine become progressively hypoactive and hypophagic causing lethality around the time of weaning (Szczyпка et al., 1999). Both the arcuate nucleus

and the substantia nigra; areas of dopamine production in the brain, show overlap in the expression of Six3 and Gad1 mRNA. While not producing or secreting dopamine itself, the SNpr, is thought to regulate dopaminergic activity within the pars compacta (Deniau et al., 1982). We hypothesize that the deletion of Six3 from the arcuate and/or SNpr plays a role in the ability of these nuclei to produce functional levels of dopamine for maintaining aspects of appetite and motivation (Salamone and Correa, 2009; Fulton, 2010; Kurniawan et al., 2011). It is known that in addition to the production of dopamine, the arcuate nuclei are responsible for secreting growth hormone releasing hormone, neuropeptide Y, and agouti-related proteins that act on hypothalamic nuclei and aid in regulation of growth and appetite (Broberger et al., 1998; Schwartz et al., 2000; Williams et al., 2001; Minor et al., 2009). The role of Six3 deletion on these critical functions of the arcuate could shed light on the resulting growth deficiencies seen in our animals.

Previous studies have implicated the TF Six3 in several aspects of cellular development including promoting proliferation (Kroll, 2007), differentiation (Kroll, 2007), and specification (Lagutin et al., 2001; Zhu et al., 2002; Ohshima et al., 2005). Here we reveal that Six3 does not play a role in the specification of at least several TF or peptidergic phenotypes in postmitotic SCN neurons. However, it is likely that Six3 is playing a role in either the specification or function of nuclei necessary for growth, which may include areas responsible for regulation of growth signals, appetite, or motivation. Future studies will need to determine the key genes necessary for regulation of the distinct stages of cellular development of SCN neurons. Better understanding of the

functionality of these genes will advance our knowledge of how the SCN and its subdivisions are developmentally specialized to create and maintain this unique time keeping system.

References

- Broberger C, Johansen J, Johansson C, Schalling M, Hokfelt T (1998) The neuropeptide Y/agouti gene-related protein (AGRP) brain circuitry in normal, anorectic, and monosodium glutamate-treated mice. *Proc Natl Acad Sci U S A* 95:15043-15048.
- Conte I, Morcillo J, Bovolenta P (2005) Comparative analysis of Six 3 and Six 6 distribution in the developing and adult mouse brain. *Dev Dyn* 234:718-725.
- Del Bene F, Tessmar-Raible K, Wittbrodt J (2004) Direct interaction of geminin and Six3 in eye development. *Nature* 427:745-749.
- Deniau JM, Kitai ST, Donoghue JP, Grofova I (1982) Neuronal interactions in the substantia nigra pars reticulata through axon collaterals of the projection neurons. An electrophysiological and morphological study. *Exp Brain Res* 47:105-113.
- Fulton S (2010) Appetite and reward. *Front Neuroendocrinol* 31:85-103.
- Geng X, Speirs C, Lagutin O, Inbal A, Liu W, Solnica-Krezel L, Jeong Y, Epstein DJ, Oliver G (2008) Haploinsufficiency of Six3 fails to activate Sonic hedgehog expression in the ventral forebrain and causes holoprosencephaly. *Dev Cell* 15:236-247.
- Gestri G, Carl M, Appolloni I, Wilson SW, Barsacchi G, Andreazzoli M (2005) Six3 functions in anterior neural plate specification by promoting cell proliferation and inhibiting Bmp4 expression. *Development* 132:2401-2413.
- Gray PA, Fu H, Luo P, Zhao Q, Yu J, Ferrari A, Tenzen T, Yuk DI, Tsung EF, Cai Z, Alberta JA, Cheng LP, Liu Y, Stenman JM, Valerius MT, Billings N, Kim HA,

- Greenberg ME, McMahon AP, Rowitch DH, Stiles CD, Ma Q (2004) Mouse brain organization revealed through direct genome-scale TF expression analysis. *Science* 306:2255-2257.
- Ko CH, Takahashi JS (2006) Molecular components of the mammalian circadian clock. *Hum Mol Genet* 15 Spec No 2:R271-277.
- Kobayashi D, Kobayashi M, Matsumoto K, Ogura T, Nakafuku M, Shimamura K (2002) Early subdivisions in the neural plate define distinct competence for inductive signals. *Development* 129:83-93.
- Kroll KL (2007) Geminin in embryonic development: coordinating transcription and the cell cycle during differentiation. *Front Biosci* 12:1395-1409.
- Kurniawan IT, Guitart-Masip M, Dolan RJ (2011) Dopamine and effort-based decision making. *Front Neurosci* 5:81.
- Lagutin O, Zhu CC, Furuta Y, Rowitch DH, McMahon AP, Oliver G (2001) Six3 promotes the formation of ectopic optic vesicle-like structures in mouse embryos. *Dev Dyn* 221:342-349.
- Lagutin OV, Zhu CC, Kobayashi D, Topczewski J, Shimamura K, Puellas L, Russell HR, McKinnon PJ, Solnica-Krezel L, Oliver G (2003) Six3 repression of Wnt signaling in the anterior neuroectoderm is essential for vertebrate forebrain development. *Genes Dev* 17:368-379.

- Lavado A, Lagutin OV, Oliver G (2008) Six3 inactivation causes progressive caudalization and aberrant patterning of the mammalian diencephalon. *Development* 135:441-450.
- Lein ES, Hawrylycz MJ, Ao N, Ayres M, Bensinger A, Bernard A, Boe AF, Boguski MS, Brockway KS, Byrnes EJ, Chen L, Chen L, Chen TM, Chin MC, Chong J, Crook BE, Czaplinska A, Dang CN, Datta S, Dee NR, et al. (2007) Genome-wide atlas of gene expression in the adult mouse brain. *Nature* 445:168-176.
- Liu W, Lagutin OV, Mende M, Streit A, Oliver G (2006) Six3 activation of Pax6 expression is essential for mammalian lens induction and specification. *Embo J* 25:5383-5395.
- Liu W, Lagutin O, Swindell E, Jamrich M, Oliver G (2010) Neuroretina specification in mouse embryos requires Six3-mediated suppression of Wnt8b in the anterior neural plate. *J Clin Invest* 120:3568-3577.
- Madisen L, Zwingman TA, Sunkin SM, Oh SW, Zariwala HA, Gu H, Ng LL, Palmiter RD, Hawrylycz MJ, Jones AR, Lein ES, Zeng H (2010) A robust and high-throughput Cre reporting and characterization system for the whole mouse brain. *Nat Neurosci* 13:133-140.
- Manavathi B, Peng S, Rayala SK, Talukder AH, Wang MH, Wang RA, Balasenthil S, Agarwal N, Frishman LJ, Kumar R (2007) Repression of Six3 by a corepressor regulates rhodopsin expression. *Proc Natl Acad Sci U S A* 104:13128-13133.

- McCormick DA, Bal T (1994) Sensory gating mechanisms of the thalamus. *Curr Opin Neurobiol* 4:550-556.
- Minor RK, Chang JW, de Cabo R (2009) Hungry for life: How the arcuate nucleus and neuropeptide Y may play a critical role in mediating the benefits of calorie restriction. *Mol Cell Endocrinol* 299:79-88.
- Ohyama K, Ellis P, Kimura S, Placzek M (2005) Directed differentiation of neural cells to hypothalamic dopaminergic neurons. *Development* 132:5185-5197.
- Okamura H, Abitbol M, Julien JF, Dumas S, Berod A, Geffard M, Kitahama K, Bobillier P, Mallet J, Wiklund L (1990) Neurons containing messenger RNA encoding glutamate decarboxylase in rat hypothalamus demonstrated by in situ hybridization, with special emphasis on cell groups in medial preoptic area, anterior hypothalamic area and dorsomedial hypothalamic nucleus. *Neuroscience* 39:675-699.
- Salamone JD, Correa M (2009) Dopamine/adenosine interactions involved in effort-related aspects of food motivation. *Appetite* 53:422-425.
- Sam S, Frohman LA (2008) Normal physiology of hypothalamic pituitary regulation. *Endocrinol Metab Clin North Am* 37:1-22, vii.
- Schwartz MW, Woods SC, Porte D, Jr., Seeley RJ, Baskin DG (2000) Central nervous system control of food intake. *Nature* 404:661-671.

- Shimogori T, Lee DA, Miranda-Angulo A, Yang Y, Wang H, Jiang L, Yoshida AC, Kataoka A, Mashiko H, Avetisyan M, Qi L, Qian J, Blackshaw S (2010) A genomic atlas of mouse hypothalamic development. *Nat Neurosci* 13:767-775.
- Szczyepka MS, Rainey MA, Kim DS, Alaynick WA, Marck BT, Matsumoto AM, Palmiter RD (1999) Feeding behavior in dopamine-deficient mice. *Proc Natl Acad Sci U S A* 96:12138-12143.
- Taniguchi H, He M, Wu P, Kim S, Paik R, Sugino K, Kvitsani D, Fu Y, Lu J, Lin Y, Miyoshi G, Shima Y, Fishell G, Nelson SB, Huang ZJ (2011) A resource of cre driver lines for genetic targeting of GABAergic neurons in cerebral cortex. *Neuron* 71:995-1013.
- VanDunk C, Hunter LA, Gray PA (2011) Development, maturation, and necessity of transcription factors in the mouse suprachiasmatic nucleus. *J Neurosci* 31:6457-6467.
- Williams G, Bing C, Cai XJ, Harrold JA, King PJ, Liu XH (2001) The hypothalamus and the control of energy homeostasis: different circuits, different purposes. *Physiol Behav* 74:683-701.
- Zhu CC, Dyer MA, Uchikawa M, Kondoh H, Lagutin OV, Oliver G (2002) Six3-mediated auto repression and eye development requires its interaction with members of the Groucho-related family of co-repressors. *Development* 129:2835-2849.

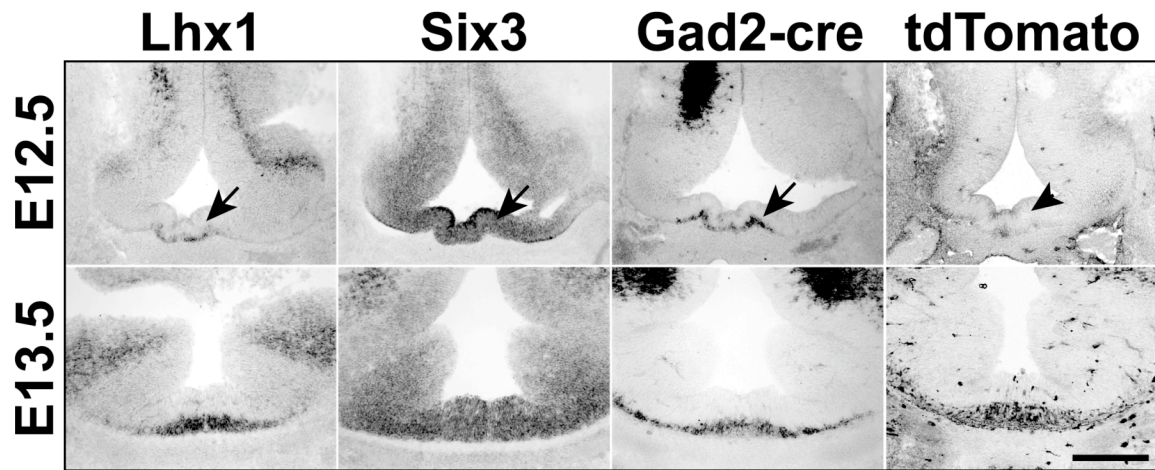


Figure 1. Gad2-cre induces successful recombination within the SCN. Representative ISH images in adjacent transverse sections through the developing SCN show expression of Lhx1, Six3, Gad2-cre, and intrinsic tdTomato at E12.5 and E13.5. Image depicts the overlap of expression of Gad2-cre recombinase and Six3 within the early SCN, marked by the expression of Lhx1 (arrows in E12.5 tissue), and the successful recombination leading to tdTomato expression present by E13.5. Arrowhead points to absence of tdTomato signal at E12.5. Scale bar, 250 μ m.

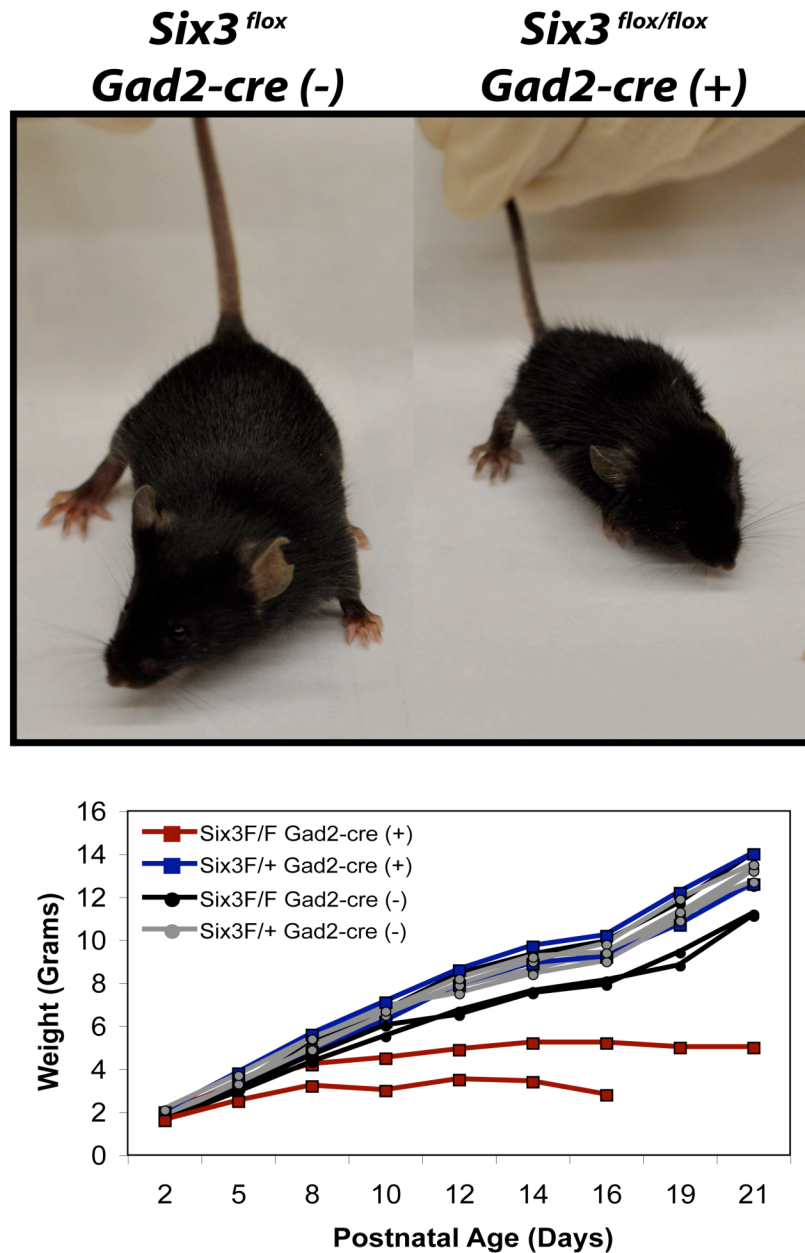


Figure 2. *Six3*^{flox/flox}/*Gad2-cre* (+) mice display severe growth deficiencies visible by P10. *Top*, photograph of control *Six3*^{flox}/*Gad2-cre*(-) mouse (left) shown beside a *Six3*^{flox/flox}/*Gad2-cre*(+) experimental littermate (right) imaged at P23. *Bottom*, bar graph traces the weights (g) of 12 pups from a cross between *Six3*^{flox/+}/*Gad2-cre*(+) male x *Six3*^{flox/flox} female showing that experimental pups are born at a normal weight but stop increasing in size approximately eight days after birth.

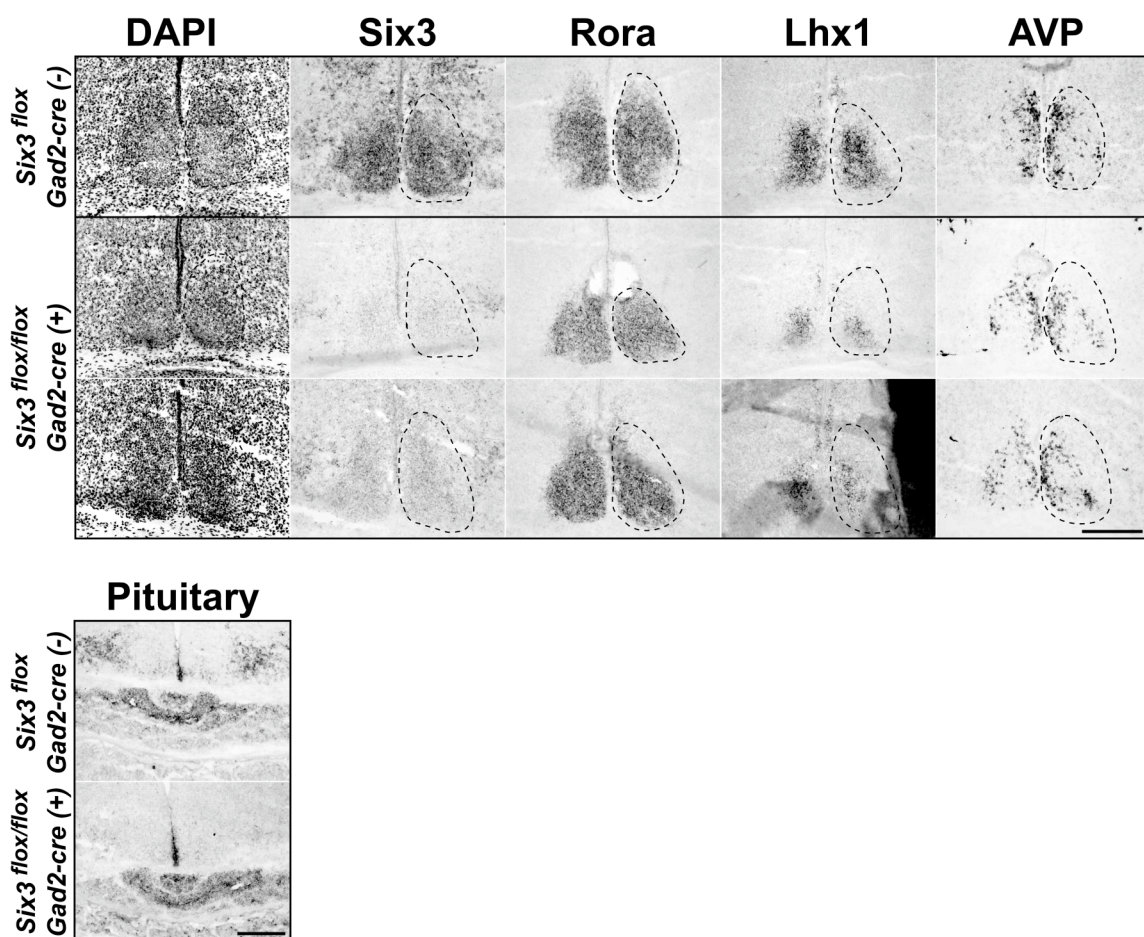


Figure 3. Neonatal localization of SCN transcription factors and peptide expression persist in $Six3^{flox/flox}/Gad2-cre(+)$ mice. Inverted nuclear DAPI staining and ISH images show cell density and expression of Six3, Rora, Lhx1, and AVP in two P2 $Six3^{flox/flox}/Gad2-cre(+)$ mice compared with a $Six3^{flox}/Gad2-cre(-)$ littermate control. Postmitotic Six3 knock-outs display complete Six3 loss in GABA-ergic cells of the SCN while sparing Six3 expression within regions not expressing GABA, such as the pituitary gland. Expression of Rora, Lhx1, and AVP remain present and appropriately localized in $Six3^{flox/flox}/Gad2-cre(+)$ experimental animals. Dotted lines indicate margins of the SCN estimated from DAPI stain. Scale bar, 250 μ m.

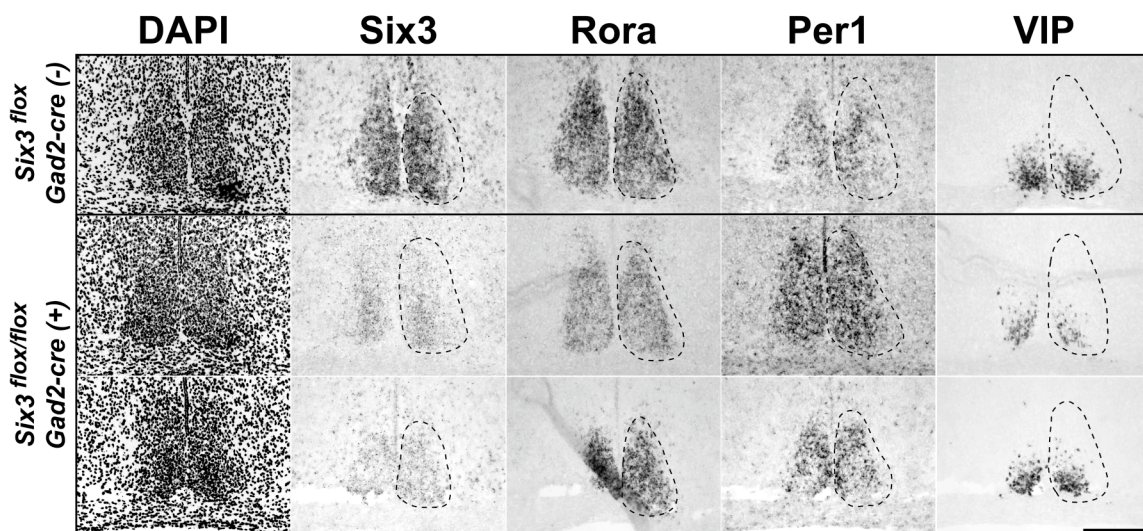


Figure 4. Postmitotic loss of *Six3* does not affect mature transcription factor expression or peptide localization. Inverted nuclear DAPI staining and ISH images show cell density and expression of *Six3*, *Rora*, *Per1*, and *VIP* in two P21 *Six3^{flox/flox}/Gad2-cre(+)* mice compared with a *Six3^{flox}/Gad2-cre(-)* littermate control. ISH for *Six3* mRNA reveals near complete loss in the SCN. Expression of *Rora*, *Per1*, and *VIP* remain present and localized in *Six3^{flox/flox}/Gad2-cre(+)* experimental animals. Dotted lines indicate margins of the SCN estimated from the cell density marker DAPI. Scale bar, 250 μ m.

Table 1. SCN size is maintained in animals with postmitotic deletion of Six3.

Age, Genotype	Average mid-SCN Area (square microns)	Rostral to Caudal Length (um)	mid-SCN width (um)
P2, Six3F Gad2-cre (-)	106,114 ± 2,190	370 ± 50.00	311.63 ± 12.18
P2, Six3F/F Gad2-cre (+)	97,293 ± 4,773 <i>p</i> =0.165	370 ± 50.00	289.37 ± 12.46 <i>p</i> =0.249
P21, Six3F Gad2-cre (-)	99,759 ± 3,537	470 ± 50.00	274.21 ± 14.12
P21, Six3F/F Gad2-cre (+)	86,942 ± 13,664 <i>p</i> =0.424	420 ± 0.00	259.05 ± 17.23 <i>p</i> =0.461

Table displays mid-SCN area (calculated by averaging measurements of right and left nuclei for each animal), rostral to caudal length, and mid-SCN width of SCN nuclei (\pm s.e.m.), showing no overall changes in SCN size in P2 or P21 mice after postmitotic deletion of Six3.

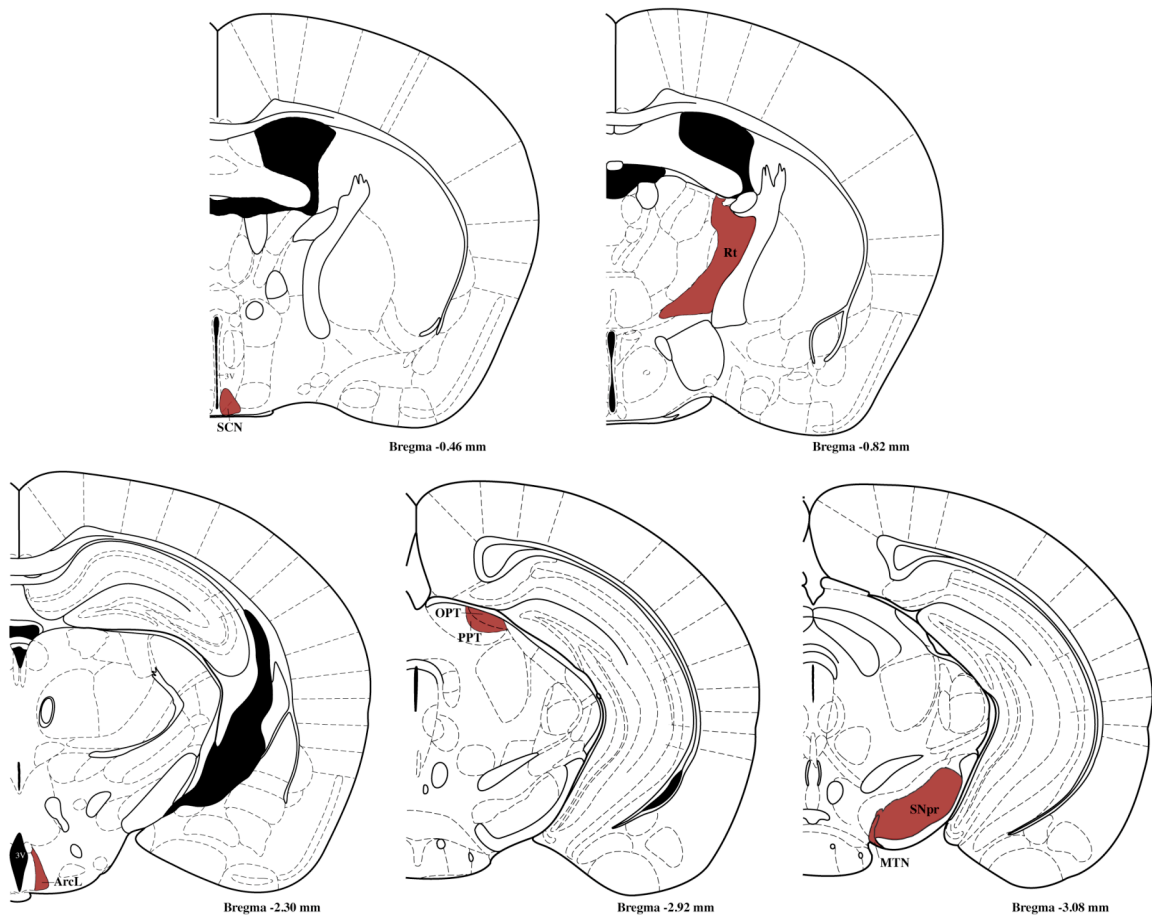


FIGURE 5A

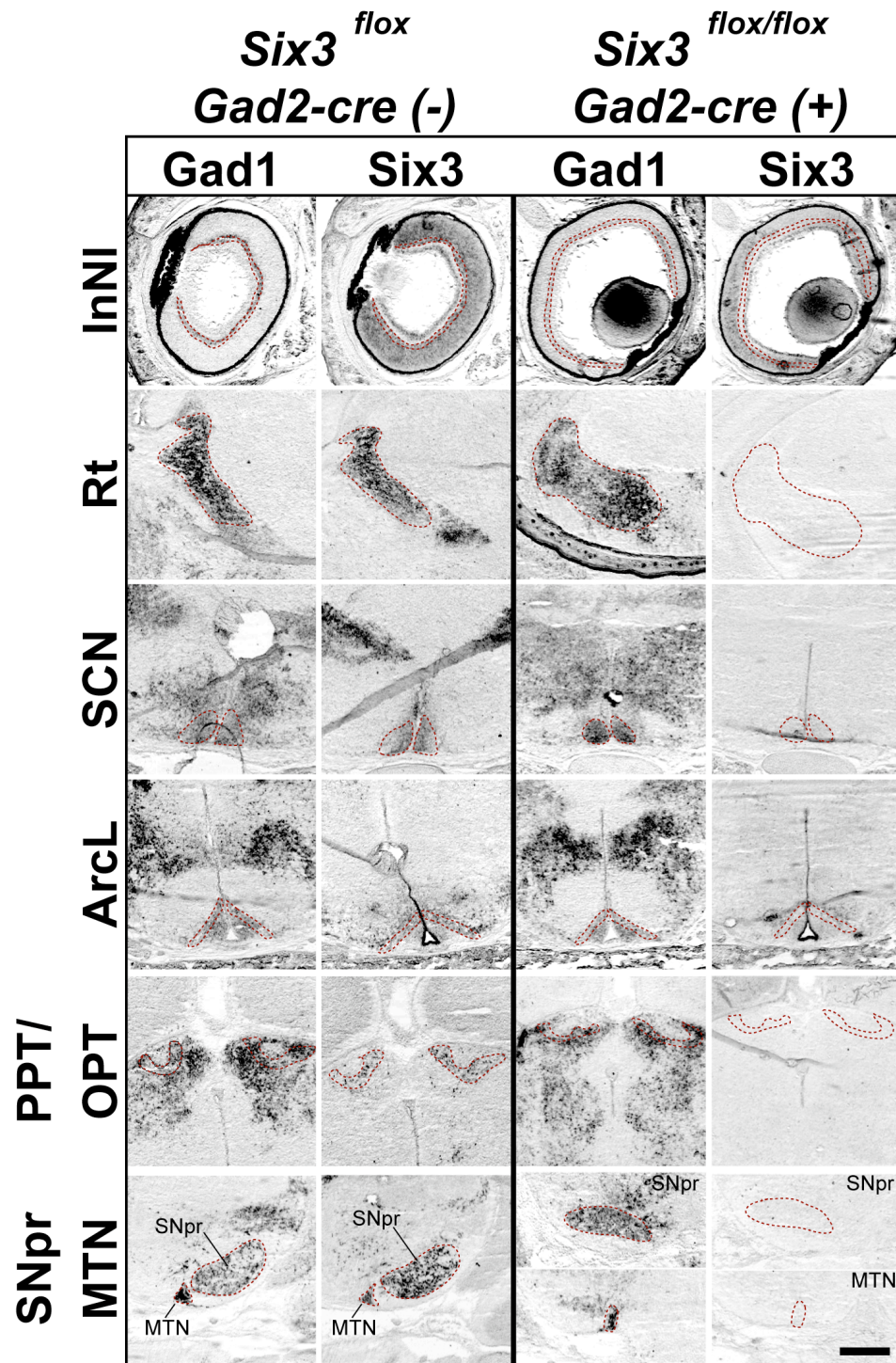


FIGURE 5B

Figure 5. Co-expression of Gad1 and Six3 mRNA is not exclusive to the SCN. Regions of most significant overlap between the expression of Gad1 and Six3 mRNA observed in P2 mice are displayed as red filled in regions within sections from an illustrated Adult mouse atlas (Paxinos and Franklin, 2001) in transverse section (**A**) and dotted red outlines in representative ISH images from adjacent transverse sections of control and *Six3^{flox/flox}/Gad2-cre(+)* mutant mice (**B**). Figures depict significant overlap in amacrine cells of the inner nuclear layer of the retina (InNI), Suprachiasmatic nuclei (SCN), Reticular nuclei (Rt), lateral Arcuate nuclei (ArcL), Posterior pretecal nuclei (PPT)/Optic pretecal nuclei (OPT), Substantia nigra pars reticulata (SNpr) and medial terminal nucleus of the accessory optic tract (MTN). *Six3^{flox/flox}/Gad2-cre(+)* homozygous mutants show successful deletion of Six3 from all regions of overlap. Scale bar, 500 μm .

Supplemental Table 1. Regions of overlap of Six3 and Gad1 mRNA in P2 mouse neural tissue.

Regions of potential overlap
Amacrine cells of the inner nuclear layer, retina
Accumbens nucleus, core
Stria terminalis
Septohypothalamic nucleus
Reticular thalamic nucleus
Zona inserta
Suprachiasmatic nucleus
Anterior amygdala area basolateral
Paraventricular hypothalamic nucleus, medial parvicellular part
Interstitial nucleus of the posterior limb of the anterior commissure
medial preoptic nucleus, medial part
Aruate hypothalamic nucleus, lateral part
Posterior pretectal nucleus/Olivary pretectal nucleus
Posterior hypothalamic nucleus
Retroparafascicular nucleus
Interstitial nucleus of Cajal
Substantial nigra, pars reticulata
Nucleus of Darkschewitsch
Medial geniculate nucleus
Subbrachial nucleus

Table lists all the potential brain regions with overlapping expression of Six3 and Gad1 mRNA in order from rostral to caudal.

-CHAPTER 5-

Conclusions and Future Directions

The primary goal of this thesis was to identify genes expressed by SCN neurons outside of those involved in the molecular clock, and to use those genes to elucidate mechanisms necessary for specification and development of SCN neurons, the SCN network, and circadian function. The SCN are not only essential nuclei necessary for regulating homeostatic processes but represent highly specialized nuclei with a distinct function and thus can be utilized as a model for understanding the direct relationships between genes and rhythmic behavior.

Combinations of transcription factors (TFs), in part, specify the diverse number of cell types that reside in and generate the complexity of the brain; however the direct relationship between TFs and the SCN has never been explored. We pioneered this relationship by utilizing a pre-existing TF screen (Gray et al., 2004) to identify candidate TFs expressed relatively specifically within the prenatal and postnatal SCN (Chapter 2). These candidate TFs allowed us to not only characterize postnatal development of the SCN, outside of the consideration of clock genes but more importantly provide the first descriptions of prenatal maturation of SCN nuclei. In addition, these descriptions provided a tool with which we could investigate the contribution of other elements on development of SCN network organization by assessing the maintenance of mature TF patterns. Finally, we took the first steps into identifying TFs responsible for SCN development by demonstrating the necessity of *Six3* in both SCN formation and specification. Thus, this work has given the field of circadian biology a foundation for understanding the development of the mammalian principal circadian rhythm generators.

Development of SCN neuronal subtypes

A reoccurring theme in the field of circadian biology is how to reconcile the heterogeneity of SCN cellular subtypes (differences in afferent input, connectivity, neuropeptide content, etc.) with possible regions of functional differences and the homogeneous nature of rhythmic capacity within SCN neurons. The presence of cellular heterogeneity has prompted the division of the SCN into anatomically and functionally discrete zones. Classification using different subtypes yields different, not always opposing, ways in which to classify regions of the SCN. Our data demonstrate that the SCN can be subdivided in yet another way based on adult patterns of TF expression that partially overlap with classic peptidergic divisions. Specifically, we find mature localization in expression of *Lhx1* in a central region of the SCN partially overlapping regions expressing both AVP, as well as VIP. We also find the expression of *Rora* is mainly limited to regions containing AVP expressing cells. However, both *Rora* and *Lhx1* expression can be seen in cells that do not express either VIP or AVP. This additional method of dividing SCN neurons into subtypes reiterates the claims argued by Morin, 2007 that broad anatomical classification of SCN subdivisions are an oversimplification and that the SCN reflects subtypes much more diverse (Morin, 2007). Even still, understanding the relationships of these subtypes with one another may lead to a more thorough view of SCN network function.

Early studies performed by Altman and Bayer (1986) describe SCN neurons being derived from two distinct neuroepithelial zones, giving rise to the hypothesis that

SCN precursor cells may exist with distinctly restricted fates even before cells become postmitotic. In this work, we developed tools that allowed us to test the hypothesis that SCN precursors exhibit different genetic markers prior to SCN formation. Our results do not support a genetic distinction in the neuroepithelium from which SCN neurons are derived. On the contrary, we find the entire SCN neuroepithelium expresses a combination of Six3, Six6, and Fzd5. Additionally, SCN neurons progress through the same gene cascade from the time of precursors to being postmitotic. From the proliferative neuroepithelium cells undergo mitosis and lose expression of Fzd5 and begin expressing Dlx2. Once cells become postmitotic they transiently express Dlx2 followed by Lhx1. The first sign of variability between cells is in the onset of peptide expression and the loss of Lhx1 expression in cells located in the outer SCN, leading to the visual appearance of centralization of Lhx1, present by E18.5. Thus, the genetic markers developed support the idea that SCN neurons are derived from the same precursor population.

Several studies indicate that cell-to-cell signaling in the SCN promotes rhythmicity in a subset of SCN neurons (Yamaguchi et al., 2003; Aton et al., 2005; Maywood et al., 2007). Thus, although each cell has the capacity to create rhythms, some produce autonomous rhythms, while others can be driven to rhythmicity through network function. Webb and colleagues (2009) have shown that neurons displaying cell-autonomous rhythms can express VIP, AVP, or neither peptide, suggesting no one peptidergic subtype of SCN neuron can be attributed to those displaying cell autonomous

rhythm-generating properties. They also demonstrate that single cells have the ability to shift between rhythmic modalities.

Taken together these results give rise to the hypothesis that all SCN cells are innately similar. SCN precursors follow the same gene cascade that specifies them to be “SCN” neurons and intrinsic oscillators. As they develop, these unstable oscillators undergo further specialization in order to become a functional network. Differentiation of these neural precursors into unique subtypes may then arise from one or several sources such as morphogens or signaling elements, connectivity, environmental influences, innervation, or other genes yet to be discovered. Interestingly, it has been suggested that variability in capabilities of single oscillators to maintain similar amplitude and periodicities from cell to cell aids in robustness and plasticity of the circadian clock network (Webb et al., 2009). We further hypothesize that diversity in neurotransmitter phenotype, response to stimuli, or TF expression of individual oscillators may also contribute to the plasticity of the network.

Differential gene expression and the impact of retinal innervation on SCN development

Several researchers have found differential expression of clock genes across the SCN at mid-day time points, namely in the expression of *Per1* and *Per2* isolated to the SCN shell. In Chapter 2 we find that the mature SCN displays patterns of *Rora* expression similar to that described for *Per1* and *Per2*. This pattern of expression is

progressively localized through development. Interestingly, expression of another gene in this study, *Lhx1*, moves centrally during prenatal development. As of yet, the meaning behind the localization of these TFs is unknown, but it is tempting to speculate that the localization could form a functional division in the SCN. The progressive regionalization of *Rora* is coincident with several anatomical and functional changes within the nuclei including retinal innervation and synaptogenesis. We hypothesize that the progressive change in postnatal (and prenatal) TF localization may represent functional or induced changes within the nuclei.

In Chapter 3 we investigated the role of two crucial aspects of the circadian system in shaping SCN development. We find that the circadian pacemaker develops anatomically independent of retinal innervation or VIP/VPAC₂ signaling. Specifically, when VIP, VPAC₂, or retinal innervation are eliminated we found that subdivisions, in way of peptide segregation and TF localization, are formed and SCN cell number and nuclei size persist.

Despite the lack of gross anatomical changes, effects on circadian period have been repeatedly reported in animals lacking retinal innervation. Effects of circadian period lengthening have been observed in mice with both genetic (Wee et al., 2002) and naturally occurring models (Laemle and Ottenweller, 1998) of enucleation. In addition, it has been shown that altering the photoperiod of neonatal mice can impact the developed circadian period (Ciarleglio et al., 2011). These findings suggest that although not necessary for development of the anatomical timekeeping system that retinal innervation

and/or light input may be necessary to initially set the timing of the circadian period by an unknown mechanism. These results are consistent with there being a baseline innate system of individual clocks that would then need to be structured on a molecular level to set the timing of the network.

Role for Six3 in development

In Chapter 2 we identified the homeobox gene, Six3, as critical for formation and early specification of the SCN. The premitotic loss of Six3 led to loss of cell dense clusters along the ventral surface of the developing telencephalon/diencephalon indicating loss of nuclei formation. In addition, loss of Six3 led to the lack of cells expressing key downstream genes such as Lhx1 and Rora. This represents the first gene to be discovered as playing an early critical role in development of the SCN.

Six3 expression is maintained in several nuclei in mature animals. The prolonged expression of Six3; a gene predominately thought of as involved in early patterning, led to the possibility of additional roles for this gene in postmitotic development and function. In order to target deletion from the SCN postmitotically, we generated mice with deletion of Six3 driven by Gad2, a precursor to GABA, expressed by SCN neurons (Okamura et al., 1990). We find that Gad2 recombination is apparent by approximately two days after cells exit the cell cycle. In Chapter 4 we demonstrate that postmitotic loss of Six3 had gross effects on the development of mice containing homozygous mutations, leading to severe growth deficiencies and early lethality. This indicated two things; first,

Six3 plays an active role in cells postmitotically and second, that Six3 may have a strong role in postmitotic regulation of nuclei responsible for coordinating growth. We find postmitotic deletion of Six3 within the SCN had no effect on the subsequent expression and localization of TFs and peptides; however a role in function has not yet been investigated.

Future Directions

SCN formation and specification

Early specification relies not only on locally expressed TFs but also on extrinsic morphogens and other signaling peptides. Through our characterizations we found Lhx1 and Six3 could mark the early developing SCN. We then used these markers to identify, for the first time, where the immature SCN is located within the complex early signaling environment of the developing forebrain. Hedgehog, Wnt, bone morphogenetic protein (BMP), and fibroblast growth factor (FGF) signaling have all been implicated in shaping aspects of early telencephalon/diencephalon development (Hogan, 1999). In Chapter 2 we looked for the expression of a subset of signaling receptors and cues within the SCN. We found the SCN neuroepithelium expressed Fzd5, a receptor for Wnt signaling, but did not express SHH, the SHH receptor, Patched1, or BMP7. Future work should seek to further identify the signaling molecules and gradients that aid in the specification of SCN neurons. Understanding if different dorsal to ventral regions of the early SCN

neuroepithelium are responding differentially to signaling morphogens would shed light on the how SCN neuronal subtypes might be formed.

Six3 and the SCN

While we were able to demonstrate the essential involvement of Six3 in the early development of the SCN, many questions remain. Future work should focus on investigating (1) how Six3 regulates initial SCN specification (2) possible mechanisms for Six3 in SCN functionality and (3) use of Six3 for genetic ablation of the SCN.

Six3 has been shown to interact with a number of genes to direct early forebrain patterning, cell proliferation, specification, and differentiation (Del Bene et al., 2004; Liu et al., 2006; Manavathi et al., 2007; Liu et al., 2010). However, the possible relationship between these genes, such as Geminin (Kroll, 2007) and Pax6 (Liu et al., 2006) and the SCN is unknown. In order to understand how Six3 directs formation of the SCN, further experiments focusing on the presence of Six3 target genes within the developing SCN need to be conducted. Assessing genes elevated or reduced in the absence of Six3, through a DNA microarray, could aid in selection of downstream target candidates.

In Chapter 4 we assessed the role of Six3 in postmitotic development of the SCN. Investigation in this manner addressed the role for Six3 in postmitotic cellular/ network development as well as maintenance of nuclei function. We found postmitotic deletion of Six3 did not affect the specification of SCN TF-expressing or peptidergic neuronal subtypes; however assessment of contribution into functional elements could not be

assessed by traditional methods due to early lethality. Multi-electrode array recordings, as well as luciferase conjugated constructs have proven to be valuable resources to assess SCN network function and connectivity in addition to the rhythmicity of individual cells (Welsh et al., 1995; Liu et al., 2007). These methods normally utilize tissue taken from animals within the first ten postnatal days, thus these alternative methods could be very useful in identifying any changes in SCN network function or rhythmic properties of single cells using the *Six3^{flox/flox}/Gad2-cre(+)* mice we have generated. Alternatively, the runting phenotype could be alleviated by conditional deletion of *Six3* after a mature network has been formed. This could be achieved through use of mice with an inducible form of cre recombinase (ie. tamoxifen) driven by a promoter expressed by SCN neurons (such as the existing *Six3CreER^{T2}* (Geng et al., 2008)). The inducing agent could be administered to the entire animal (IP injection or oral gavage) or stereotaxically injected into the SCN for targeted *Six3* deletion. Animals with postnatal deletion of *Six3* could then be tested for SCN function through assessment of wheel running activity within multiple lighting paradigms.

The severe growth deficits seen within postmitotic *Six3* homozygous mutants provides evidence that *Six3* is playing critical roles in either the postmitotic specification or regulation of cells/nuclei necessary for growth. Assessment of regions with overlap of *Six3* and *Gad1* mRNA expression allow us to pinpoint potential nuclei responsible for these changes. However, given that *Six3* remains transient for a number of populations (Conte et al., 2005; VanDunk et al., 2011), assessment at P2 may not be sufficient for

determining the breadth or number of nuclei affected. Assessment at earlier stages in development may provide a more accurate understanding of the type of nuclei that may be affected by the conditional deletion. Alternatively, whole brain or isolated tissue lysates could be tested for changes in the overall levels of major neurohormones as deficits in growth and early lethality have been linked to a number of factors including reduced dopamine (Kobayashi et al., 2004) and PACAP (Gray et al., 2001; Sherwood et al., 2007). Identifying hormones affected would aid in detection of nuclei requiring postmitotic Six3.

Six3 is not exclusively expressed by the SCN neuroepithelium but rather is broadly expressed within the anterior forebrain early in development (Seo et al., 1999). In Chapter 2 we used a Nestin driven cre recombinase to remove Six3 expression from neural precursors. We found that Six3 deletion in this manner completely eliminated SCN formation and TF expression. In addition, we found no gross effects in neural morphology; however, postnatally these mice mimicked the phenotype of animals with postmitotic Six3 deletion and displayed severe growth deficiencies. It cannot be known whether this phenotype is due to effects on neuroepithelium of other forebrain nuclei influencing initial development or an effect of postmitotic control of nuclei regulating growth.

We find that the proliferative zone of the SCN neuroepithelium expresses Fzd5 and that cells of the SCN transiently express Dlx2 before becoming postmitotic. Using a Cre/loxP method with focus on these gene targets would aid in the isolation of Six3

deletion specifically from SCN precursors. Isolation of Six3 deletion specifically from SCN neuroepithelium would allow for more precise investigation into the role of Six3 in SCN development by eliminating the caveat of deletion from surrounding tissue. In addition, this specific deletion, if shown to alleviate effects on animal growth, could then be used as a model of genetic SCN ablation. A model of SCN ablation could be used to further studies on the impact of the SCN on development and rhythms within peripheral clocks as well as implications of loss of clock function on body temperature, sleep, and other homeostatic functions. Disruption of these key homeostatic mechanisms has been shown to lead to higher prevalence of both mental and physical disease (for review (Maywood et al., 2006; Bechtold et al., 2010)).

In conclusion, our efforts have created an invaluable list of TFs that serve as candidates for roles in SCN specification, development, and function. Even further we provide direct evidence that understanding the roles of TFs expressed within the SCN can reveal not only how these complex nuclei are formed and develop but also could provide critical tools for understanding the role of the SCN in animal behavior, homeostasis, and disease.

References

- Aton SJ, Colwell CS, Harmar AJ, Waschek J, Herzog ED (2005) Vasoactive intestinal polypeptide mediates circadian rhythmicity and synchrony in mammalian clock neurons. *Nat Neurosci* 8:476-483.
- Bechtold DA, Gibbs JE, Loudon AS (2010) Circadian dysfunction in disease. *Trends Pharmacol Sci* 31:191-198.
- Ciarleglio CM, Axley JC, Strauss BR, Gamble KL, McMahon DG (2011) Perinatal photoperiod imprints the circadian clock. *Nat Neurosci* 14:25-27.
- Conte I, Morcillo J, Bovolenta P (2005) Comparative analysis of Six 3 and Six 6 distribution in the developing and adult mouse brain. *Dev Dyn* 234:718-725.
- Del Bene F, Tessmar-Raible K, Wittbrodt J (2004) Direct interaction of geminin and Six3 in eye development. *Nature* 427:745-749.
- Geng X, Speirs C, Lagutin O, Inbal A, Liu W, Solnica-Krezel L, Jeong Y, Epstein DJ, Oliver G (2008) Haploinsufficiency of Six3 fails to activate Sonic hedgehog expression in the ventral forebrain and causes holoprosencephaly. *Dev Cell* 15:236-247.
- Gray PA, Fu H, Luo P, Zhao Q, Yu J, Ferrari A, Tenzen T, Yuk DI, Tsung EF, Cai Z, Alberta JA, Cheng LP, Liu Y, Stenman JM, Valerius MT, Billings N, Kim HA, Greenberg ME, McMahon AP, Rowitch DH, Stiles CD, Ma Q (2004) Mouse brain organization revealed through direct genome-scale TF expression analysis. *Science* 306:2255-2257.

- Gray SL, Cummings KJ, Jirik FR, Sherwood NM (2001) Targeted disruption of the pituitary adenylate cyclase-activating polypeptide gene results in early postnatal death associated with dysfunction of lipid and carbohydrate metabolism. *Mol Endocrinol* 15:1739-1747.
- Hogan BL (1999) Morphogenesis. *Cell* 96:225-233.
- Kobayashi M, Iaccarino C, Saiardi A, Heidt V, Bozzi Y, Picetti R, Vitale C, Westphal H, Drago J, Borrelli E (2004) Simultaneous absence of dopamine D1 and D2 receptor-mediated signaling is lethal in mice. *Proc Natl Acad Sci U S A* 101:11465-11470.
- Kroll KL (2007) Geminin in embryonic development: coordinating transcription and the cell cycle during differentiation. *Front Biosci* 12:1395-1409.
- Laemle LK, Ottenweller JE (1998) Daily patterns of running wheel activity in male anophthalmic mice. *Physiol Behav* 64:165-171.
- Liu AC, Welsh DK, Ko CH, Tran HG, Zhang EE, Priest AA, Buhr ED, Singer O, Meeker K, Verma IM, Doyle FJ, 3rd, Takahashi JS, Kay SA (2007) Intercellular coupling confers robustness against mutations in the SCN circadian clock network. *Cell* 129:605-616.
- Liu W, Lagutin OV, Mende M, Streit A, Oliver G (2006) Six3 activation of Pax6 expression is essential for mammalian lens induction and specification. *Embo J* 25:5383-5395.

- Liu W, Lagutin O, Swindell E, Jamrich M, Oliver G (2010) Neuroretina specification in mouse embryos requires Six3-mediated suppression of Wnt8b in the anterior neural plate. *J Clin Invest* 120:3568-3577.
- Manavathi B, Peng S, Rayala SK, Talukder AH, Wang MH, Wang RA, Balasenthil S, Agarwal N, Frishman LJ, Kumar R (2007) Repression of Six3 by a corepressor regulates rhodopsin expression. *Proc Natl Acad Sci U S A* 104:13128-13133.
- Maywood ES, O'Neill JS, Chesham JE, Hastings MH (2007) Minireview: The circadian clockwork of the suprachiasmatic nuclei--analysis of a cellular oscillator that drives endocrine rhythms. *Endocrinology* 148:5624-5634.
- Maywood ES, O'Neill J, Wong GK, Reddy AB, Hastings MH (2006) Circadian timing in health and disease. *Prog Brain Res* 153:253-269.
- Morin LP (2007) SCN organization reconsidered. *J Biol Rhythms* 22:3-13.
- Okamura H, Abitbol M, Julien JF, Dumas S, Berod A, Geffard M, Kitahama K, Bobillier P, Mallet J, Wiklund L (1990) Neurons containing messenger RNA encoding glutamate decarboxylase in rat hypothalamus demonstrated by in situ hybridization, with special emphasis on cell groups in medial preoptic area, anterior hypothalamic area and dorsomedial hypothalamic nucleus. *Neuroscience* 39:675-699.
- Seo HC, Curtiss J, Mlodzik M, Fjose A (1999) Six class homeobox genes in drosophila belong to three distinct families and are involved in head development. *Mech Dev* 83:127-139.

- Sherwood NM, Adams BA, Isaac ER, Wu S, Fradinger EA (2007) Knocked down and out: PACAP in development, reproduction and feeding. *Peptides* 28:1680-1687.
- VanDunk C, Hunter LA, Gray PA (2011) Development, maturation, and necessity of transcription factors in the mouse suprachiasmatic nucleus. *J Neurosci* 31:6457-6467.
- Webb AB, Angelo N, Huettner JE, Herzog ED (2009) Intrinsic, nondeterministic circadian rhythm generation in identified mammalian neurons. *Proc Natl Acad Sci U S A* 106:16493-16498.
- Wee R, Castrucci AM, Provencio I, Gan L, Van Gelder RN (2002) Loss of photic entrainment and altered free-running circadian rhythms in *math5*^{-/-} mice. *J Neurosci* 22:10427-10433.
- Welsh DK, Logothetis DE, Meister M, Reppert SM (1995) Individual neurons dissociated from rat suprachiasmatic nucleus express independently phased circadian firing rhythms. *Neuron* 14:697-706.
- Yamaguchi S, Isejima H, Matsuo T, Okura R, Yagita K, Kobayashi M, Okamura H (2003) Synchronization of cellular clocks in the suprachiasmatic nucleus. *Science* 302:1408-1412.

CASSANDRA MARIE VANDUNK

EDUCATION

- August 2005-present** **Washington University in Saint Louis**, Saint Louis, MO
Doctoral Candidate
- June – July 2008** **Marine Biological Laboratories**, Woods Hole, MA
Neural Systems and Behavior, Course Participant
- August 1999 – May 2003** **Albion College**, Albion, MI
B.A. Biology

RESEARCH EXPERIENCE

August 2005-present: **Doctoral Research**

Laboratory of Dr. Paul A. Gray, Washington University in Saint Louis, Saint Louis, MO

Characterized the specific origins, dynamic maturation, and the necessity of transcription factors in suprachiasmatic nuclei development

June 2004- June 2005: **Post Baccalaureate Intramural Research Training Award Fellow**

Laboratory of Dr. Michael O'Donovan, National Institutes of Health, Bethesda, MD

Used anatomical and genetic analysis to investigate the development of specific populations of neurons within the lumbar spinal cord

June 2003-June 2004: **Post Baccalaureate Intramural Research Training Award Fellow**

Laboratory of Dr. Phillip Nelson, National Institutes of Health, Bethesda, MD

Investigated the use of neurotrophins as potential biological markers of Autism in blood spots, eluate, plasma, and serum

June – August 2001, 2002 Summer Research Assistant

Laboratory of Dr. Pamela Swiatek, Van Andel Research Institute, Grand Rapids, MI

Improved the technique of in-vitro fertilization and sperm cryopreservation and established embryonic stem cell lines from C57BL/6 mice within the Lab of Germline Modification.

Techniques: microsurgery, sterile tissue culture, microinjection

AWARDS AND FELLOWSHIPS

Carl Storm Underrepresented Minority Fellowship, Gordon Research Conference 2009
Surdna Foundation Scholarship, Marine Biological Laboratories April 2008
John Merlie Fellowship, Washington University March 2008
Recipient of Special Act/Service Award, National Institutes of Health 2004

PUBLICATIONS

VanDunk C, Hunter L, Gray P. Development, Maturation, and Necessity of Transcription Factors in the Mouse Suprachiasmatic Nucleus. *Journal of Neuroscience*, 2011 April;27; 31(17) 6457-6467

Pagliardini S, Ren J, Gray PA, **VanDunk C**, Gross M, Goulding M, Greer JJ. Central respiratory rhythmogenesis is abnormal in *lhx1*-deficient mice. *Journal of Neuroscience*, 2008 Oct;22;28(43):11030-41

Song EY, **VanDunk C**, Kuddo T, Nelso PG. Measurement of vasoactive intestinal peptide using a competitive fluorescent microsphere immunoassay or ELISA in human blood samples. *Journal of Immunological Methods*, 2005 May: 300(1-2): 63-73.

Nelson PG, Kuddo T, Song EY, Dambrosia JM, Kohler S, Satyanarayana G, **VanDunk C**, Grether JK, Nelson KB. Selected neurotrophins, neuropeptides, and cytokines: developmental trajectory and concentrations in neonatal blood of children with autism or Down syndrome. *International Journal of Developmental Neuroscience*, 2006 Feb: 24(1): 73-80.

Song EY, **VanDunk C**, Kuddo T, Nelson PG. Measurement of CGRP in dried blood spots using a modified sandwich enzyme immunoassay. *Journal of Neuroscience Methods*, 2006 Jul; 155(1): 92-7.

ABSTRACTS

2011 VanDunk C, **Gray PA**

SCN Formation and Maturation: Influence of transcription factors, retinal innervation, and Vip signaling

Gordon Research Conference on Chronobiology, Lucca, Italy

2010 **VanDunk C**, Gray PA

Specific origin, dynamic maturation, and the necessity of Six3 in SCN development

Society for Neuroscience Conference, SanDiego, CA

VanDunk C, Gray PA

Transcription Factor Coding of the Mouse SCN

Sleep Research and Biological Rhythms Conference, Destin FL.

2009 **VanDunk C**, Gray PA

Ontogeny of the Mouse Suprachiasmatic Nucleus

Gordon Research Conference on Chronobiology, Newport, RI.

2008 **VanDunk C**, Gray PA

Characterization of gene expression profiles in the mouse suprachiasmatic nucleus Society for Neuroscience Conference, Washington D.C.

2007 Gray PA, **VanDunk C**

Developmental origins of ventral medullary NK1R neurons.

Society for Neuroscience Conference, SanDiego, CA

2005 Nelson PG, Kuddo T, Song E, Dambrosia J, Kohler S, Satyanarayana G, **VanDunk C**, Grether J, Nelson KB.

Measurement of trophins, peptides, and cytokines in blood of Down syndrome and autistic newborns and controls

Society for Neuroscience Conference, Washington D.C.

2004 Song EY, **VanDunk C**, Kuddo T, Nelson PG.
Measurement of vasoactive intestinal peptide using a competitive fluorescent
microsphere immunoassay or ELISA in human blood samples.
Society for Neuroscience Conference, San Diego, CA

PROFESSIONAL AFFILIATIONS

Society for Neuroscience